In vitro validation of multifunctional liposomes for leukaemia and prostate cancer therapy – the folate receptor and the prostate-specific membrane antigen as targets for drug delivery

By
Ida Mostrøm Nilssen

A thesis submitted in partial fulfilment of the requirements for the degree of Master of Pharmacy

Centre for Pharmacy and Institute for Biomedicine
University of Bergen, Norway

Acknowledgements

The work performed in this thesis was conducted at the Institute for Biomedicine from August 2011 to May 2012 with the support from Centre for Pharmacy and the Faculty of Medicine and Dentistry, University of Bergen.

First, I would like to thank my supervisor Lars Herfindal for all your help and guidance throughout the fulfilment of this thesis. Thank you for always taking the time to answer my questions, for the contribution with all your knowledge and for the training in the making of liposomes. I would also like to thank my co-supervisor Stein Ove Døskeland for making the fulfilment of my thesis possible.

Next, my gratitude goes towards the TSG group and all its members. Especially I would like to thank Nina Lied Larsen for training in cell culturing and lab techniques, and for help with Western blot execution towards a stressful end of the fulfilment of my thesis. I would also like to thank Lene Myhren for training in SDS-PAGE and Western blot technique, and for help with data analysis in flow cytometry. Next, my thanks goes to Siri Strømsøy and Kirsten Brønstad for lab training and help throughout the last 10 months. The TSG group has been a positive environment to work in and all your help and knowledge is highly appreciated.

I would also like to thank my fellow students at Institute for Biomedicine for helping keeping up the motivation and for good conversations. Further, my thanks goes to my pharmacy co-students for five great years at the University of Bergen.

Finally, I would like to thank my family and friends for support and understanding. Special thanks goes to my fiancée Tim Eirik Kallekleiv for all your love and support.

Bergen, May 2012

Ida Mostrøm Nilssen

Abbreviations

ADT	Androgen deprivation therapy
AML	Acute myleoid leukaemia
APL	Acute promyelocytic leukaemia
ATCC	American Type Culture Collection
ATRA	All-trans retinoic acid
AUC	Area under curve
BSA	Bovine serum albumine
CHX	Cycloheximide
CR	Complete remission
DLS	Dynamic light scattering
DMEM	Dulbecco's Modified Eagle's Medium
DMSO	Dimethyl sulphoxide
DNA	Deoxyribonucleic acid
DNR	Daunorubicin
DOX	Doxorubicin
DSPE-PEG	1,2-Disteraoyl-sn-glycero-3-Phosphoetanolamine-N-[Methoxy(Polyethylene glycol)-2000]
DSPE-PEG-FA	1,2-disteraoyl-sn-glycero-3-phosphoetanolamine-N-((polyethylene glycol-5000)folate
EME	Emetine
EPR	Enhanced permeability and retention
FBS	Foetal bovine serum
FA	Folic acid
FAB	French-American-British
FDA	Food and Drug Administration
FOLR2	Folate recetor β
FR	Folate receptor
GFP	Green fluorescent protein
GPI	Glycosyl phosphatidylinositol
h	hours
HEPC	Hydrogenated egg phosphatidylcholine
IMDM	Iscove's Modified Dulbecco's Medium
IV	Intravenous
Kd	Dissociation constant

LAF	Laminar air flow
LHRH	Luteinising hormone-releasing hormone
LSC	Leukaemia stem cell
MDR	Multidrug resistance
min	minutes
MLV	Multi lamellar vesicles
MPS	Mononuclear phagocyte system
MQ	Milli Q
PBS	Phosphate buffered saline
PC	Phosphatidylcholine
PdI	Polydispersity index
PEG	Polyethylene glycol
PEG-FA	PEG-conjugated and FA-conjugated
P-gp	P-glycoprotein
PSA	Prostate-specific antigen
PSMA	Prostate-specific membrane antigen
PVDF	Polyvinylidene difluoride
RFC	Reduced folate carrier
RNA	Ribo nucleic acid
s	seconds
SCT	Stem cell transplantation
SDS	Sodium dodecyl sulphate
SDS-PAGE	Sodium dodecyl sulphate polyacrylamide gel electrophoresis
TNM	Tumour, lymph Nodes, Metastasis
TSG	Translational Signalling Group
wt	Wild type
WST	Water soluble tetrazolium salt
ZP	Zeta potential

Table of contents

1. Introduction

1.1 Acute myeloid leukaemia and the folate receptor as a target for drug delivery

1.1.1 Acute myeloid leukaemia (AML): Disease characteristics and current treatment strategies

Acute leukaemia is a cancer where haemopoietic blasts cells constitute more than 20% of the bone marrow or peripheral blood cells; usually accumulating in the blood, infiltrating other tissues and causing bone marrow failure (1-3). Two main groups of acute leukaemia exist: acute lymphoblastic leukaemia (ALL) and acute myeloid leukaemia (AML) (1, 3). The focus in this master thesis will be on AML.

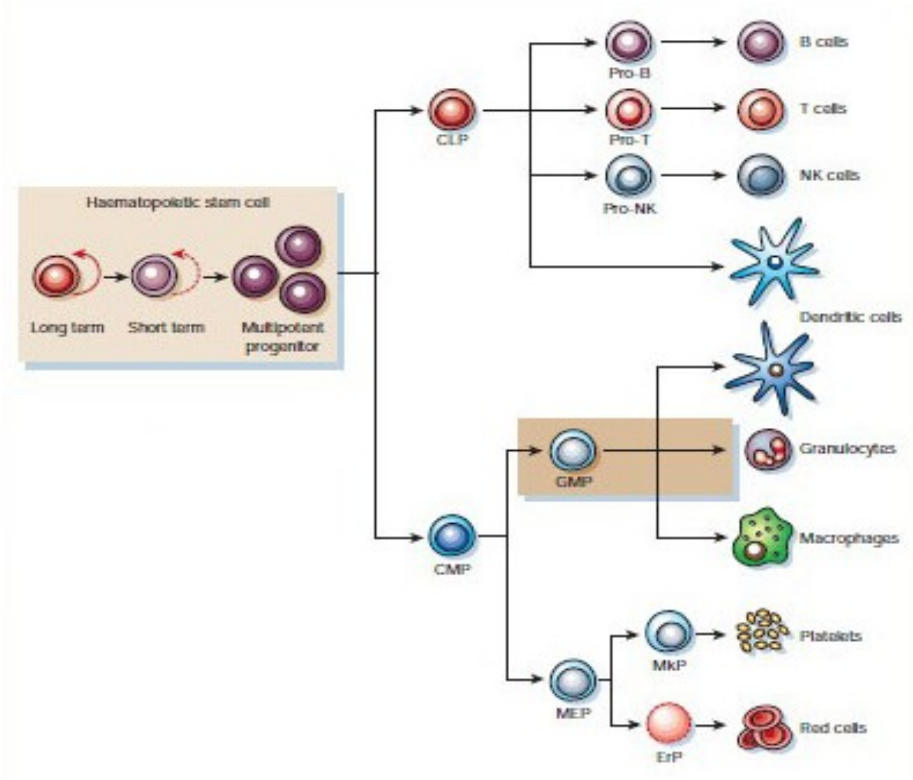

Figure 1.1: Hematopoiesis. Picture from (4). *CLP = common lymphoid progenitors, CMP = common myeloid progenitors. AML arises from the CMP compartment* (3).

AML is an uncommon cancer (3, 5), and in the US, UK and Norway about 12000 (6), 1000 (1), and 100 (7) new cases are diagnosed each year, respectively. The disease occurs at all ages but is most common in the elderly; the median age of presentation being in the late 60s (1, 5). Clinical manifestations include dyspnoea, weakness, infections and bleeding due to bone marrow failure syndrome producing anaemia, granulocytopenia and thrombocytopenia (8). AML is a highly heterogeneous disease clinically and biologically, with eight WHO sub-classifications (2008) based on morphology, immunophenotype, cytochemistry and cytogenetics (1-3, 5, 6). The MOLM-13 cell line used in this master thesis is classified as M5a (acute monocytic leukaemia) according to the French-American-British (FAB) AML classification (9), which is based on differentiation level and morphologic evaluation of blasts (3). Cytogenetic and molecular changes are highly prognostic indicators in AML, and patients can be defined to be at favourable, intermediate or unfavourable risk based on this information (1, 2, 5, 6). Acute promyelocytic leukaemia (APL), FAB classification M3 (3, 7), is often considered in an own category, given that this AML subtype has a different treatment regime and a more favourable treatment outcome (3, 10). APL will not be discussed further in this thesis. The risk-stratification allows for better treatment planning for AML patients (6). Usually, AML is fatal within weeks from the time of diagnosis if it is left untreated (8).

AML therapy is primarily divided into two phases; remission induction and post-induction therapy (1, 5-7, 11). The treatment approach depends on the age of the patient (2, 5). Treatment of childhood AML will not be described here. The standard remission induction therapy in adults has not changed much over several decades, and treatment outcomes remains suboptimal (6). Also, several novel and targeted agents have failed to improve patient outcomes in randomised trials (11). Relatively few new AML drugs have been approved in the past 20 years (5).

For patients between 18 and 60 years old, the standard of care for induction therapy remains a combination of 3 days of daunorubicin and 7 days of cytosine arabinoside (cytarabine), also called the “3 + 7” protocol (2, 3, 5, 11). In this regime, cytarabine (100 – 200 mg/m^2/day) is given as a continuous IV infusion over 7 days and an anthracycline, normally daunorubicin (45 – 90 mg/m^2), is given as an IV infusion for the first 3 days (2, 3, 6, 7). Cytarabine acts as a competitive inhibitor of DNA polymerase, and it can also act as a substrate for the enzyme; incorporation leading to chain termination or preventing DNA replication (12). Daunorubicin is described thoroughly in section 1.3.3. Addition of other agents or multidrug resistance modulators has not improved outcomes for induction chemotherapy (2, 6). Complete remission (CR) is defined as marrow blasts lower than 5% and recovery of peripheral counts, and is assessed after one or two induction treatments (5). The aim of remission induction is CR, but without further treatment after reaching CR a very high proportion of the patients will relapse (3, 5). Therefore, post-induction therapy is necessary (3, 5).

For patients younger than 60, this consists of further chemotherapy or stem cell transplantation (SCT) (5, 6). High-dose cytarabin 3 g/m^2 per 12 hours on day 1, 3 and 5 given for a total of 4 courses is the most widely accepted schedule, particularly for favourable risk patients (5-7). SCT from a well-matched sibling donor is an alternative approach, and offers the best option for unfavourable risk patients (2, 5, 6). The current treatment outcome is that 40 to 45% of AML patients younger than 60 years will be cured (5).

The majority of AML patients, however, are older than 60 years (5). Lower CR rates can be predicted in older patients based on prognostic factors such as increasing age, poor performance status, comorbidities, secondary leukaemia, P-glycoprotein (P-gp) overexpression leading to chemotherapy resistance, adverse cytogenetics, splenomegaly and extramedullary disease (2, 3, 5). Induction therapy is less effective in older patients due to patient-related and disease-related factors (6). Disease-characteristics associated with poor outcome occur more frequently in older patients (2, 6). Also, intensive chemotherapy treatment is problematic due to toxicity concerns (5, 7). Low-intensity induction with low-dose cytarabin has been a standard treatment over the last several decades, aiming to preserve efficacy while reducing toxicity in older patients (2, 11). However, for selected elderly patients intensive remission induction therapy, hence a 3 days of daunorubicin (45 to 50 mg/m^2) and 7 to 10 days of cytarabine (100 to 200 mg/m^2) regime, provides a superior approach to a wait-and-watch or dose-attenuated cytoreductive treatment (2, 5, 11). CR after remission induction is normally short-lived in the elderly, and there is no established post-induction therapy for these patients (2, 5). For patients at least up to age 70 who reach CR, an option is reduced-intensity conditioning and SCT (6). Currently, several novel agents are under investigation for treatment in older AML patients, including clofarabine, decitabine, azactidine and tipifarnib (6). The overall survival probability for patients older than 60 years is around 10% 5 years from the diagnosis (5).

Patients that are not fit for intensive treatment because they are medically unfit or unlikely to benefit from treatment due to the nature of their disease have been treated with low-dose cytarabin, hydroxyurea, hypomethylating agents or supportive care (2, 5).

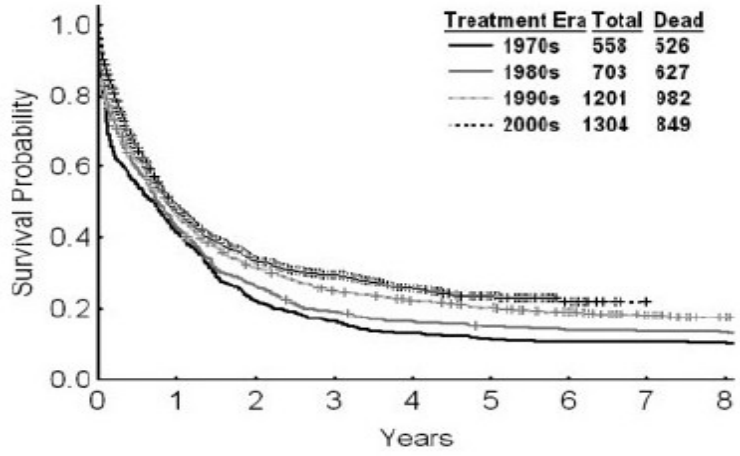

Figure 1.2: Overall AML survival in patients. Data from 3766 patients with newly diagnosed AML referred to the Leukaemia Department of the M.D. Anderson Cancer Center from 1973 to 2008. Picture from (13).

A 1975-2001 annual US report on cancer stated that AML remains a highly fatal malignancy (14). The 5-year relative survival was improved from 6% to 17% over 20 years, and this was stated to may be attributed in part to supportive care improvements (14). See Figure 1.2 for overall AML survival in different treatment eras.

The majority of AML patients will die from their disease. This warrants for the investigation of new and more effective treatment approaches. In the following section, the folate receptor is described as a target for drug delivery in AML.

1.1.2 The folate receptor and its role in AML targeted drug delivery

Vitamin B9 is a co-enzyme that occurs physiologically in reduced forms, of which folate is one (15, 16). Reduced folates have essential roles in one-carbon transfers and in biological methylation reactions (17, 18). At least three different transporters mediates cellular folate uptake (15, 17). The reduced folate carrier (RFC) is the predominant transporter, mediating transmembrane transport of 5-methyltetrahydrofolate and is expressed throughout development and in normal adult tissues (15, 17, 19). A proton-coupled high-affinity folate transporter has been shown to be the major transporter of folate under low pH conditions and for intestinal absorption of the vitamin (15, 17, 20). The third folate transporter is the folate receptor (FR), a high-affinity folate binding protein that binds folic acid (FA) as well as reduced folates, antifolates and folate conjugates (15, 16). Compared to the RFC, FRs have a more than 10^3 fold higher affinity for folate and have a highly restricted

expression among tissues (19). At least 4 isoforms of FRs exists; α, β, γ/γ' and δ, and the isoforms share 68 – 79% sequence identity (15, 16, 19). The α, β and δ isoforms are cell surface glycosyl phosphatidylinositol (GPI)-anchored membrane proteins, whereas γ/γ' isoforms are constitutively secreted (19). The literature to date has mostly been focused on FR-α and FR-β (19). FR-α and FR-β are N-glycosylated proteins with affinities for folic acid in the nanomolar range (Kd ~ 0.1 – 1 nM) (15, 19).

The expression of functional FR is low or absent in normal tissues (16, 19). The FR-α isoform is expressed in the luminal surface of polarised epithelial cells and also on epithelial cells in the kidney proximal tubules (15, 19). The epithelial cells have limited accessibility from the bloodstream, and larger folate conjugates, like nanocarriers, are not accessible to the kidneys due to their inability to be filtered through the glomerulus (15, 19).

The FR-β isoform is expressed in normal myelopoiesis and is a differentiation marker in the myelomonocytic lineage (15, 16, 19). It is also expressed in placenta (15, 16). The form of FR-β expressed in normal hematopoietic cells, however, is unable to bind to folate due to aberrant post-translational modifications (15, 19). The FR-β is also expressed in a functional form in activated macrophages associated with most inflammatory diseases (19, 21).

Otherwise, the FR-α and FR-β are selectively expressed in functional forms in several carcinomas (15). The FR-β is expressed in approximately 70% of AML cases and therefore most AML cells may be targeted by this receptor (15, 16, 19, 22). Considerations supporting the view that FR-β is a potentially valuable target in AML treatment are: the described expression pattern and the non-functionality of the receptor form expressed by normal hematopoietic cells, the accessibility of the target cells in the bone marrow and peripheral blood and finally the likeliness that engrafting leukaemia stem cells carry functional FR-β because of frequent co-expression with CD34 (15, 23). Leukaemia stem cells (LSCs) represent a rare population of AML cells capable of endless self-renewal, proliferation and differentiation into malignant blasts (24). LSCs are an important potential target for drug delivery, especially since cytarabine is ineffective against these cells (11).

FR has advantages as a target for cancer therapy in that the receptor binds tight and specifically to FA, a small, presumably non-immunogenic water soluble molecule that can be chemically conjugated to drug molecules or nanoparticles without disrupting its binding properties (15, 19). FRs in the cell membrane recycle between the cell surface and intracellular compartments, internalising receptor-bound folate conjugates by receptor-mediated endocytosis (15, 16, 19).

Targeted drug delivery effectiveness is limited by FR abundance on the target cell surface (19). FR expression in vitro is most often absent in cell lines derived from established FR-expressing malignant tissues (16). FR expression can be up-regulated in a variety of cells by

lowering the extracellular folate concentration (16). FR-β can be up-regulated by treatment with all-trans retinoic acid (ATRA) and other retinoid nuclear receptor agonists (15, 16, 22, 23).

Conjugation of FA to liposomes has been successfully conducted and shown increased efficacy in FR-expressing cells compared to plain or PEGylated liposomes in several in vitro studies (22, 23, 25-29). AML cells have been targeted by PEG-FA-conjugated liposomes, showing increased in vitro cytotoxicity compared to PEG-conjugated liposomes and also targeting of AML clonogenic cells (LSCs) through the FR-β (22, 23). PEG-FA-conjugated liposomes were also demonstrated to prolong animal survival in in vivo studies (23). FA-conjugated liposomes have been suggested to be internalised in FR-β expressing AML cells by receptor-mediated endocytosis (23).

1.2 Prostate cancer and the PSMA

1.2.1 Prostate cancer: Disease characteristics and treatment strategies

Most prostate cancers are adenocarcinoma, i.e. of prostatic glandular origin, although occasionally other forms of cancer can arise within the prostate such as transitional cell and small cell carcinomas (30, 31). Both genetic and physiological factors contribute to the development of prostate cancer, which contributes to a heterogenic nature of the disease (30). Diagnosis of prostate cancer is based on clinical, biochemical, radiological and histological grounds (30). Histopathology can provide important prognostic information guiding patient management, most importantly by grading the tumour (30). The Gleason system is used to grade prostatic adenocarcinoma based on architectural features (30). Prostate cancer is also categorised according to stage using the TNM (Tumour, lymph Nodes, Metastasis) system (31).

Prostate cancer is the most commonly diagnosed cancer in American and Norwegian men, with approximately 200000 and 4300 new cases in 2009, respectively, and is the second leading cause of male cancer death in these countries (32-34). The incidence increases rapidly with age (33). Introduction of the test for prostate-specific antigen (PSA) has led to earlier detection of the disease, and the serum PSA level and velocity provides prognostic information (14, 31). However, concerns have been risen regarding the prevalence of prostate cancer overdiagnosis due to PSA screening; assigning diagnosis to men who would not suffer from reduced quantity or quality of life if the cancer was never detected (35). The majority of men are now diagnosed with localised disease (30, 35, 36). Early prostate cancer is invariably asymptomatic, whereas advanced disease can

present with local or distant symptoms such as obstructive lower urinary tract symptoms, haematuria or haematospermia, pain, erectile dysfunction, bone pain, pathological fracture, anaemia, oedema or hypercalcaemia (30). Metastatic prostate cancer is most commonly located in bone (30). A significant number of men diagnosed with prostate cancer will experience relapse, requiring surveillance and therapy (36). The focus in this thesis is on advanced prostate cancers.

Prostate cancer has different treatment strategies depending on whether the disease is localised or metastatic. Active surveillance is a management option for selected low-risk patients (30, 35, 37). Localised early disease is treated with surgical removal of the prostate, i.e. radical prostatectomy, radiotherapy (prostate brachytherapy) or high-intensity focused ultrasound (30, 31). Radical prostatectomy is also used in selected cases of locally advanced disease (30). Cryotherapy is used to treat prostate confined, locally advanced disease and for salvage after failed radiotherapy (30).

Advanced disease is primarily treated with hormonal therapy; relieving symptoms and delaying progression (30, 31, 36, 38). Hormonal therapy is also used in earlier stages of the disease, adjuvant and neo-adjuvant to radiotherapy (30, 31, 39). Different types of hormonal therapy are androgen deprivation therapy (ADT) and treatment with antiandrogens (22). ADT targets testicular Leydig cell testosterone production, and can be achieved surgically by castration or medically through manipulation of the hypothalamic-pitituary-testicular axis (31, 36, 38). As the disease progresses, however, the tumour can become resistant to testosterone depletion with proliferation of androgen-independent cells (30, 36, 39). Other hormone manipulations, such as antiandrogens, oestrogens and steroids, can be added sequentially at this stage, but the response is often short-lived (30, 36). Hormonal therapy is associated with numerous side-effects, including erectile dysfunction, reduced libido, hot flushes, osteoporosis, reduced muscle mass, breast swelling and mastalgia, weight gain, lethargy, anaemia, mood swings, depression and metabolic complications (30, 36, 38, 39).

Patients with castrate-resistant cancers have a generally poor survival (30). Chemotherapy with docetaxel is the mainstay treatment for these patients who have metastatic or progressive disease, and can improve survival for some (30, 36). Docetaxel is a taxane promoting microtubuli polymerisation and inhibiting microtubuli disassembly (27). Zoledronic acid, a bisphosphonate, is used for the treatment of bone metastases in patients with castrate-resistant cancers (27). Radiation therapy is used for palliation of symptoms from metastatic disease (36).

A number of new prostate cancer agents are available on the market or undergoing clinical trials (36). Three new therapies recently gained FDA approval for castration-resistant prostate cancer: sipuleucel-T (Provenge), cabazitaxel (Jevtana) and abiraterone acetate (Zytiga) (40). Other

novel prostate cancer drugs are in late-stage developments (40).

A 1975-2001 annual US report on cancer stated that the 5-year survival rate for prostate cancer increased significantly from 70% in the 70s to 99% between 1995 – 2000 (14). Both PSA-related early detection and improved treatments was believed to have contributed to this decrease in mortality (14).

Still, prostate cancer is the leading cause of cancer and the second leading cause of cancer death in men, and this warrants the search for new and effective treatment strategies. ADT, the mainstay treatment of choice for advanced prostate cancer, has effect for a limited period of time and is associated with serious side-effects. Active targeting strategies have the potential of reducing side-effects by limiting treatment to cancer cells. The disease-specific prostate-specific membrane antigen (PSMA) will be described in the next section as a goal for targeted drug delivery.

1.2.2 The prostate-specific membrane antigen (PSMA): role in prostate cancer and targeting strategies for drug delivery

Prostate-specific membrane antigen (PSMA) is a type II membrane glycoprotein that is over-expressed in all stages of prostate cancer (32, 33, 41-43). The PSMA is expressed in the secretory epithelial cells of the normal prostate, and also at lower levels in the spine, brain, peripheral nervous system, kidney, striated muscle, small intestine, colon and the salivary gland (33, 43). It is also expressed in endothelial cells of the neovasculature in virtually all solid tumours, but not in neovasculature associated with normal tissues (33, 43). PSMA expression is suppressed by androgens (23).

PSMA exists in at least three variants due to alternative splicing, but the implication of these splice variants in prostate cancer is not known (41). The protein exhibits two unique enzymatic functions: NAALADase activity and folate hydrolase activity (33, 41, 42). The folate hydrolase activity will be the focus is this thesis. PSMA folate hydrolase activity catalyses cleavage of the terminal glutamates from γ-linked poly-glutamates (41, 42).

PSMA expression in prostate cancer tissues correlates with the stage of the disease, the Gleason score, is higher in hormone-refractory cancers and has been shown to be an independent marker of disease recurrence (32, 33). As prostate cells become cancerous, more membrane bound PSMA is expressed and the folate hydrolase activity is increased (32). The prostate has an especially high folate requirement and at physiologically relevant folate levels, it has been shown that PSMA offers a growth advantage for prostate cancer cells (32). This can be due to that PSMA converts the extracellular poly-γ-glutamated folate to non-glutamated folate that can be taken up by

cells (32). PSMA expression has also been shown to significantly increase cellular uptake of folic acid under low folate conditions (32).

PSMA undergoes internalisation constitutively through clathrin-coated pits (32, 41, 43). Monoclonal antibody – PSMA complex formation often results in internalisation resembling receptor-mediated endocytosis (41). It is proposed that since PSMA internalises folates, it may have some transport property for it that is not yet fully understood (32, 41). PSMA could possibly bind and transport folates into the cell, potentially implicating it as a novel folate receptor (32). PSMA's internalisation function and regulation can be exploited in cancer therapeutics, allowing for a targeted therapy approach (41).

PSMA represents an excellent target for prostate cancer imaging and therapy, being a cell surface protein expressed in thousand-fold greater levels in cancer compared to normal tissues (41). PSMA is also over-expressed in neovasculature of most solid tumours and plays an important role in angiogenesis, making it a possible goal for targeted vasculotoxic therapy of solid cancers as well (32, 41, 43). The focus in this thesis is PSMA as a target in prostate cancer therapy.

PSMA-specific antibodies have been developed for targeted drug delivery; anti-PSMA radiotherapy and anti-PSMA immunotoxins (43). Docetaxel-encapsulated aptamer-conjugated nanoparticles have been developed that bind to and are taken up by PSMA-expressing LNCaP cells (25). Also, bispecific antibodies re-targeting immune cells to PSMA-expressing cells and PSMA vaccines have been developed, utilising PSMA as a target for cancer therapy (43).

Targeting PSMA for drug delivery may be particularly useful in metastatic prostate cancer, where new and targeted approaches are needed to improve survival.

1.3 Nanocarriers

Drug delivery systems are developed for three main reasons: protecting the drug against inactivation, protecting healthy tissues from the drug and favourably changing and controlling drug pharmacokinetics (44). In this section, nanocarriers in general and liposomes especially are described as drug delivery systems for anticancer therapeutics.

1.3.1 Nanomedicine: Background information and advantages of the use of drug delivery nanosystems in cancer therapy

Nanotechnology concerns the study of man-made devices that are in the 1-1000 nm range in at least

one dimension (45). Pharmaceutical nanotechnologies are usually defined as nanomedicine (44).

Nanoparticles are engineered and constructed systems in the nanometer size range that can be used as vehicles for drug delivery (46). Examples of nanoparticles for drug delivery – also called nanocarriers – are dendrimers, micelles, polymeric nanoparticles, nanocapsules, fullerenes, nanotubes and liposomes (46, 47). Liposomes are described in section 1.3.2.

Nanocarriers possess the advantages of high drug-loading capacity and prolonged circulation times (47). The encapsulated drug is protected from degradation, and at the same time side effects can be reduced by focused delivery of the drug (45, 48). Limitations of the drug can also be addressed by use of nanocarriers, including poor aqueous solubility, low bioavailabilty and unfavourable pharmacokinetic properties such as rapid elimination by the kidneys (47).

Delivery of anticancer therapeutics from nanoparticles can be categorised as passive or active (46, 47). Passive targeting refers to selective transport through tumour vasculature and subsequent retention of the nanoparticles (46, 47). This effect rises from abnormality of tumour vessels; tumour endothelial cells have gaps in between them ranging from 100 to 780 nm that allows nanoparticles to extravasate into the tumour (46). In comparison, normal vessels have tight endothelial junctions typically of a 5 to 10 nm size (46). Also, tumours lack effective lymphatic drainage that can cause extended retention times for the nanoparticles (46, 49). This is termed the enhanced permeability and retention (EPR) effect (46, 49).

Active targeting refers to drug delivery based on molecular interactions between the nanoparticle and the target cell, providing enhanced selectivity (44-46). Examples of commonly used receptor targets for nanocarriers are the folate receptor (FR), the vascular endothelial growth factor (VEGF) receptor, the transferrin receptor and the CD20 antigen (47). The targeting ligand, which can be an antibody, an engineered protein, an aptamer or a peptide, can be coupled to the nanocarrier by physical interaction or chemical conjugation (47). Active targeting strategies may trigger receptor-mediated endocytosis, which promotes internalisation of nanocarriers (47). It has also shown the potential of suppressing multidrug resistance (MDR) via bypassing P-gp-mediated drug efflux (29, 47).

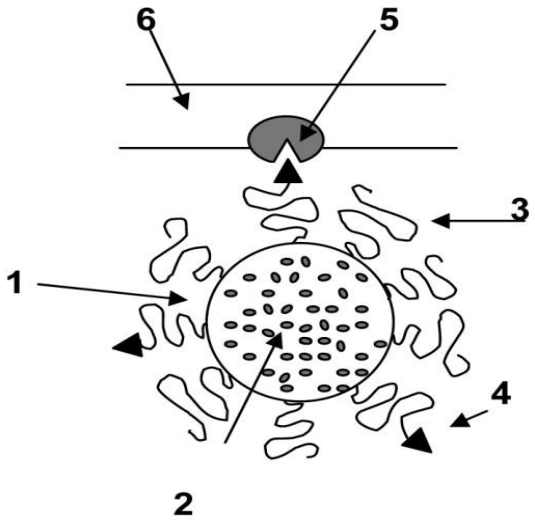

Figure 1.3: Multifunctional nanocarrier. 1: nanocarrier, 2: drugs, 3: sterically protecting polymer (PEG), 4: targeting ligand (such as FA), 5: specific receptor (such as FR) targeted with the ligand, 6: cell membrane. Picture from (50).

Multifunctional nanocarriers are nanoparticles with several integrated properties, such as drug or imaging agent delivery, targetability, prolonged circulation, PEGylation (see section 1.3.2) and stimuli-sensitivity (44, 47).

1.3.2 Liposomes as drug delivery vehicles in cancer therapy

Liposomes are vesicles with phospholipid bilayer membrane structures and sizes from approximately 50 – 1000 nm in diameter (44, 48, 51). The phospholipids form bilayers in aqueous solutions due to their amphipathic nature, thereby lowering the energy of the system (48). The resulting lipid membrane has a very low permeability for ions and polar molecules, while water molecules traverse quite easily (48).

Liposomes have a compartmental structure enabling them to function as a storage and drug carrier, protecting its contents from degradation (48). Hydrophilic drugs can be encapsulated in the aqueous core of liposomes (52). The hydrophobic membrane prevents leakage of hydrophilic substances from the aqueous core, and it can also encapsulate hydrophobic drugs (52). Liposomes are considered biocompatible and biodegradable due to their lipidic composition (48, 51).

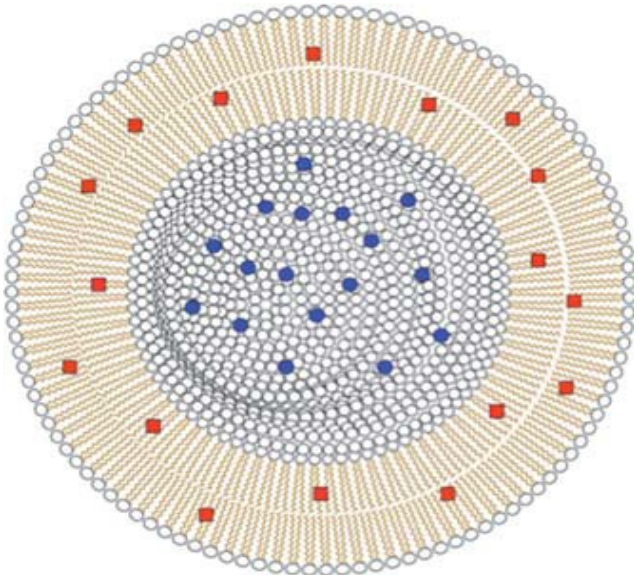

Figure 1.4: Liposome structure. Hydrophilic drugs (blue) encapsulated in the aqueous core and lipophilic drugs (red) encapsulated in the lipid bilayer. Picture from (53).

To increase the stability of liposomes in a physiological environment, cholesterol can be incorporated into the phospholipid bilayer (44, 48). Then the lipids become more densely packed and the membrane is rigidified by cholesterol aligning in the hydrophobic core (48).

Pharmacokinetic properties of liposomes are important parameters, because the drug will adopt the pharmacokinetic disposition from its carrier until they are released from it (44, 48). Hence, liposomes can change the tissue distribution and the clearance rate of the drug (48). The pharmacokinetic behaviour of liposomes depends on physiochemical properties such as size, surface charge, membrane lipid packing, steric stabilisation and route of administration (44, 48). A liposome size of 80 to 200 nm is considered to give a satisfactory reservoir capacity and at the same time having an adequate bioavailability – larger particles are eliminated more rapidly by the mononuclear phagocyte system (MPS) (48).

Elimination of liposomes takes place by escape of the drug from circulating liposomes, local metabolic elimination in tumour tissues and by the mononuclear phagocyte system (MPS) (48). Conventional liposomes and other nanocarriers undergo rapid elimination from the blood by the MPS (44, 48). Plasma proteins are absorbed onto the liposomal membrane, causing opsonisation and recognition by the cells of the MPS, and finally accumulation in the liver and metabolism by specialised Kuppfer cells (48). To slow down the MPS recognition of liposomes, polyethylene glycol (PEG) chains can be attached to the membrane surface, creating long-circulating liposomes

(44, 54, 55). PEG is a biocompatible, non-toxic and highly soluble polymer that causes very low stimulation of the immune system (44, 48). The flexible polymeric chains form a sterically protective hydrophilic film over the surface that also improves formulation stability by preventing liposomes from aggregating (44, 48). Liposomes have a tendency to aggregate and fuse if the resultant of electrostatic interactions, steric properties and hydration forces allow it (48). Compared to conventional liposomes, PEGylated liposomes have a longer half-life, an improved tissue distribution by avoiding accumulation in healthy tissues, low systemic plasma clearance, low volume of distribution and greater Area Under Curve (AUC) values (48). Sometimes however, PEGylated liposomes can experience difficulty in releasing the drug and killing tumour cells (51).

The drug can be delivered from liposomes to target cells by one or several of the following mechanisms: absorption of liposomes on the cell membrane, fusion of liposomes with the cell membrane, receptor-mediated endocytosis (particle size <150 nm in diameter) or transfer of the drug from the liposomes to plasma lipoproteins (48). Receptor-mediated endocytosis by ligand attachment of liposomes increases intracellular drug levels, but the endocytosed material is subjected to lysosomal degradation, which can result in reduced biological activity (51).

In summary, liposomes serve as an attractive drug delivery system for anticancer drugs due to increasing drug solubility, elongation of circulation times and focused delivery of the drug (48). Passive and active targeting strategies can be applied to liposomes, as described in section 1.3.1. Folic acid (FA) can be conjugated to liposomes and as a targeting ligand it has advantages of simple conjugation chemistry, non-immunogenicity and low cost (47). FA-conjugated liposomes have been shown to facilitate cancer-specific drug delivery (47).

By encapsulation in liposomes, the therapeutic index of the drug is improved and multidrug resistance can be bypassed (48). Liposomes are well tolerated and have a similar structure to biological membranes that makes them less likely to be accumulated in the body over long time, which is a concern for many other nanocarriers (48).

Liposomes were first discovered in 1961, and today several liposomal formulations are available in the market or undergoing clinical trials (44, 48). Examples of liposomal formulations in clinical use today are Caelyx® (PEGylated liposomal doxorubicin), DaunoXome® (liposomal daunorubicin) and Myocet® (liposomal doxorubicin) (44, 46).

1.4 Daunorubicin (DNR) and emetin (EME): choice of drugs for encapsulation in multifunctional liposomes

Anthracyclines, with doxorubicin (DOX) and daunorubicin (DNR) first isolated from *Streptomyces peucetius* in the 1960s, remain among the most effective anticancer drugs developed (56). The anticancer mechanism of action of anthracyclines is still a controversial matter, and the mode of action seems to be concentration-dependent (56). The following mechanisms have been suggested: DNA intercalation, generation of free radicals causing DNA damage or lipid peroxidation, DNA binding and alkylation, cross-linking of DNA, interference with DNA unwinding/strand separation and helicase activity, direct membrane effects and topoisomerase II inhibition initiating DNA damage or inducing apoptosis (56).

DNR has activity against AML, and has been used as a part of standard AML treatment for several decades (11, 56). However, the clinical use of DNR faces serious challenges such as resistance development in cancer cells and toxicity in healthy tissues (56). Anthracycline treatment is most notably associated with a dose-dependent cardiotoxicity in the form of chronic cardiomyopathy and congestive heart failure (56). Tumour-targeted nanocarriers have been developed for improving the efficacy and cardiac safety of currently approved anthracyclines (56-58).

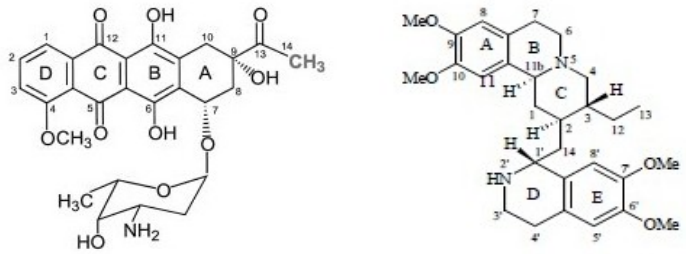

Figure 1.5: Chemical structure of DNR and EME. Picture of DNR from (56) *to the left, picture of EME from* (59) *to the right.*

On the basis of the work performed by Gausdal et al. (60), it was decided to investigate a potential synergism between DNR and a protein synthesis inhibitor. Gausdal et al. demonstrated a synergistic effect of cycloheximide (CHX) and DNR in several AML cell lines in vitro and also in in vivo experiments (60). In this thesis, emetin (EME) was chosen as protein synthesis inhibitor on the basis of its isoelectric point, which is quite similar to that of DNR (Figure 1.6). Also, unlike CHX, EME has approval for use in humans (61) and has been studied in both animals and humans

and therefore has a shorter way towards regulatory approval (62, 63). Hence, EME offers a shorter way towards clinical use compared to CHX, and it is more likely that EME treatment can be approved. A potential synergism of DNR and EME offers possibilities for improved therapeutic outcome in AML, a highly fatal malignancy. The drugs were to be combined in a single, multifunctional PEG-FA-conjugated liposome, reducing drug toxicity and targeting cancer cells specifically.

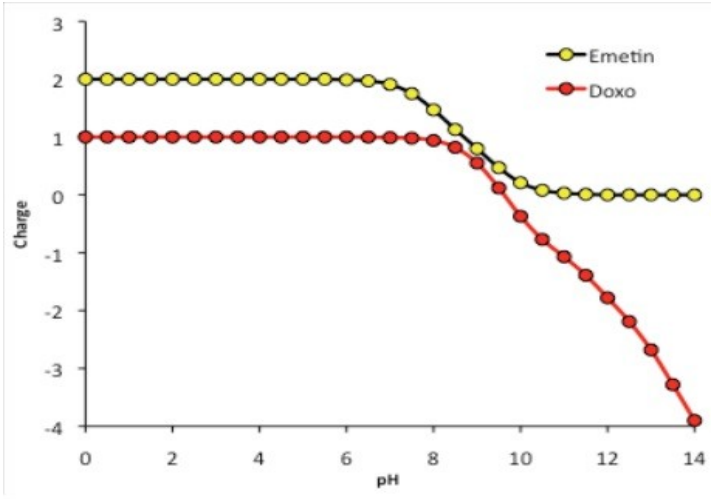

Figure 1.6: Charge - pH relationship of EME and DOX (unpublished data from Lars Herfindal). The isoelectric point for DOX and DNR is identical, pH 9.1 (Herfindal, 2011, unpublished data). The isoelectric point of the drugs is exploited in the acid precipitation method drug loading of liposomes, as described in section 3.5.1.

EME is an alkaloid, found in *Psychotria ipecacuanha* (59, 64). The earliest use of ipecac in traditional medicine was as an emetic and expectorant (59). EME has been used extensively as an antiparasitic drug against amoebiasis and amoebic dysentry caused by *Entamoeba histolytica,* but its use was discouraged due to excessive toxicity (59, 64). EME is a protein, DNA and RNA synthesis inhibitor, and it has antiviral and anticancer activities (59). It has proved to exhibit cytotoxity in several cancer cell lines, including different leukaemia cell lines, and the cytotoxic mechanism is considered to be caused by protein synthesis inhibition and DNA interaction (59). Recently, it has been shown that EME is a substrate of P-gp, offering a potential use of overcoming multidrug resistance in cancer therapy (59, 65). Studies have been performed combining EME with other therapeutic agents in cancer drug discovery research (59). An additive effect was observed when EME was combined with doxorubicin in human neuroendocrine tumour cell lines (65). EME was combined with cisplatin in a leukaemia cell line (Jurkat T-cells) in vitro, enhancing apoptosis in

an additive but synergistic fashion, and also showing that emetine itself was a powerful inducer of apoptosis in leukaemia cells (64). The medical use of EME has been discouraged due to its toxicity, and chronic usage has been associated with myopathy and cardiotoxicity (59).

1.5 Aim of study

The aim of this study was to synthesise FA-conjugated and PEGylated liposomes for investigation of targeted drug delivery to FA-expressing AML cell lines and PSMA-expressing prostate cancer cell lines. PEGylated (PEG-conjugated) liposomes were synthesised to compare the effect of targeted and non-targeted liposomes. PEGylated and FA-conjugated (PEG-FA-conjugated) liposomes have previously been shown to give an increased anticancer efficacy in FA-expressing cell lines compared to PEG-conjugated liposomes (22, 23, 25, 26).

The liposomes were made using hydrogenated egg phosphatidylcholine and cholesterol to create a reinforced lipid bilayer with a relatively high lipid transition temperature (60°C) to improve physiological stability. DSPE-PEG was incorporated to slow down MPS recognition of liposomes and finally, DSPE-PEG-FA was incorporated to target liposomes to FR on AML cells, or to prostate cancer cells expressing PSMA. DNR and EME were chosen as drugs for incorporation in the liposomes, as described in section 1.4.

The main focus in this thesis was on AML, with MOLM-13 as the cell line of investigation. We wanted to validate the expression of FR-β in this cell line, and to see if it indeed could be used as a target for drug delivery by FA-conjugated multifunctional liposomes. As mentioned in section 1.1.1, AML remains a highly fatal malignancy and there is a need for developing more effective therapeutics. Liposomal targeted drug delivery via FR offers a possibility of improving therapeutic outcomes, reducing mortality and reducing side-effects. Combining DNR and EME in a single multifunctional liposome would offer a new approach in the treatment of AML, and the synergistic effect of these drugs was to be investigated.

On the basis of promising results using multifunctional liposomes in the PSMA-expressing prostate cancer cell line LNCaP (41), obtained by Herfindal in 2011 (unpublished data), it was decided to perform experiments in this cell line as well. PSMA represents a target for drug delivery, and we wanted to investigate if its function as a folate hydrolase could be exploited by FA-conjugated liposomes. The LNCaP cell line is p53 positive, and the PC-3 prostate cancer cell line was included due to its status as p53 deficient (66) to investigate a potential synergism between DNR and EME. p53 deficient cells have been shown to be particularly sensitive towards the

combination of DNR and a protein synthesis inhibitor (unpublished data, Gausdal) (60). The PC-3 cell line was to be transiently transfected with PSMA to investigate if this expression led to higher efficacy of the FA-conjugated liposomes. DNR and EME were used as the liposomal drugs in these cell lines as well, offering a potentially new treatment for prostate cancer. The synergistic effect of DNR and EME was investigated in these cell lines as well.

2. Materials

2.1 Cell lines

Cell line	ATCC® number	Supplier
HEK293	CRL-1573	American Type Culture Collection (ATCC)
LNCaP	CRL-1740	American Type Culture Collection (ATCC)
MOLM-13 (wt original)		Supplied by prof. Bjørn Tore Gjertsen, Univ. Bergen Origin of the cell line described by (9).
MOLM-13 SH p53 (silenced p53)		Produced at TSG, Univ. Bergen
MV4-11	CRL-9591	American Type Culture Collection (ATCC)
NRK	CRL-1570	American Type Culture Collection (ATCC)
PC-3	CRL-1435	American Type Culture Collection (ATCC)

2.2 Materials used in cell culture

Material	Catalogue number	Supplier
BisBenzimide H33342 trihydrochloride (Hoechst)	B2261-100MG	Sigma-Aldrich
Cell proliferation Reagent WST-1	11644807001	Roche
Dulbecco's modified eagles medium 10x without folic acid with L-glutamine and $NaHCO_3$	D2429	Sigma-Aldrich
Dulbecco's Modified Eagle's Medium with glucose/L, L-glutamine, $NaHCO_3$, pyridoxine HCl	D5796	Sigma-Aldrich
Fetal bovine serum (FBS) Standard quality	A15-101	PAA Laboratories GmbH
Iscove's Modified Dulbecco's Medium	I3390	Sigma-Aldrich
Penicillin-Streptomycin	P0781-100ML	Sigma-Aldrich
Plasmids: PSMA-encoding DNA plasmids GFP-encoding DNA plasmids		Supplied by prof. Dean Bacich, Univ. Pittsburgh (PSMA) and prof. James Lorens, Univ.

Empty vector DNA plasmids		Bergen
RPMI-1640 medium with L-glutamine and $NaHCO_3$	R8758	Sigma-Aldrich
Trypsin 1:250	T-0646	Sigma-Aldrich

2.3 Liposome materials

Material	**Catalogue number**	**Supplier**
Cholesterol	C8667-5G	Sigma-Aldrich
DSPE-PEG-FA (1,2-disteraoyl-sn-glycero-3-phosphoetanolamine-N-((polyethylene glycol-5000)folate) (ammonium salt) (Reconstituted in 5 ml ethanol)	880123P	Avanti® Polar Lipids
Hydrogenated Egg Phosphatidyl Choline (HEPC)	E PC-3	Lipoid
DSPE-PEG (1,2-Disteraoyl-sn-glycero-3-Phosphoetanolamine-N-[Methoxy(Polyethylene glycol)-2000]) (ammonium salt)	880120P	Avanti® Polar Lipids
Texas Red® DHPE (Texas Red® 1,2 Dihexadecanoyl-*sn*-Glycero-3-Phosphoethanolamine, Triethyl ammonium salt)	T1395MP	Invitrogen

2.4 Drugs

Material	**Catalogue number**	**Supplier**
Cerubidin® 20 mg, daunorubicin (Reconstituted in 5 ml milli Q water)	01 74 59	Sanofi Aventis
Emetine dihydrochloride hydrate	E-2375	Sigma-Aldrich

2.5 Antibodies

Material	**Catalogue number**	**Supplier**
Anti-beta actin antibody [AC-15]	ab6276	Abcam
Anti-FOLR2, 500 µg/mL	ab56067	Abcam

Anti-mouse IgG (whole molecule) alkaline phosphatase produced in goat	A3562-.5ML	Sigma-Aldrich
Anti-PSMA (C-terminal) polyclonal antibody, 0,25 mg/ml	AB10614	Millipore
Anti-rabbit IgG (whole molecule) alkaline phosphatase conjugate antibody developed in goat	A-3687	Sigma-Aldrich

2.6 Phosphatidylcholine Assay Kit ingredients

The Phosphatidylcholine Assay Kit, catalogue number 10009926, was provided by Cayman Chemical Company.

PC buffer, 30 ml
3 ml PC buffer concentrate, cat.no 10010066, final buffer of
  50 mM Tris-HCl, pH 8.0
  0.66 mM $CaCl_2$
27 ml milli Q water
PC colour detector, 3 ml
PC colour detector, cat.no 10010067, lyophilised powder of
  DAOS (N-ethyl-N-(2-hydroxy-3-sulfopropyl)-3,5-dimethoxyaniline)
  4-aminoantipyrine
3 ml PC buffer
PC enzyme mixture, 1 ml
PC enzyme mixture, cat.no 10010068, lyophilised powder of
  choline oxidase
  horseradish peroxidase
1 ml PC buffer
PC-specific PLD, cat.no 10010069, containing a solution of
phosphatidylcholine-specific phospholipase D
Phosphatidylcholine Standard, 1 ml
Phosphatidylcholine Standard, cat.no 10010070, lyophilised powder of
  phosphatidylcholine
1 ml detergent solution
Phosphatidylcholine Stock Standard 200 mg/dl, 1.5 ml
200 µl Phosphatidylcholine Standard
1.3 ml detergent solution
PC detergent solution, cat.no 10010071, containing a solution of
triton X-100

2.7 Reagents and chemicals

Material	**Catalogue number**	**Supplier**
30% Acrylamide/Bis solution	151-0158	Bio-Rad Laboratories
Ammonium persulfate (APS)	161-0700	BioRad

Ammonium sulphate	1.01217.1000	Merck
Bromophenol blue (BFB)	80-1129-15	Pharmacia
Calcium chloride dihydrate ($CaCl_2 \cdot 2H_2O$)	2382	Merck
CDP-star®	MSC100	Tropix
Chloroform ($CHCl_3$)	2447	Merck
Chloroquine	C-6628	Sigma-Aldrich
Complete Mini	11836153001	Roche
Deoxycholic acid (NaDOC)	D-2510	Sigma-Aldrich
Diethanolamine (DEA)	D8885-500G	Sigma-Aldrich
Dimethyl sulphoxide (DMSO)	D2650	Sigma-Aldrich
1,4 Dithioerythritol (DTE)	1.24511.0025	Merck
Ethanol absolute	32221-2,5L	Sigma-Aldrich
Ethylene dinitril tetraacetic acid (EDTA) disodium salt dihydrate	1.12029.1000	Merck
Formaldehyde solution min. 37%	1.04003	Merck
D (+) Glucose	24371.264	VWR International
L-Glutamine, non-animal source	G8540-100G	Sigma-Aldrich
Glycerol about 80%	1.04094.1000	Merck
Glycine ($C_2H_5NO_2$)	8.16013.1000	Merck
Hepes sodium salt	H7006	Sigma-Aldrich
I-block ™	A1300	Tropix
Isobutanol	1.00984.1000	Merck
Lipofectamine™ 2000	11668-027	Invitrogen
Magnesium chloride hexahydrate ($MgCl_2 \cdot 6H_2O$)	31413	Sigma-Aldrich
Methanol (CH_4O)	24229-2.5L-R	Sigma-Aldrich
Nitro-Block II ™	T2184	Applied Biosystems
Nitrogen (N_2) for lipid extrusion	7727-37-9	Yara
Nonidet P-40 (NP-40)	74385	Fluka
Phenol Red solution 0.5% in DPBS	P-0290	Sigma-Aldrich
Potassium Chloride (KCl)	1.04936.1000	Merck KGaA
Potassium dihydrogen phosphate (KH_2PO_4)	1.04873.1000	Merck

Precision Plus Protein® All Blue Standards	161-0373	BioRad
Protein Assay Dye Reagent Concentrate	500-0006	BioRad Laboratories
Protein standard II Bovine Serum Albumin (BSA)	500-007	BioRad
Re-Blot Plus Strong Solution 10x	2504	Millipore
Sephadex ™ G-25 Medium	17-0033-01	Amersham Biosciences
Sodium azide (NaN_3)	S8032-25G	Sigma-Aldrich
Sodium chloride (NaCl)	1.06404.1000	Merck
Sodium dodecyl sulphate (SDS)	L5750-500G	Sigma-Aldrich
Sodium hydrogen carbonate ($NaHCO_3$)	1.06329.1000	Merck
di-Sodium hydrogen phosphate dihydrate ($Na_2HPO_4 \cdot 2H_2O$)	1.06580.1000	Merck
Sucrose	1.7660-3	BDH AnalaR Kebo Lab AB
N, N, N', N'-Tetramethylethylenediamine (TEMED)	T9281	Sigma-Aldrich
Tris (hydroxymethyl) - aminomethane	1.08382.2500	Merck KGaA
Tween® 20	P5927-500ML	Sigma-Aldrich

2.8 Technical equipment and instruments

Name	**Supplier**
Cary quarts cuvette	Starna®
Cell counting chamber 0.100 mm depth	Bürker
Econo-Columns®: 1.5x15 cm and 0.7x10 cm	BioRad
LIPEX™ extruder	Northern Lipids
Pellet pestle® homogeniser	Kontes
SDS-PAGE gel electrophoresis and Western blotting equipment	BioRad
Instruments:	
Axiovert 200M Fluorescence/Live cell imaging microscope	Zeiss
Balances	Mettler Toledo
C6 flow cytometer	Accuri®
CKX31 microscope	Olympus

Electrophoresis power supply EPS 301	Amersham pharmacia biotech
HAAKE C10-K10 Heating circulator	Thermo electron corporation
Holten Lamin Air Safety bench/Lab hood (vevskultur)	Holten
Labofuge 400 centrifuge	Heraeus
LAS 3000 imager	Fujifilm
Locator 8 plus Cryo Biological storage system	Thermolyne®
Membrane vacuum pump MZ 2C	Vacuubrand
Microcentrifuge Biofuge Fresco	Heraeus
Milli-Q® integral water purification system: For the making of Milli Q (MQ) water	Millipore
Mini Centrifuge	Costar®
MS2 Minishaker	IKA®
Peristaltic pump XX80 202 30	Millipore
RCT basic magnetic stirrer hotplate	IKA Labortechnik
Rotary Evaporator Laborota 4000	Heidolph instruments
Steri – Cycle CO_2 Incubator	Thermo Forma
Swip shaker	Edmund Bühler
UVM 340 microplate spectrophotometer	ASYS
UV-visible spectrophotometer	Varian Cary
Vario Vacuum pump	Vacuubrand
Zetasizer Nanoseries Nano-ZS	Malvern Instruments Nordic

2.9 Computer software

Name	**Supplier**
AxioVision	Carl Zeiss
Cary Win UV	Agilent Technologies
DigiRead	Asys
FlowJo	TreeStar
Image Reader LAS-3000	FUJIFILM
ScanPlus	Asys
Zetasizer software	Malvern

2.10 Solutions, buffers, media

Cell culturing:
RPMI-1640 cell medium with L-glutamine and $NaHCO_3$
500 ml RPMI-1640 added 50 ml FBS and 5 ml Penicillin/Streptomycin (final 100 IU/ml penicillin

and 100 µg/ml streptomycin)
Dulbecco's Modified Eagle's Medium (DMEM)
500 ml Dulbecco's Modified Eagles Medium added 50 ml FBS and 5 ml Penicillin/Streptomycin (final 100 IU/ml penicillin and 100 µg/ml streptomycin)
Dulbecco's Modified Eagles Medium (DMEM) without folic acid
50 ml Dulbecco's Modified Eagles Medium 10x added 450 ml milli Q water, 0.15 g L-glutamine, 1.0 g sodium bicarbonate NaHCO3, sterile filtered at 0.2 µm then added 50 ml FBS and 5 ml Penicillin/Streptomycin (final 100 IU/ml penicillin and 100 µg/ml streptomycin)
Iscove's Modified Dulbecco's Medium (IMDM)
500 ml Iscove's Modified Dulbecco's Medium added 50 ml FBS and 5 ml Penicillin/Streptomycin (final 100 IU/ml penicillin and 100 µg/ml streptomycin)
1xPhosphate Buffered Saline (PBS), 500 ml
0.1 g KCl, 0.1 g KH_2PO_4, 0.675 g $Na_2HPO_4 \cdot 2H_2O$, 4 g NaCl and 450 ml milli Q water. pH adjusted to 7.4 using 1M NaOH, volume adjusted to 500 ml and the solution was autoclaved
Trypsin-EDTA, 200 mL
40 mg EDTA disodium salt, 200 mg Glucose, 80 mg KCl, 1600 mg NaCl, 0.4 mg Phenol red solution, 116 mg $NaHCO_3$, 100 mg trypsin. Milli Q water added to a total of 200 mL. The solution was sterile filtered.
2xHEPES buffer for transfection 500 ml
8.0 g NaCl, 6.5 g Hepes sodium salt and 5.25 g Na_2HPO_4 dissolved in 500 ml milli Q water. pH adjusted to 7
4% FIX solution, 500 ml
54 ml Formaldehyde solution 37%, 446 ml PBS. pH adjusted to 7.4 by NaOH or HCl
FIX solution with DNR 0.1 µg/ml 50 ml
50 ml 4% FIX solution added 10 µl Cerubidin® daunorubicin 5 mg/ml

Western blotting:
RIPA buffer with Complete, 100 ml
1 ml NP-40, 0.5 ml SDS 10%, 0.5 g Na DOC, 0.606 g Tris, 0.876 g NaCl, 2 Complete Mini tablets. Milli Q water added to a total volume of 100 ml.
20% SDS, 1 l
200 g SDS, milli Q water added to a total volume of 1 l
0.5 M Tris-HCl, 500 ml
30.29 g Tris. Water added to a total volume of 500 ml and the pH of the solution adjusted to 6.8 using HCl
1.0 M Tris-HCl, 1 l
121.14 g Tris. Water added to a total volume of 1 l and the pH of the solution adjusted to 8.7 using HCl
5xSDS sample buffer, 1ml
6.25 ml 20% SDS, 14.35 ml Glycerol. Bromophenol blue added until the solution was blue, then added 965 mg DTE and 3.0 ml 0.5 M Tris-HCl pH ~ 6.8. Milli Q water added to a total volume of 1 ml
5x Running buffer, 5 l
151.2 g Tris, 720 g Glycine, 125 ml 20% SDS. Water added to a total volume of 5 l
10xBlotting buffer, 1 l
30.0 g Tris, 144.0 g Glycine. Milli Q water added to a total volume of 1 l.
Blotting buffer, 2000 ml
200 ml 10xBlotting buffer added 300 ml Methanol and 1500 ml milli Q water
PBS Tween, 5l
5 l 1xPBS added 10 ml Tween 20 and 5 g $MgCl_2$

WB 2 – blocking buffer 1 l 1xPBS added 2 g I-Block. The solution was heated to 70 °C using a magnet stirrer, then cooled to room temperature. Next it was added 1 ml Tween, 1 g $MgCl_2$ and 1 ml Sodium Azid NaN_3 20% solution 1xDiethanolamine (DEA) buffer reagent, 100 ml 1.1 ml Diethanolamine added some milli Q water was added to dissolve the DEA. pH was adjusted to 9.5 with concentrated HCl. Next it was added 0.02 g $MgCl_2$ and milli Q water to a total volume of 100 ml Substrate solution 45 ml 1xDEA added 225 µl CDP-star and 450 µl Nitro-Block
Liposomes: 250 mM ammonium sulphate pH 5.5, 100 ml 3.3035 g ammonium sulphate added 100 ml milli Q water. pH was adjusted to 5.5 by 25% NH_4^+ 5% sucrose solution, 50 ml 2.5 g sucrose added 50 ml milli Q water

2.11 Disposable equipment and consumables

Name	Supplier
15 and 50 mL sterile PP-tubes Cellstar®	Greiner Bio-One
Amersham Hybond™-P	GE Healthcare
Aspirations – pipette 2 mL	Sarstedt
Disposable cuvettes 1.5 ml, cat number: 7590 15	Brand
Easy flask 25 and 75 V/C	Nunc ™
Filtropur L 0.2 µm pressure filtration units	Sarstedt
Glass beads 0.45 mm	Biospec Products
Microtubes 1.5 mL MCT-150-C	Genuine Axygen Quality
Nucleopore® track-etch membranes (25 mm diameter) for lipid extrusion. Pore sizes: 0.8 µm, 0.4 µm, 0.2 µm and 0.1 µm	Whatman®
Nunc® CryoTube 1.8 ml	Thermo Fisher Scientific
Pipette tips 1000, 200, 100 and 10 µL	Gilson
Pipette tips 1000, 200, 100 and 10 µL	Corning
Serological pipettes 10 and 5 ml	VWR
Single-use Insulin syringe OmniCan® 50	Braun
Syringes 1 ml, 3 ml, 5 ml	BD Medical
Tissue culture dishes: Nunclon surface Multidish 6-wells, 12-wells, 48-wells and 96-wells	Nunc ™
Transfer pipettes 3.5 ml and 2 ml	Sarstedt
Zetasizer nanoseries folded capillary cells	Malvern

3. Methods

3.1 Cell culturing

All cell culturing and other work with cell lines was performed in a sterile environment, using a Holten Laminar Air Flow (LAF) safety bench. All cell lines were examined in an Olympus CKX31 microscope on a regular basis, ensuring healthy cells free of bacterial contamination. Cell media were supplemented with 100 IU/ml penicillin and 100 μg/ml streptomycin to avoid bacterial growth and 10% foetal bovine serum (FBS) unless otherwise specified. Centrifugation of cells was performed at 160 x g in a Heraeus Labofuge 400 centrifuge or a Costar® Mini centrifuge. The cells were cultured in a humidified Steri – Cycle CO_2 Incubator at 37°C, 6% CO_2.

3.1.1 Culturing of suspension cells: MOLM-13 and MV4-11 cell lines

The MOLM-13 wt and the MOLM-13 SH p53 (silenced p53) cell line were cultured in Dulbecco's Modified Eagle's Medium (DMEM) without FA because culturing of FR-expressing cells in FA-free medium is shown to enhance the expression of FR (16, 67, 68). Both cell lines were cultured in FA-free DMEM without any negative effects on the cells for 3 – 4 weeks. To prevent a negative effect from either FA depletion or DMEM medium, the cells were replaced with cells from backup cell lines cultured in RPMI-1640 medium after this period of time. For the preparation of cell lysates for Western blotting, the MOLM-13 cell lines were also cultured in RPMI-1640 medium.

The MV4-11 cell line was cultured in DMEM without FA in order to enhance the expression of the FR (67, 68). Culturing in this medium was without negative adverse effects for 2 – 3 weeks. Like previously described for the MOLM-13 cell lines, the cells were replaced with cells from backup cell lines cultured in Iscove's Modified Dulbecco's Medium (IMDM) after this period of time. IMDM is the preferred culturing medium for this cell line and it was difficult to culture the cells in other media; negative effects were visible after a period of time in terms of a high proportion of cell death.

All suspension cell lines were cultured in FA-free DMEM medium in dilution series in a 12-well tissue culture dish. New dilution series were made every week.

To expand suspension cells for experiments or Western blotting, the cells were cultured in 10-ml medium Nunc™ easy flasks. Cells were allowed to condition in FA-free medium for at least 4 days prior to experiments. The cells were kept at a concentration between $0.4 \cdot 10^5$ and $8 \cdot 10^5$

cells/ml, and dilution was done by removing cell suspension and adding fresh medium. Cell number was estimated with a Bürker cell counting chamber.

3.1.2 Culturing of adherent cells: PC-3, LNCaP and NRK cell lines

The PC-3 cell line was cultured in RPMI-1640 medium. The cells were cultured in 10-ml or 20-ml medium Nunc™ easy flasks, where the medium was monitored by visual inspection on a regular basis and replaced when it had a yellow colour. When the cells had reached 70 – 90% confluence, they were detached as described in section 3.1.3 and reseeded in a new flask at a minimum of 10% confluence or in a tissue culture dish. Cells were detached and reseeded or medium was changed at least three times per week.

The LNCaP cell line was cultured in RPMI-1640 medium. The cells were cultured in 10-ml or 20-ml medium Nunc™ easy flasks, and the medium was replaced regularly as described for the PC-3 cell line. When the cells had reached 70 – 90% confluence, they were detached by flushing 5 – 8 ml PBS (see Table 2.10 for content) at room temperature repeatedly using a pipette. Next, the cells were centrifuged for 4 min, re-suspended in fresh medium and reseeded in a new flask at a minimum of 15% confluence or in a tissue culture dish. Cells were detached and reseeded or medium was changed at least 2 times per week.

The NRK cell line was cultured in 10-ml Nunc™ easy flasks in DMEM medium. When the cells had reached 70 – 90% confluence, they were detached as described in section 3.1.3. Reseeding in a new flask was performed at a minimum of 10% confluence.

All adherent cell lines were cultured until a maximum of 15 generations in total. After this they were replaced with newly defrosted cells.

3.1.3 Protocol for trypsin-aided detachment of adherent cells

Medium was removed and the cells were rinsed with PBS at room temperature. Next, PBS and trypsin-EDTA (see Table 2.10 for content) were added in a 1:2 relationship and the cells were incubated at 37°C, 6% CO_2 until the cells had detached from the flask, i.e. would move when examined in the light microscope. Trypsin was inactivated by adding an equal volume of fresh medium to the PBS/trypsin-EDTA/cell mixture, and the cell suspension was centrifuged for 4 min. The cell pellet was re-suspended in fresh medium and reseeded as described in section 3.1.2.

3.1.4 Freezing and defrosting of cells from liquid nitrogen

Freezing: The cell suspension was centrifuged for 4 min and re-suspended in fresh medium to a concentration of 7 – $10 \cdot 10^6$ cells/ml. 500 µl FCS with 20% DMSO was added to 500 µl cell suspension, mixed gently and transferred to a sterile 1.8 ml Nunc™ cryo tube. The tube was wrapped in tissue paper and put in a Styrofoam box to ensure slow freezing. The box was frozen at -80ºC for 24 – 48 h before transferring the Nunc™ cryo tubes to liquid nitrogen.

Defrosting: Defrosting of cells was performed as rapid as possible to avoid cellular damage and death. First, the Nunc™ cryo tube was removed from the liquid nitrogen and wrapped in paper to keep it frozen until installed in the LAF hood. The tube was opened slightly, allowing controlled pressure release and next thawed quickly by holding it in the hand. When the frozen contents had loosened from the tube, it was transferred to a sterile 15 ml tube. 10 ml pre-heated medium at 37ºC was poured drop-wise over the frozen cells. Finally, the cell suspension was transferred to one or two 10-ml flasks and the medium was changed the next day to remove DMSO.

3.2 SDS-PAGE and Western blotting

The contents of all solutions and buffers used for SDS-PAGE and Western blotting are described in Table 2.10.

3.2.1 Preparation of cell lysates for SDS-PAGE and Western blotting

The cell suspension was centrifuged for 5 min and the resulting pellet re-suspended in 10 ml cold PBS. The suspension was re-pelleted by another 5 min centrifugation, and next re-suspended in 1 ml cold PBS. The suspension was centrifuged for 4 min and the PBS carefully removed from the pellet. Finally, the pellet was re-suspended in 50 – 100 µl cold RIPA buffer with Complete to lyse the cells and frozen at -80°C. The cell lysates were kept cold during preparation and stored cold to avoid degradation of the proteins.

3.2.2 Protocol for protein measurement

The cell lysates were thawed on ice and the pellets re-suspended using a homogeniser (Kontes Pellet pestle®). Next the samples were centrifuged at 9450 x g in a Heraeus Microcentrifuge

Biofuge Fresco for 20 min at 4°C, and the supernatant containing proteins collected and stored on ice. Solutions for a protein standard curve were made using ingredients in amounts described in Table 3.1. The samples were diluted in MQ water to a total volume of 50 µl. 3 ml Bio-Rad Protein Assay Dye Reagent Concentrate was diluted in 12 ml water, the solution was filtered and 750 µl of this solution was added to each of the tubes for the standard curve and the samples. Two parallels of 280 µl for each solution were added to a 96-well Nunclon multidish and the absorbance of the solutions at 595 nm was determined using an ASYS UVM 340 microplate spectrophotometer. The software KIMpro was used to control the instrument and analyse measurements. A standard curve was calculated by the software and the protein concentration in the samples determined based upon this.

Table 3.1: Solutions for the making of a protein standard curve.

Concentration, mg/ml	BSA 1 mg/ml volume, µl	Water volume, µl
0.8	40	10
0.6	30	20
0.4	20	30
0.2	10	40
0.1#	10	90
0.05#	10	190
0	0	50

# of these solutions 50 µl was pipetted into a new tube and this was used in further analysis.

3.2.3 Protocol for SDS-PAGE

A 12.5% acrylamide separation gel was made by mixing the ingredients described in Table 3.2, with 10% APS and TEMED added as the last ingredients to start the polymerisation. The gel solution was applied between the plates up to 3 cm below the top, isobutanol was applied to even out the surface and the gel was left to solidify for 20 – 30 min. The isobutanol was removed from the solidified gel and a 5.4% acrylamide stacking gel was made in a similar way using the ingredients described in Table 3.3. The stacking gel solution was applied on top of the separation gel and left to solidify for 20 – 30 min.

Table 3.2: 12.5% acrylamide separation gel ingredients

Ingredient	**Amount for the making of 2 gels**
30% Acrylamide/Bis	6.3 ml
1 M TrisHCl pH 8.7	5.7 ml
Milli Q water	2.7 ml
20% SDS	152 µl
10% APS	135.2 µl
TEMED	13.6 µl

Table 3.3: 5.4% acrylamide stacking gel ingredients

Ingredient	**Amount for the making of 2 gels**
30% Acrylamide/Bis	1.36 ml
0.5 M TrisHCl pH 6.8	2 ml
Milli Q water	4.1 ml
20% SDS	40 µl
10% APS	40 µl x 2 = 80 µl
TEMED	5.25 µl x 2 = 10.5 µl

Samples with determined protein content (see section 3.2.2) were prepared for loading on the gel. An equal protein amount for each sample was diluted in 5xSDS sample buffer and MQ water to a total concentration of 1xSDS sample buffer to denaturate the proteins. The samples were heated at 96°C for 5 min to reduce disulphide linkages.

The running chamber was prepared and filled with running buffer. The samples and the standard were transferred to the wells using a pipette with loading tips. Voltage was applied, first 160 V for 5 min to compress the proteins in the stacking gel and next 120 V for 2 – 2 ½ h to separate the proteins by size in the separation gel.

3.2.4 Protocol for Western blotting

The membrane (Amersham Hybond™-P, PVDF) was activated by incubation with methanol for 5 min. The membrane with the separation gel on top was placed in blotting cassette, the cassette was transferred to the blotting chamber and blotting buffer poured over to cover the cassette. A magnet stirrer and a cooling system were used to obtain circulation in the liquid and avoid melting of the gel. Finally, the proteins were blotted onto the membrane using a current of 200 mA for 16 – 18 h, the membrane facing the positive pole and the gel facing the negative pole.

The membrane was washed with PBS Tween for 5 min and non-specific binding of antibody to the membrane was blocked by incubation with blocking buffer (WB2) for 1 – 2 h. Next, the membrane was incubated with primary antibody, see Table 3.4 for anti-FOLR2 antibody and Table 3.5 for anti-PSMA antibody preparation. The FOLR2 and PSMA blots were incubated at 4°C over the night, for 16 – 18 h.

The membrane was washed with PBS Tween for 4x15 min and next incubated with alkaline phosphatase-coupled secondary antibody anti-rabbit 1:20 000 diluted in WB2 solution for 2 h at room temperature. The secondary antibody and incubation times were identical for the FOLR2 and PSMA blots. The membrane was washed with PBS Tween for 4x15 min, incubated with 1xDEA for 2x2 min and next with substrate solution for 20 min with minimal light exposure. Finally, images of the blot were processed using a Fujifilm LAS 3000 Imager and the Image Reader LAS-3000 software was used to control the instrument and to process images.

An actin measurement was next performed on the same blot by following the same procedure as described for FOLR2 and PSMA. First, the blot was stripped by incubation with Re-blot solution for 15 min, followed by blocking and incubation with anti-actin primary antibody 1:10 000 (see Table 3.6 for contents) for 24 – 72 h at 4°C. Next, the blot was washed and incubated with secondary antibody alkaline phosphatase-coupled anti-mouse 1:10 000 diluted in WB 2 for 2 hours at room temperature shaking. The blot was washed again, incubated with 1xDEA and finally substrate solution for 20 min before processing of images.

All incubations of the blot were performed while shaking, using an Edmund Bühler Swip shaker.

Table 3.4: FOLR2 antibody solution preparation, 1 µg/ml

Ingredient	Amount for 1 µg/ml (recommended dilution)
Anti-FOLR2: ab56067 (abcam) 500 µg/ml	10 µl
WB 2 (blocking buffer)	5 ml

Table 3.5: PSMA antibody solution preparation, 1.25 µg/ml

Ingredient	Amount for 1.25 µg/ml (recommended dilution 1-3 µg/ml)
Anti-PSMA: AB10614 (Millipore) 250 µg/ml	30 µl
WB 2 (blocking buffer)	5 ml

Table 3.6: Actin antibody 1:10 000 solution preparation

Ingredient	Amount
Actin antibody	3 µl
WB2 (blocking buffer)	30 ml

3.3 Transient transfection of PSMA in the PC-3 cell line

3.3.1 Protocol for PSMA transfection by lipofectamine

Plasmids encoding GFP (supplied by prof. James Lorens, Univ. Bergen), PSMA (supplied by prof. Dean Bacich, Univ. Pittsburgh) or empty vector (supplied by prof. James Lorens, Univ. Bergen) were maxi-prepped by Nina Lied Larsen. PC-3 cells were cultured in a Nunc™ 6-well tissue culture dish four days prior to the transfection, and had reached about 90% confluence at the day of transfection. 2 ml DMEM medium supplemented with 10% FBS but without antibiotics was added to each well and 4 tubes were prepared using ingredients described in Table 3.7 and 3.8. The contents of Tube 1 and 2 and the contents of tube 3 and 4 were mixed thoroughly, i.e. the DNA-solutions were mixed with the lipofectamine-solutions, and incubated at room temperature for 20 min. Next, 500 µl of the DNA-lipofectamine mixture was added to each well; 3 wells were transfected with PSMA (4 µg/well) and GFP (0.4 µg/well)-encoding DNA and another 3 wells with empty vector (4 µg/well) and GFP (0.4 µg/well)-encoding DNA. GFP was used as a means of visualising successful transfection. The wells were incubated at 37°C, 6% CO_2 for 6 h, and the medium was changed to fresh RPMI-1640 supplemented with 10% FBS and antibiotics. GFP expression was detected after 24 h by examination in a Zeiss Axiovert 200M Fluorescence/Live cell imaging microscope using a FITC laser, see Figure 4.20 for GFP-positive cells. Cells for experiments were detached by trypsin treatment and reseeded in 48-well tissue culture dishes. Cell lysates for Western blotting were prepared (see section 3.2.1) from the contents of two 6-well dishes, one transfected with PSMA and one with empty vector.

Table 3.7: Lipofectamine transfection ingredients for 3 wells: PSMA – encoding DNA + 10% GFP – encoding DNA

Tube number	**Ingredient**	**Amount for 3 wells, µg**	**Concentration, µg/µl**	**Amount of solution for 3 wells, µl**
1	GFP – DNA	1.2	1	1.2

	PSMA – DNA	12	1.1	10.91
	DMEM medium (- FCS, - P/S)	-	-	738
2	Lipofectamine	-	-	30
	DMEM medium (- FCS, - P/S)	-	-	720

Table 3.8: Lipofectamine transfection ingredients for 3 wells: Empty vector – DNA + 10% GFP – encoding DNA

Tube number	**Ingredient**	**Amount for 3 wells, µg**	**Concentration, µg/µl**	**Amount of solution for 3 wells, µl**
3	GFP – DNA	1.2	1	1.2
	Empty vector – DNA	12	0.7	17.14
	DMEM medium (- FCS, - P/S)	-	-	732
4	Lipofectamine	-	-	30
	DMEM medium (- FCS, - P/S)	-	-	720

3.3.2 Protocol for PSMA transfection by calcium phosphate

PC-3 cells were cultured in a Nunc™ multidish 6-well two days prior to transfection, and had reached about 70% confluence at the day of transfection. 2 ml DMEM medium supplemented with 10% FBS but without antibiotics and 2 µl 25 mM chloroquine was added to each well. Transfection reagents containing plasmids were prepared, see contents in Table 3.9 and 3.10. 2xHEPES buffer was added as the last ingredient followed by aeration of the solutions for 20 – 30 s. Immediately after this, 500 µl of the solutions was added to each well; 3 wells were transfected with the PSMA (2 µg) and GFP-encoding DNA (0.2 µg) and another 3 wells with empty vector (2 µg) and GFP-encoding DNA (0.2 µg). The wells were incubated at 37°C, 6% CO_2 for 5 – 6 h and the medium was changed to fresh RPMI-1640 supplemented with 10% FBS and antibiotics. The wells were incubated for a total time of 48 h after the transfection and examined for GFP expression as described in section 3.4.1. See Table 2.10 for the contents of 2xHEPES buffer.

Table 3.9: Calcium phosphate transfection ingredients for 3.2 wells: PSMA and 10% GFP-encoding DNA

Ingredient	**Amount for 1 well, µg**	**Concentration**	**Amount of solution for 3.2 wells, µl**
GFP – DNA	0.2	1 µg/µl	6.4*
PSMA – DNA	2	1.1 µg/µl	5.82
MQ water	-	-	685
$CaCl_2$	-	2 M	102.4
2xHEPES buffer	-	-	800

*A 1:10 dilution of GFP-encoding DNA was made

Table 3.10: Calcium phosphate transfection ingredients for 3.2 wells: empty vector and 10% GFP-encoding DNA

Ingredient	**Amount for 1 well, µg**	**Concentration**	**Amount of solution for 3.2 wells, µl**
GFP – DNA	0.2	1 µg/µl	6.4*
Empty vector – DNA	2	0.7 µg/µl	9.15
MQ water	-	-	682
$CaCl_2$	-	2 M	102.4
2xHEPES buffer	-	-	800

*A 1:10 dilution of GFP-encoding DNA was made

3.4 Cell experiments

3.4.1 Protocol for cell experiments with suspension cell lines

Cells were seeded in the desired concentration (40000 – 300000 cells/well) in a 12 or 48-well tissue culture dish. Next, drug or liposome solutions were added to the wells, and the plate was incubated at 37°C, 6% CO_2 for 20 or 30 min. The cells were washed 3 times by this procedure: the plate was centrifuged at 160 x g in a Heraeus Labofuge 400 centrifuge for 4 min, medium was gently removed and fresh medium was added. The cells were next incubated at 37°C, 6% CO_2 for 24 or 48 h and WST-1 viability assay was performed as described in section 3.5.3. The cells were fixed by addition of 4% FIX solution to a final concentration of 2% FIX. DNR was added to the fixative (0.1 µg/ml) as a fluorescent probe to stain the nuclei for cell counting. See Table 2.10 for contents of 4% FIX solution and 4% FIX solution with DNR.

3.4.2 Protocol for cell experiments with adherent cell lines

Cells were seeded in the desired concentration (3000 – 5000 cells/well) in a 48-well tissue culture dish one or two days before the experiment was performed. At the day of the experiment, the medium was replaced with fresh medium, next drug or liposome solutions were added to the wells and the plate was incubated at 37°C, 6% CO_2 for 30 min. The cells were washed 2 times by removing the medium and adding fresh medium. Next the cells were incubated at 37°C, 6% CO_2 for 48 or 72 h, and WST-1 viability assay was performed as described in section 3.5.3. The cells were fixed by addition of 4% FIX solution to a final concentration of 2% FIX. To stain the nuclei, either DNR was added to the fixative (0.1 µg/ml) or a 1:100 dilution of Hoechst 33342 in MQ water was added to the wells after fixing. The DNR staining turned out to be more powerful compared to Hoechst 33342 staining, and was therefore chosen as staining reagent in further experiments. See Table 2.10 for contents of 4% FIX solution and 4% FIX solution with DNR.

3.4.3 Cell proliferation reagent WST-1 measurements and calculations

Roche Cell proliferation Reagent WST-1 was added to the wells to a total 1:20 dilution in the tissue culture dishes containing cells. Two or three wells containing the medium only was added WST-1 and used as blanks. The dish was shaken gently and incubated at 37°C, 6% CO_2 for 2 h. The absorbance was measured at 450 nm with 620 nm as reference using an ASYS UVM 340 microplate spectrophotometer and the software DigiRead or ScanPlus was used to control the instrument and perform measurements.

Calculations: See calculations formula 1 for calculation of adjusted absorbance of treated divided by adjusted absorbance of control cells. The average values of the parallels for different treatments were calculated and a bar graph was made, plotting treatment against treatment/control values. For experiments with two parallels, the variation between the measurements was calculated by subtracting one of the measurements from the average value and error bars were inserted using these values. For experiments with three or more parallels, the standard error was calculated (see calculations formula 2 and 3) and error bars were inserted using these values. T-tests were performed between comparable treatments with similar doses when three parallels or more were performed. P-values were marked in the graph this way: $P < 0.05$ *, $P < 0.01$ **, $P < 0.005$ *** and $P < 0.001$ ****.

Calculations formulas:

$$(|(drug\,treated)|-|(blank)|)\div(|(control)|-|(blank)|) \quad (1)$$

$$SE = s \div \sqrt{n} \quad (2)$$

$$s = \sqrt{((1\div(N-1))\times\sum((xi-x)^2))} \quad (3)$$

3.4.4 Fluorescence microscope cell counting, calculations and processing of images

Counting of cells was performed using a Zeiss Axiovert 200M Fluorescence/Live cell imaging microscope. The nucleus morphology was examined using DNR or Hoechst 33342 as a fluorescent probe, at 40x or 20x cy3.5 for DNR and 40x or 20x DAPI for Hoechst. See Figure 4.11 for DNR staining in MOLM-13 wt cells and Figure 4.18 for Hoechst staining in LNCaP cells and. Cells having condensed or fragmented nuclei were counted as dead and cells having whole nuclei were counted as living at the time of fixing. For adherent cell lines, cell death was also determined on the basis of the appearance of the cells in the light microscope; cells that had a rounded appearance, surface membrane blebs, were detached from the wells and/or had a destroyed cell membrane were counted as dead. A minimum of 100 cells were counted per well unless otherwise specified.

Calculations: The percentage of dead cells was calculated for all parallels (see calculations formula 4), and the adjusted % cell death for different treatments calculated by using calculations formula 5 to account for cell death among the controls. The average values of the parallels for different treatments were calculated and a bar graph was made, plotting treatment against adjusted % cell death values. Error bars were made and T-tests were performed as described in section 3.5.3.

Images of the cells were obtained by the software AxioVision 3.1, using the Zeiss microscope described at 40x magnification. Phase contrast, and the cy3.5, DAPI and FITC lasers were used.

Calculations formulas:

$$Cell\,death = Dead \div (Dead + Living)\times 100 \quad (4)$$

$$Adjusted\ \ cell\,death = ((\,cell\,death) - (\,cell\,death\,control))\times(100\div(100-(\,cell\,death\,control))) \quad (5)$$

3.4.5 Flow cytometry cell experiment

MOLM-13 SH p53 cells were used for a flow cytometry-analysis experiment. Liposomes with the Texas Red fluorochrome as described in Table 3.13 and 3.14 were made by Lars Herfindal. 300000

cells/well were seeded in a 12-well tissue culture dish and liposomes were added at 3%, 1% and 0.3% of the total volume in 2 parallels per liposome batch (PEG and PEG-FA). The plate was incubated for 10 min at 37°C, 6% CO_2. Washing of the cells was performed twice as described in section 3.5.1 and the plate was incubated for 30 min at 37°C, 6% CO_2. Next, the cell suspensions were washed with PBS twice and the cell pellets finally re-suspended in 300 µl 2% FIX. Flow cytometry was performed using an Accuri® C6 Flow cytometer, 3 blue and 1 red laser at FL3, 610/20 filters. The instrument was controlled by and data analysis was performed using the FlowJo software.

3.5 Preparation and measurements of liposomes

3.5.1 Preparation of liposomes

HEPC, cholesterol and DSPE-PEG were weighed out and dissolved in chloroform separately. See Table 3.11 – 3.14 for contents of different liposome batches of 5 ml, all the batches had a molar ratio of 1,81 HEPC : 1 cholesterol : 0,15 DSPE-PEG. The ingredients were mixed and for FA-conjugated liposomes, the DSPE-PEG-FA dissolved in ethanol was added. A thin, even lipid film was made by evaporation of the chloroform in a Rotary Evaporator at 150 mBar, ~ 90 rpm and the film was left at maximum vacuum pump capacity for 30 – 60 min to remove all chloroform. The lipid film was rehydrated in 250 mM ammonium sulphate pH 5.5 (see Table 2.10) by vortexing at 60 – 65°C, which is above the lipid transition temperature. 15 – 20 clean glass beads (0.45 mm) were used to aid the rehydration. Next, the flask with the hydrated multi-lamellar vesicles (MLV) was gently shaken under heating (90 – 100 rpm, 60°C) for 30 min to ensure mixing of the contents. Finally the MLV were extruded through Whatman® Nucleopore® track-etch membranes for lipid extrusion at 65°C using a Northern Lipids LIPEX™ extruder 5 times at 0.8 and 0.4 µm 5 times, and 10 times at 0.2 and 0.1 µm. This created monolamellar liposomes of a size between 110 and 124 nm in diameter. The particle size was measured before, during and after lipid extrusion by Dynamic Light Scattering (DLS, see section 3.6.3).

To change the buffer on the outside of the liposomes, the liposome solution was gel filtrated (see section 3.6.2) through a 1.5x15 cm BioRad Econo-Column filled with Sephadex ™ G-25 Medium. Fractions of 1 ml were gel filtrated using PBS pH 8 as eluting buffer and the column was washed with 30 ml PBS between each fraction. Based on previous experiments (Herfindal, Univ.Bergen 2011, pers.comm.), the liposomes were diluted 1.6 times during the extrusion and gel

filtration, and the lipid concentration in the liposome solution was 2.7 mg/ml (Herfindal, 2011 pers.comm.).

Next, the cytostatics were incorporated into the liposomes, using the acid precipitation method. This method takes advantage of that the drugs are neutral in slightly alkaline solutions, but protonated in acidic solutions (see Figure 1.6), hence when the drugs are internalised they can no longer pass the lipid bilayer and precipitates (69). 1 mg DNR and/or 1 mg EME per 10 mg lipids was added to the liposome suspensions, and the mixtures were incubated at 60°C for 2 h. The mixtures were shaken every 30 min.

The liposomes were then gel filtrated to remove non-incorporated cytostatics from the liposome solutions, and eluted in PBS pH 7.4. The column was washed with 100 – 150 ml PBS between each liposome fraction to wash out cytostatics from the column.

Liposomes were stored dark at 4°C to prevent chemical degradation. Liposome solutions were always shaken before use, and used for a maximum of 2 months after they were prepared.

Table 3.11: PEGylated liposomes, 5 ml batch

Ingredient	**Amount**
HEPC (Hydrogenated Egg Phosphatidylcholine)	12.0 mg
Cholesterol	3.2 mg
DSPE-PEG (1,2-Disteraoyl-sn-glycero-3-Phosphoetanolamine-N-[Methoxy(Polyethylene glycol)-2000] (ammonium salt)	3.5 mg

Table 3.12: Folic acid conjugated PEGylated liposomes, 5 ml batch

Ingredient	**Amount**
HEPC (Hydrogenated Egg Phosphatidylcholine)	12.0 mg
Cholesterol	3.2 mg
DSPE-PEG (1,2-Disteraoyl-sn-glycero-3-Phosphoetanolamine-N-[Methoxy(Polyethylene glycol)-2000] (ammonium salt)	3.5 mg
DSPE-PEG-FA (1,2-disteraoyl-sn-glycero-3-phosphoetanolamine-N-((polyethylene glycol-5000)folate) (ammonium salt)	140 µl

Table 3.13: PEGylated liposomes with the Texas red fluorochrome, 5 ml batch

Ingredient	**Amount**
HEPC (Hydrogenated Egg Phosphatidylcholine)	12.0 mg

Cholesterol	3.2 mg
DSPE-PEG (1,2-Disteraoyl-sn-glycero-3-Phosphoetanolamine-N-[Methoxy(Polyethylene glycol)-2000] (ammonium salt)	3.5 mg
Texas Red® DHPE (Texas Red® 1,2 Dihexadecanoyl-*sn*-Glycero-3-Phosphoethanolamine, Triethyl ammonium salt)	0.25 mg

Table 3.14: Folic acid conjugated PEGylated liposomes with the Texas red fluorochrome, 5 ml batch

Ingredient	**Amount**
HEPC (Hydrogenated Egg Phosphatidylcholine)	12.0 mg
Cholesterol	3.2 mg
DSPE-PEG (1,2-Disteraoyl-sn-glycero-3-Phosphoetanolamine-N-[Methoxy(Polyethylene glycol)-2000] (ammonium salt)	3.5 mg
DSPE-PEG-FA (1,2-disteraoyl-sn-glycero-3-phosphoetanolamine-N-((polyethylene glycol-5000)folate) (ammonium salt)	140 µl
Texas Red® DHPE (Texas Red® 1,2 Dihexadecanoyl-*sn*-Glycero-3-Phosphoethanolamine, Triethyl ammonium salt)	0.25 mg

3.5.2 Preparation of columns and gel filtration of liposomes

Two BioRad Econo-Columns at 1.5x15 cm and 0.7x10 cm were prepared by heating Sephadex ™ G-25 Medium and MQ water 1:2 to 90°C for 1 h. The mixture was shaken every now and then. Next, Sephadex was washed two times with MQ water and the mixture was transferred to the column using a pipette. The mobile phase was then exchanged to PBS.

All solutions were degassed before introducing them into the column. The 1.5x15 and 0.7x10 cm columns were washed before use by gel filtrating at least 30 and 5 ml eluting buffer, respectively. A fraction of empty liposomes was gel filtrated to fill up unspecific binding of liposomes to the column. Empty liposomes and liposomes containing EME were identified as an opaque solution when eluted out, whereas DNR-containing liposomes were visible as a red band in the column. The column was left standing with 20% ethanol when not used for over three days to avoid bacterial contamination.

As a quality assurance and indication of stability, fractions of the readily prepared liposomes

containing DNR were gel filtrated after a time of storage. Any leakage of DNR from the liposomes would be visible due to the red colour of the drug. The liposomes were gel filtrated on a small column using degassed PBS (pH 7.4) as the eluting buffer.

3.5.3 Size and zeta potential (ZP) measurements

A Malvern Zetasizer Nanoseries Nano-ZS with Zetasizer software was used for the size and zeta potential (ZP) measurements. In this instrument, the particle size is measured by dynamic light scattering (DLS) (70). DLS measures Brownian motion of particles, i.e. the random movement due to bombardment of solvent molecules, and relates this to the particle size (70). The diameter measured by DLS is the hydrodynamic diameter of a particle, since it refers to particle movement in a fluid (70). The Zetasizer uses the M3-PALS technique to determine the ZP (71). In this technique, the particle electrophoretic mobility is measured, which is related to the ZP by the Henry equation (71).

Size measurements: Samples for DLS size measurements were prepared by diluting one drop of liposome suspension in 1 ml suspension buffer (PBS or ammonuim sulphate). The sample was transferred to a Brand disposable cuvette. Lipids were chosen as material and dispersant set to PBS when dissolved in PBS or water when dissolved in ammonium sulphate. Three measurements were performed for each sample and the data were presented as Z-average value (nm, diameter) and polydispersity index (PdI).

ZP measurements: The liposome suspension was diluted 1:10 in 5% sucrose. With this solvent, we obtained reliable results and the size was relatively stable. PBS or diluted PBS (1:10) as solvent did not give consistent results. The sample was injected into a clear disposable zeta cuvette and the cuvette was placed in the Zetasizer instrument. Settings were changed in the software to ZP measurements. Lipids were chosen as material and dispersant set to water. Three measurements were performed for each sample. Next, the size was measured, using the same sample in the same cuvette. The data were presented as ZP (mV), ZP standard deviation for the ZP and Z-average (nm, diameter) for size measurements.

3.5.4 Drug content measurements

DNR content measurements: Samples were prepared by mixing thoroughly 100 µl of liposome or free DNR solution, 500 µl of 20% SDS (see table 2.10 for content) to lyse the liposomes and 400 µl PBS in a Brand disposable cuvette. Blank samples contained 500 µl 20% SDS

and 500 µl PBS. Measurements were done by a Varian Cary UV-visible spectrophotometer at 483 nm controlled by the CaryWin UV program in simple reads mode. The measurements were zeroed out at the blank sample, after this three measurements were made for each liposome sample. A DNR standard curve was made based on measurements of solutions of free DNR (10, 30, 60 and 100 µM) using linear regression. The equation for the straight line obtained was used to calculate the DNR content in the liposome samples. The absorbance of empty liposomes at 483 nm was subtracted from the absorbance of DNR-containing liposomes before calculations were done.

EME content measurements: Samples were prepared by mixing 75 µl of liposome or free EME solution and 75 µl of 20% SDS to lyse the liposomes. Blank samples contained 75 µl milli Q water and 75 µl 20% SDS. The samples were transferred to a Starna® Cary quartz cuvette and the absorbance was measured at 280 nm using a Varian Cary UV-visible spectrophotometer in the CayWin UV program, scan mode. An EME standard curve was made based on measurements of solutions of free EME (3, 10, 30, 60, 100 and 150 µM). The absorbance of the samples at 500 nm and the absorbance of the blank sample was subtracted from the free EME samples, and these values were plotted for the making of a standard curve. A straight line was obtained using linear regression and the equation was used to calculate the EME content in the liposome samples. The absorbance of empty liposomes at 280 nm was subtracted from the absorbance of EME-containing liposomes before calculations were done.

3.5.5 Phosphatidylcholine (PC) content measurements

A Phosphatidylcholine Assay Kit from Cayman Chemical Company was used to determine the PC content of the liposomes. First, the PC buffer, PC colour detector and the PC enzyme mixture were prepared as described by the supplier. The PC standard and 7 tubes with increasing PC concentration (0, 20, 40, 60, 80, 100 and 150 mg/dl) were prepared for the making of a standard curve and next the reaction mixture was prepared. In a 96-well multidish, two 10 µl parallels of each of the PC standards and three 10 µl parallels of undiluted liposome samples (PEG-FA and PEG-conjugated empty liposomes) were added. 100 µl of reaction mixture was added to each well, and the plate was shaken carefully to mix the contents. The plate was incubated at 37°C for 60 min and the absorbance measured at 585 – 600 nm in an ASYS UVM 340 microplate spectrophotometer. The software DigiRead was used to perform measurements and control the instrument.

Calculations were performed and a standard curve was made. All samples and the standard solutions were subtracted the absorbance of the blank solution. A standard curve was made based on

the subtracted absorbance values of the standards and a straight line was obtained using linear regression. The equation was used to calculate the PC contents in the liposome samples.

4. Results

4.1 Liposome drug loading and characteristics

Four different liposome batches were used in the work performed in this master thesis; Batch 1 (02.11.11), 2 (03.01.12) and 3 (12.03.12) consisted of PEG and PEG-FA liposomes (see Table 3.11 and 3.12). Batch 4 consisted of PEG Texas Red and PEG-FA Texas Red liposomes (see Table 3.13 and 3.14), these liposomes were not filled with cytostatics. All batches were made as described in section 3.6.1.

4.1.1 Liposome production: Characteristics, size measurements and estimation of PC content

After rehydration of the lipid film, the multilamellar large vesicles (MLV) solution had an opaque white appearance. This rehydrated solution precipitated and formed white aggregates when stored over night dark at 4°C and the aggregates were easily re-suspended when shaken. After the last extrusion (100 nm pore size), the liposome solution became less opaque, and did not form visible aggregates upon storage in the dark at 4°C.

The liposomes typically had a Z-average value of between 110 and 124 nm in diameter, and a low polydispersity index (PdI), usually below 0.05 (Table 4.1). The Texas Red-conjugated liposomes (batch 4) were somewhat larger in size (Table 4.1) Table 4.2 shows that both the Z-average and PdI values of the liposomes decrease during the extrusion, resulting in a monodisperse liposome solution. Figure 4.1 shows a typical size distribution curve.

Table 4.1: Z-average values for liposome batches 1, 2, 3 and 4 (Texas Red) after lipid extrusion

Liposomes	Batch 1		Batch 2		Batch 3		Batch 4 (Texas Red)	
	Z-average, d, nm	PdI	Z-average, d, nm	PdI	Z-average, d, nm	PdI	Z-average, d, nm	PdI
PEG	121.6	0.021	116.5	0.045	114.6	0.062	130.2	0.065
PEG-FA	110.7	0.039	119.0	0.025	123.8	0.068	126.3	0.065

Table 4.2: Z-average values for liposome batch 3 before, during and after lipid extrusion as an example of how the particle size and PdI changed during lipid extrusion

Extruded through filter	PEG liposomes		PEG-FA liposomes	
	Z-average, d, nm	PdI	Z-average, d, nm	PdI
Before extrusion	2220.0*	0.513	6290.0*	1.000
800 nm x5	450.6**	0.308	579.6**	0.487
400 nm x5	133.8	0.117	176.6	0.161
200 nm x10	131.5	0.083	208.1**	0.226
100 nm x10	114.6	0.062	123.8	0.068

Feedback from Zetasizer software:

* = Measurement results did not meet quality criteria

** = Multiple peaks in measurements

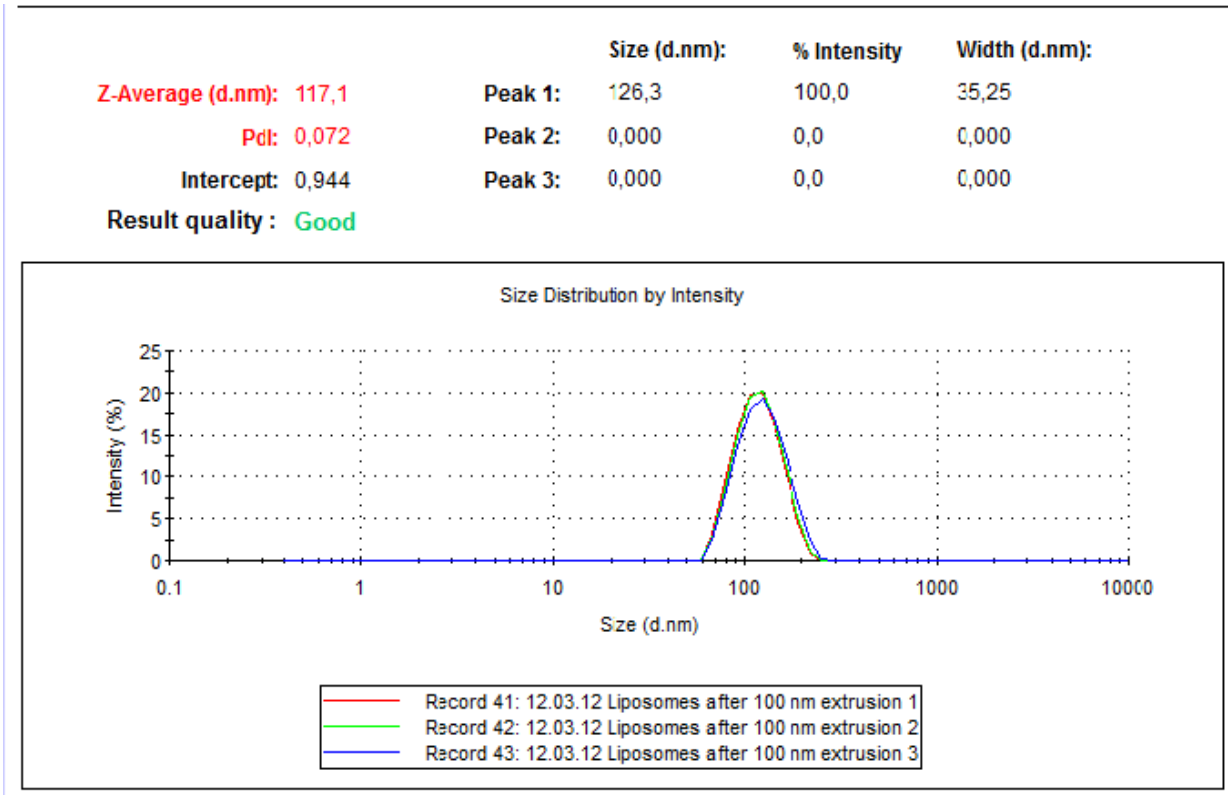

Figure 4.1: Size distribution curve for liposome batch 3 measured by DLS. The graph shows a typical size distribution for liposomes after lipid extrusion through a 100 nm membrane; PEG-liposomes after 100 nm extrusion are shown here. Three measurements are shown. The Z-average and PdI is the result for the first measurement.

In order to obtain the correct relationship between lipid and drug when the liposomes were to be loaded with DNR and EME, we measured the total PC content of the extruded liposomes.

However, the measurement results were below the dynamic range of the PC kit (20 – 150 mg/dl, see Figure 4.2) and the standard deviation of the three measurements performed for each liposome fraction was high (Table 4.3). An estimate of the PC content before gel filtration can be calculated by dividing the added PC (15.5 mg) by 5 ml, which gives a PC content of 3.1 mg/ml (310 mg/dl). Even though liposomes were gel filtrated before the PC content measurements, the measurement results of this batch were too low to be correct: 0.019 and 0.037 mg PC /ml (1.9 and 3.7 mg/dl). Previous measurements performed by Lars Herfindal showed that the lipid content of gel filtrated liposomes was 2.7 mg lipids/ml solution and this was used as an estimate in the further work with this thesis, for instance in calculations when loading liposomes with drugs.

Table 4.3: PC concentration measurement results for liposome batch 2 after buffer exchange gel filtration.

Liposomes	PC concentration, mg/dl	Standard deviation, mg/dl
PEG	1.926	1.63
PEG-FA	3.685	5.99

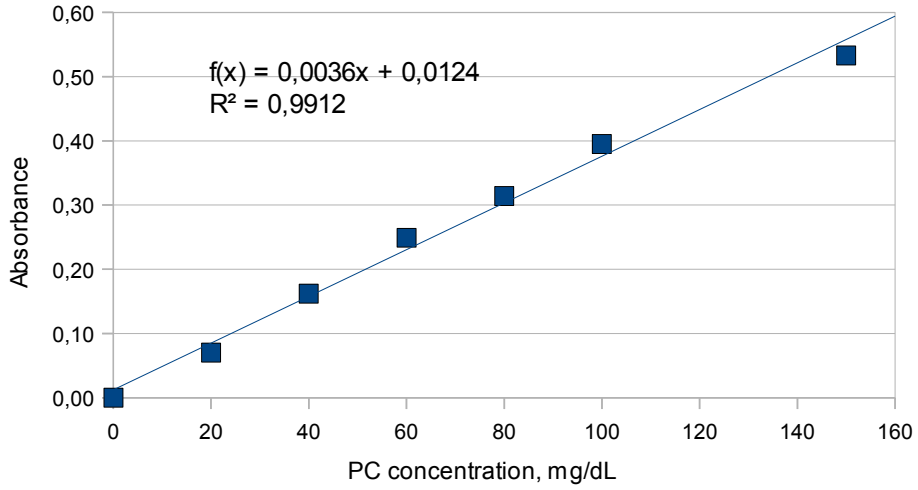

Figure 4.2: Phosphatidylcholine (PC) standard curve.

4.1.2 Drug loading of liposomes and drug content measurement results

The appearance of the drug-incorporated and gel filtrated solutions was colourless but slightly turbid for EME-containing liposomes and pink and slightly turbid for the DNR-containing liposomes.

The DNR and EME standard curves are shown in Figure 4.3 and 4.4, respectively. Results of calculated DNR and EME contents for liposome batches 1 – 3 are shown in Table 4.4. Due to previous experiences with difficulty in measuring EME content of liposomes (Herfindal 2011, pers.comm), these measurements were not performed on the first batch. The EME content of batch 1 is therefore estimated as the average of batch 2 and 3.

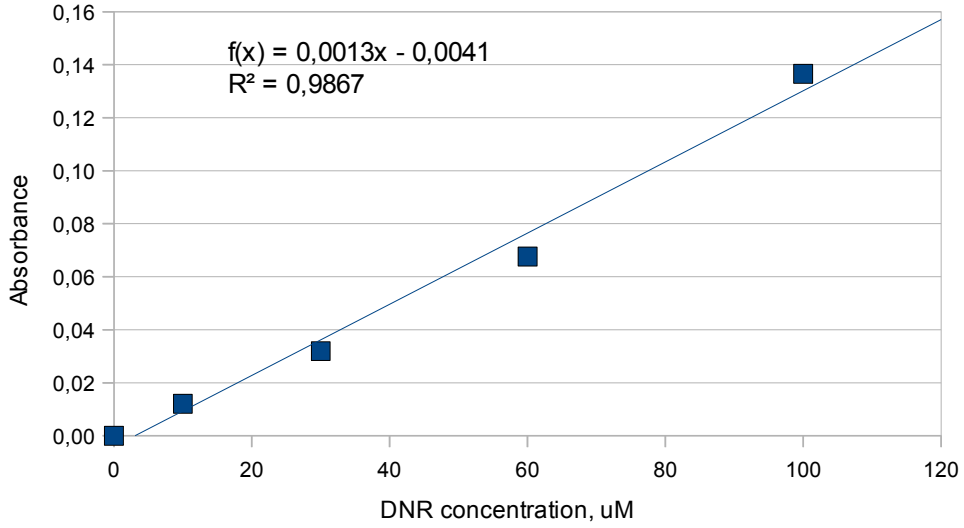

Figure 4.3: Daunorubicin standard curve. DNR absorbance measured at 483 nm

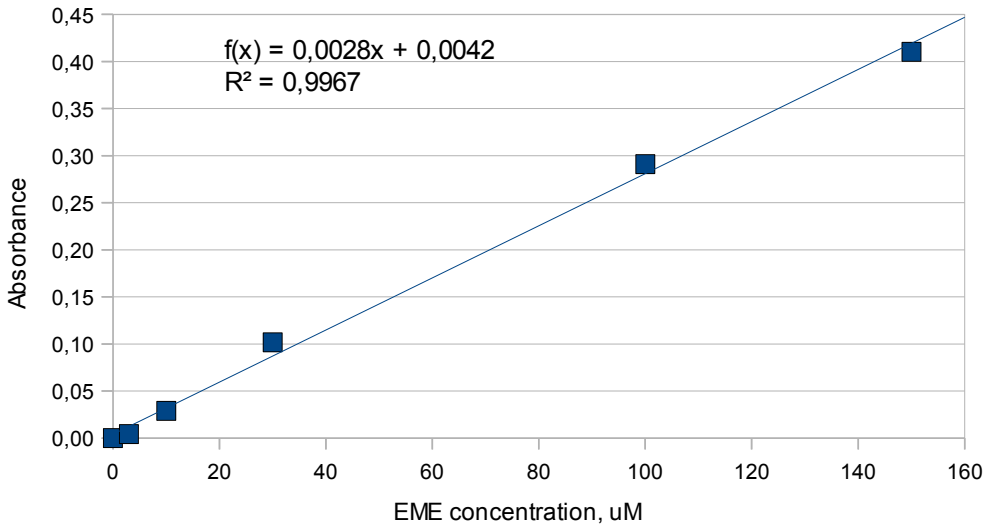

Figure 4.4: Emetin standard curve. EME absorbance measured at 280 nm

Table 4.4: Drug content of liposome batch 1, 2 and 3. The EME content of batch 1 is estimated as the average of batch 2 and 3.

Liposomes	Batch 1		Batch 2		Batch 3	
	[DNR], µM	[EME], µM	[DNR], µM	[EME], µM	[DNR], µM	[EME], µM
PEG DNR	57.00	-	95.82	-	64.90	-
PEG-FA DNR	47.54	-	56.54	-	65.59	-
PEG EME	-	131.59	-	115.07	-	148.11
PEG-FA EME	-	132.61	-	113.14	-	152.07
PEG DNR+EME	36.77	66.15	74.86	45.01	77.03	87.29
PEG-FA DNR+EME	33.08	92.53	52.18	89.80	69.59	95.25

4.1.3 Characterisation of drug-loaded liposomes: Size and zeta potential measurements and stability during storage

Size measurements were performed after drug-loading and gel filtration of the liposomes. Results for the different batches are shown in Table 4.5 – 4.7. When comparing to Table 4.1, it can be seen that the Z-average of the liposomes does not seem to change much after drug-loading. A small increase in size is seen for batch 3, for batch 2 the size is fairly constant. For batch 1, the size is also fairly constant except from the measurement of PEG liposomes with DNR+EME.

Table 4.5: Size measurement results of liposome batch 1 after drug-loading.

Liposomes	PEG		PEG-FA	
	Z-average, d, nm	PdI	Z-average, d, nm	PdI
Empty	123.3	0.055	111.2	0.054
DNR	123.7	0.084	113.2	0.058
EME	121.2	0.056	112.1	0.048
DNR+EME	183.5*	0.221	120.0	0.106

Feedback from Zetasizer software:

* The sample could be sedimenting during measurement (count size and rate decreasing). This measurement had two peaks. If the peak in the large area could be excluded from the measurements, the Z-ave could be more similar to the others.

Table 4.6: Size measurement results of liposome batch 2 after drug-loading and after 39 days of storage.

Liposomes	PEG: After drug-loading		PEG-FA: After drug-loading		PEG: After 39 days storage		PEG-FA: After 39 days storage	
	Z-average, d, nm	PdI	Z-average, d, nm	PdI	Z-average, d, nm	PdI	Z-average, d, nm	PdI
Empty	116.0	0.038	117.3	0.041	117.7	0.056	119.1	0.045
DNR	113.8	0.033	118.9	0.030	113.7	0.042	119.6	0.055
EME	116.8	0.039	119.1	0.035	117.5	0.055	121.5	0.055
DNR+EME	114.2	0.040	119.0	0.048	116.3	0.051	121.2	0.055

Table 4.7: Size measurement results of liposome batch 3 after drug-loading.

Liposomes	PEG		PEG-FA	
	Z-average, d, nm	PdI	Z-average, d, nm	PdI
Empty	116.3	0.038	126.0	0.041
DNR	116.4	0.053	127.4	0.023
EME	118.5	0.046	126.2	0.058
DNR+EME	116.4	0.048	126.0	0.029

To investigate the electronegativity of the liposomes and to see if this was influenced by drug loading, we measured the ZP. This was only done for batch 3, since the application was not available when batch 1 and 2 were made. Interestingly, the ZP increased from -26 mV in empty liposomes to between -10 and -15 mV in drug-loaded liposomes (Table 4.8). The liposomes had to be suspended in 5% sucrose in order to obtain reliable results and we experienced only a modest increase in size (Table 4.8), suggesting that the liposomes were intact. Liposomes suspended in hypotonic solution (10% PBS) underwent a large increase in size, the size increased substantially during the measurements and a large peak at approximately 5000 nm size suggested that aggregates were formed. These findings imply that the liposomes were lysed in hypotonic solution. When using undiluted PBS as solvent for ZP measurements, we were not able to obtain high enough count rates to get reliable data, and the estimated ZP differed from those reported in the literature. Probably, the ionic strength of PBS was too high to make it an appropriate solvent for these measurements. High conductivity media suppress the electrical double layer, also called the Debye length, and this in turn increases the ZP (70, 71). This is consistent with our findings, as the measured ZP was approximately -6 mV with PBS as a solvent.

Table 4.8: Zeta potential measurements for liposome batch 3. 5% sucrose was used as solvent. Size measurements were performed directly after zeta potential measurements.

Liposomes	PEG			PEG-FA		
	ZP, mV	Standard deviation ZP, mV	Z-average, d, nm	ZP, mV	Standard deviation ZP, mV	Z-average, d, nm
Empty	-25.5	1.15	131.8	-26.2*	1.45	156.0*
DNR	-13.6	0.07	127.5	-14.6	1.98	149.6*
EME	-14.7	0.57	129.9	-12.1	0.71	135.9
DNR+EME	-9.9	1.02	129.0	-12.1	0.07	142.1

Feedback from Zetasizer software:

* Sample not stable or not clean

Stability of the liposome solutions during storage was investigated by visual inspection, size measurements and gel filtration of DNR-loaded liposomes. Drug-loaded and empty liposomes were observed for a storage period of up to 4 months dark at 4°C and for this period of time they did not form visible aggregates and the colour and appearance remained constant. Size measurements were performed on batch 2 for a storage period of 39 days after drug-loading (Table 4.6). The liposome size remained fairly constant over this period of time, and some increase was seen in PdI value.

Gel filtration of DNR-containing liposomes was performed for batch 2 after a storage period of 39 days after drug incorporation. No free DNR was visible in the column during the gel filtration; the liposome solution eluted as a single pink band for all fractions. The same observation was noted for batch 3 after a storage period of 40 days after drug incorporation. In conclusion, the liposomes do not seem to suffer from DNR leakage over a period of time of 40 days.

4.2 Efficacy of drug-loaded multifunctional liposomes against AML cell lines

4.2.1 Comparing the efficacy of drug-loaded liposomes conjugated with PEG-FA to liposomes conjugated with PEG only in MOLM-13 and MV4-11 cells

We first investigated the efficacy of liposomes in the MOLM-13 and MV4-11 leukaemia cell lines in a pilot experiment, see Figure 4.5 and 4.6.

The EME and DNR doses given by the different liposomes (PEG and PEG-FA) are nearly equivalent and therefore the results are comparable. Both cell lines suffered cell death from

treatment with drug-loaded liposomes at concentrations below 0.30 μM DNR, 1.25 μM EME and 0.32/0.57 μM DNR+EME. Cell death was higher for PEG-FA liposomes than PEG liposomes. Also, cell death was substantially higher for the MV4-11 cell line than the MOLM-13 cell line for nearly equivalent DNR and EME doses. Treatment with empty liposomes with or without FA did not appear to affect cell viability or induce death (Figure 4.5 and 4.6).

The cell viability WST-1 results were not consistent (Figure 4.5 A and B, Figure 4.6 A and B). For the MOLM-13 cell line, there was more conversion of the tetrazolium salt, i.e. metabolic activity when treated with PEG-EME and PEG-DNR+EME than for empty liposomes. There was no apparent metabolic activity for PEG-DNR liposomes, while the counting of cells on nuclear morphology for this treatment showed approximately 30% cell death. The results for PEG-FA treatment in this cell line were more consistent with fluorescence microscopy cell counting, but with no apparent metabolic activity for the PEG-FA-DNR treatment (Figure 4.5).

For the MV4-11 cell line, the WST-1 data showed high metabolic activity for the cells treated with empty liposomes. There were no apparent viable cells for the PEG-DNR, PEG-DNR+EME, PEG-FA-DNR, PEG-FA-EME and PEG-FA-DNR+EME treatments and some metabolic activity for the PEG-EME treatment (Figure 4.6 A and B). These results were fairly consistent with the fluorescence microscopy cell counting, except from that the EME-liposomes induced only around 15% cell death (Figure 4.6 C and D).

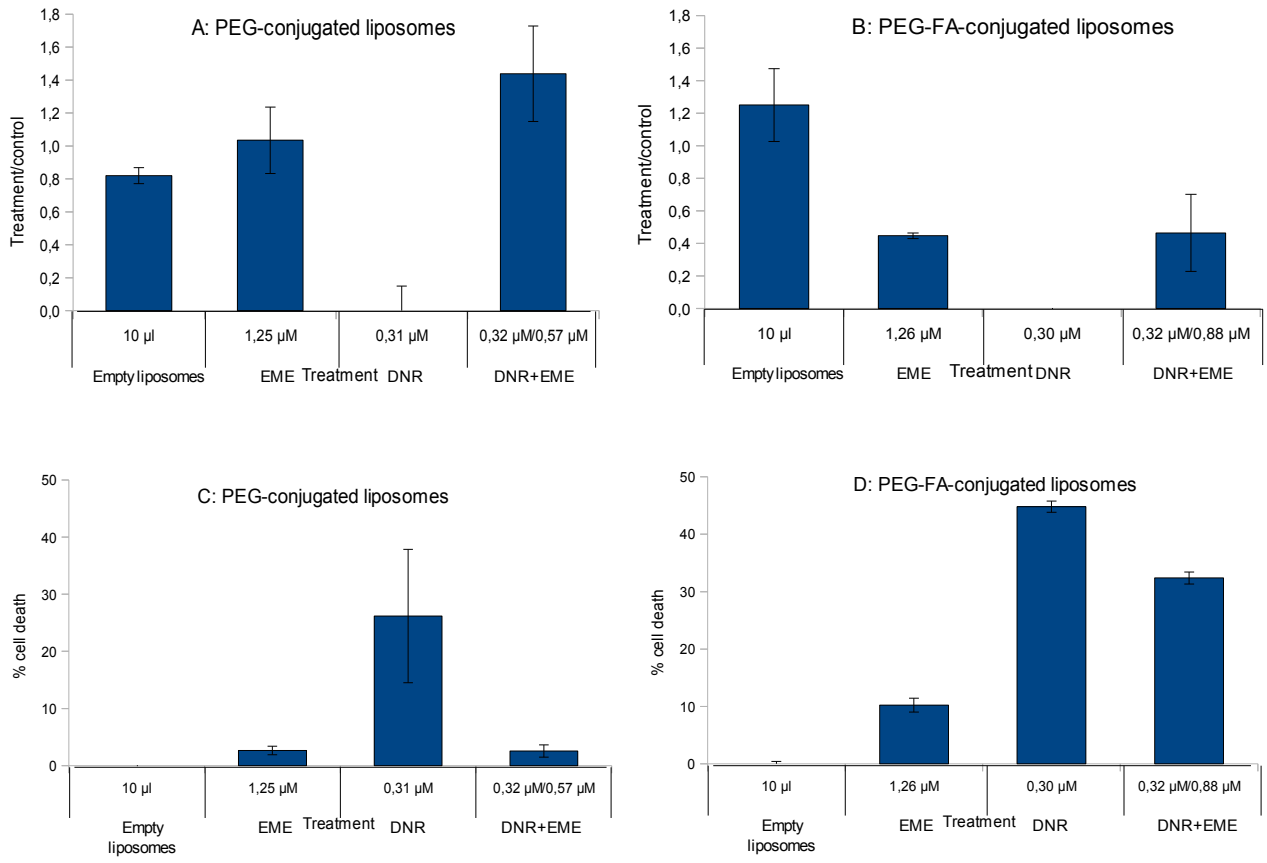

Figure 4.5: Death induction in MOLM-13 wt cells by different liposomes. Cells (44000 cells/well) were incubated with liposomes (batch 1) for 30 min in 12-well tissue culture dishes, washed 3 times, and incubated for 72 h before WST-1 measurement and fixing of cells. The cells were cultured in FA-free medium for 4 days before the experiment and the experiment was conducted in FA-free medium. Panel A and B show results from WST-1 measurements, panel C and D results from fluorescence microscope cell counting using Hoechst 33342 as a fluorescent probe. The data are average of two parallels and the deviation.

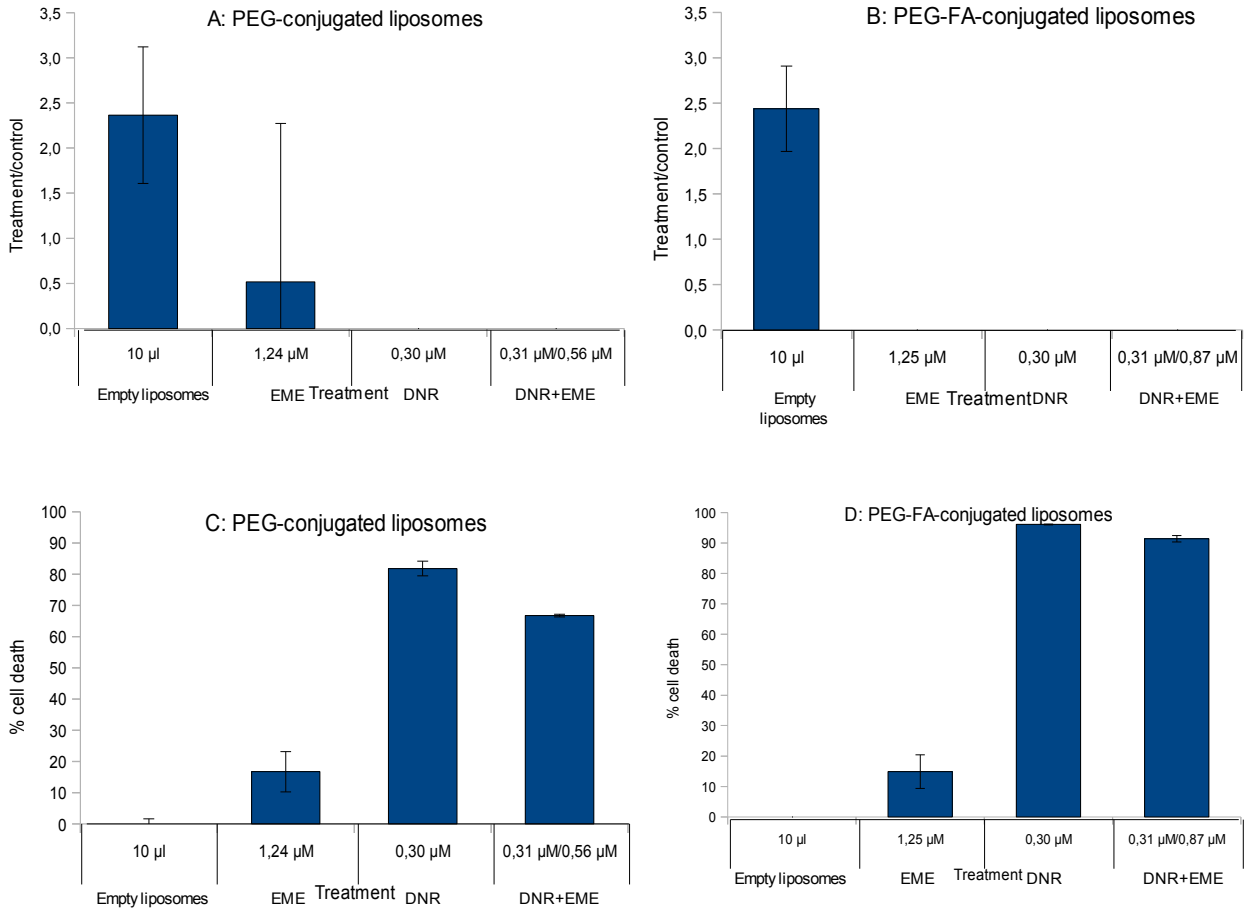

Figure 4.6: Death induction in MV4-11 cells by different liposomes. Cells (42000 cells/well) were incubated with liposomes (batch 1) for 30 min in 12-well tissue culture dishes, washed 3 times, and incubated for 72 h before WST-1 measurement and fixing of cells. The cells were cultured in FA-free medium for 4 days before the experiment and the experiment was conducted in FA-free medium. Panel A and B show results from WST-1 measurements, panel C and D results from fluorescence microscope cell counting using Hoechst 33342 as a fluorescent probe. The data are average of two parallels and the deviation.

4.2.2 Expression of folate receptor β (FOLR2) in MOLM-13 cells

Based on the results shown above, it was decided to use the MOLM-13 cells to evaluate the usefulness of the FA-conjugated liposomes in AML therapy. These cells showed a somewhat better response towards the FA-conjugated liposomes and also higher tolerance to different media than the MV4-11 cells. We found no previous studies that showed expression of FR-β in MOLM-13 cells,

and therefore wanted to verify the expression by Western blotting. SDS-PAGE and Western blotting was performed on MOLM-13 wt and MOLM-13 SH p53 (silenced p53) cell lines. The cells were cultured in medium with and without FA to investigate if FA depletion could influence the level of FR-β expression. As a negative control, we used HEK293 cells.

The FR-β blot was difficult to interpret (Figure 4.7). We identified a band most likely to be FR-β, but other bands were also present. The FR-β seemed to be expressed in both MOLM-13 cell lines, with no visible difference in expression between cells grown in medium with or without FA. The SDS-PAGE and Western blotting procedure was performed a total of three times with the same results. We suspect that the low intensity of the bands corresponding to FR-β can be due to poor quality of the anti-FOLR2 antibody: apparently it had been stored at 4°C rather than -20°C (supplier recommendations (72)) for 2 years.

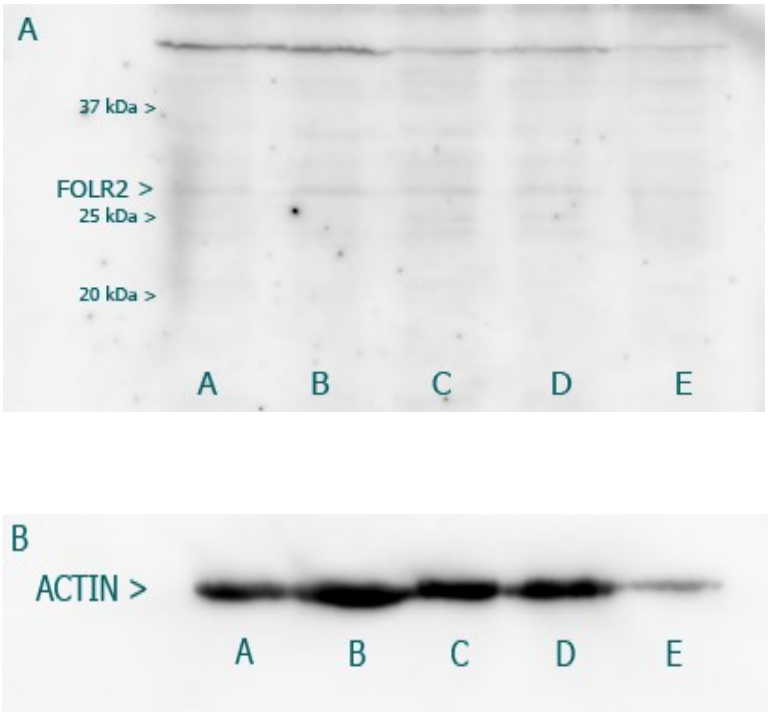

Figure 4.7: Expression of FOLR2 in MOLM-13 cells. A: FOLR2 Western blot. 50 µg protein was loaded for each sample. Lane A is MOLM-13 wt cultured in RPMI medium and lane B the same cell line cultured in FA-free medium for 33 days. Lane C is MOLM-13 SH p53 cultured in RPMI medium and lane D the same cell line cultured in FA-free medium for 4 days. Lane E is HEK293 as a negative control (cell lysate provided by Lene Myhren). B: Actin measurements performed on the same blot.

4.2.3 Evaluating effective dose and establishing difference in effect between PEG-FA-conjugated liposomes vs PEG-conjugated liposomes in MOLM-13 wt and MOLM-13 SH p53 cells

We next wanted to find the effective dose of DNR and EME in liposomes to induce cell death in MOLM-13 cells. It has previously been shown that leukaemia cells with deficient p53 are particularly sensitive to the combination of DNR and protein synthesis inhibitors (60). The MOLM-13 variant with silenced p53 (MOLM-13 SH p53) was therefore introduced in the experiments.

We found that PEG-FA-conjugated liposomes were more effective than PEG-conjugated liposomes in delivering both DNR, EME and the DNR+EME combination. A higher proportion of cell death was induced by PEG-FA-conjugated liposomes. This was true for both cell lines (Figure 4.8 – 4.10). The DNR+EME combination was found to induce less cell death than DNR alone. Also there was some batch-to-batch variation, liposome batch 2 seemed to be more effective than batch 3 (Figure 4.8 and 4.9). Comparing results between the cell lines, the MOLM-13 SH p53 cells were more vulnerable to liposome treatment than MOLM-13 wt cells (Figure 4.8 – 4.10).

In these experiments, we noted that the WST-1 data were not reliable. Figure 4.8 A and B show typical WST-1 data as examples of the inconsistent data obtained by using this assay. Fluorescence microscopy using DNR as a fluorescent probe (Figure 4.8 C and D, images in Figure 4.11) was considered a much more reliable method for death assessment.

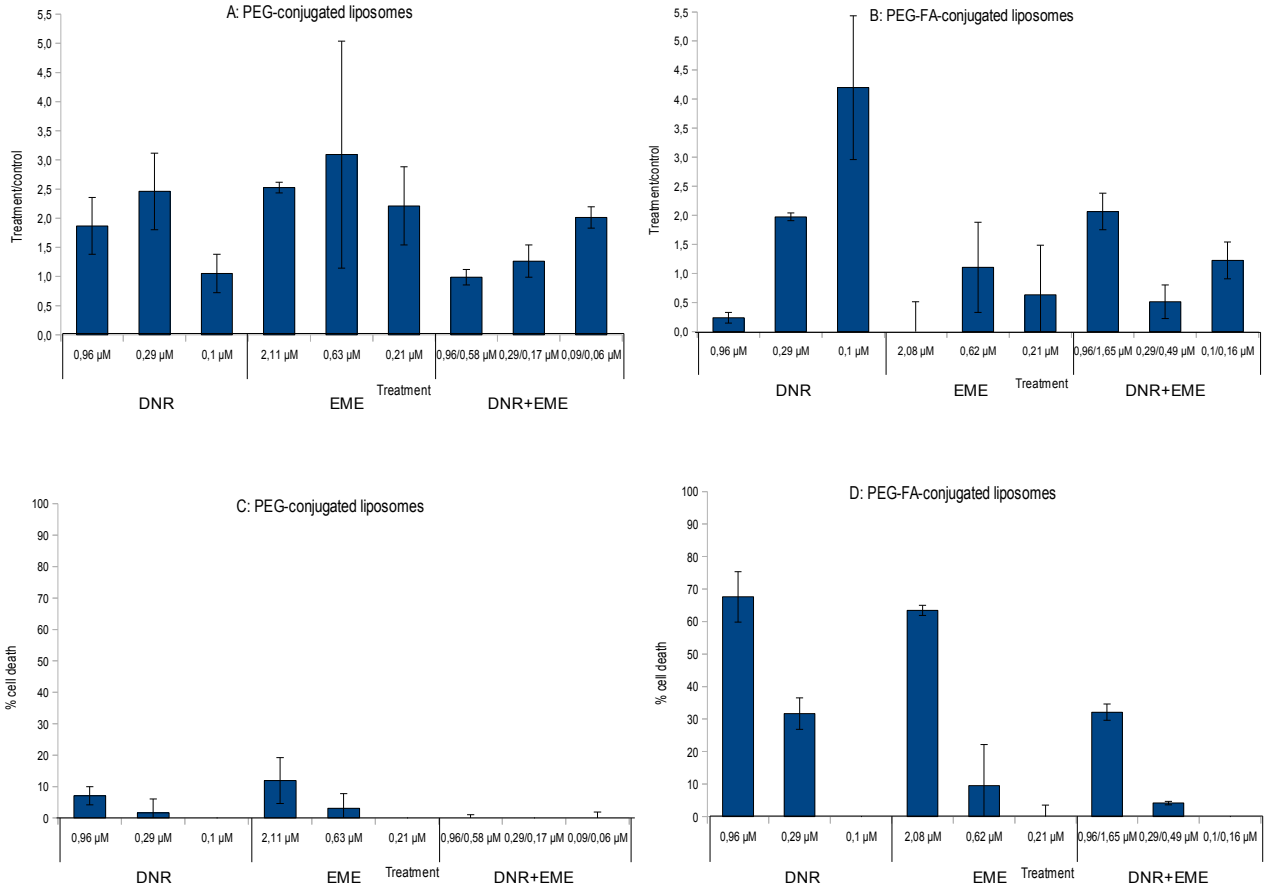

Figure 4.8: Death induction in MOLM-13 wt cells by different liposomes. Cells (40000 cells/well) were incubated with liposomes (batch 2) for 30 min in 48-well tissue culture dishes, washed 3 times, and incubated for 48 h before WST-1 measurement and fixing of cells. The cells were cultured in FA-free medium for 42 days before the experiment and the experiment was conducted in FA-free medium. Panel A and B show results from WST-1 measurements, panel C and D results from fluorescence microscope cell counting on nucleus morphology using DNR as a fluorescent probe. The data are average of two parallels and the deviation.

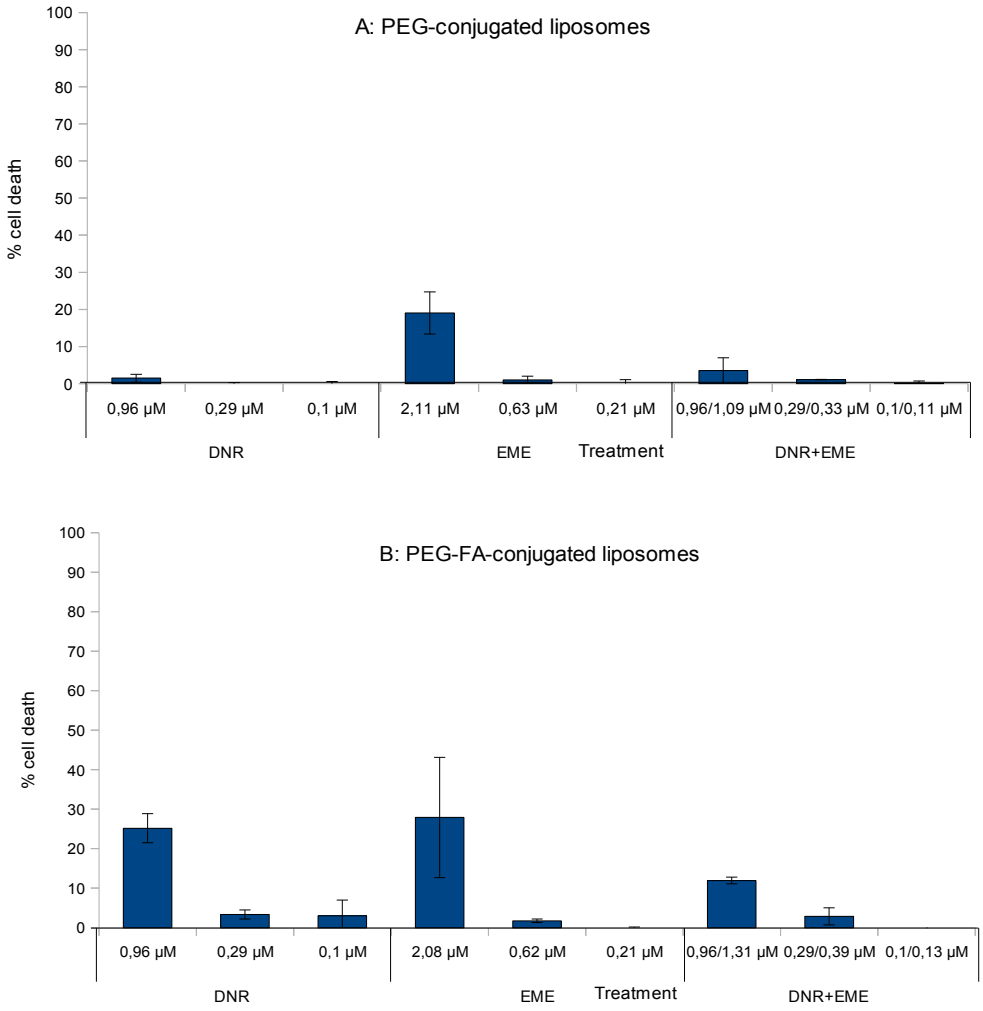

Figure 4.9: Death induction in MOLM-13 wt cells by different liposomes. Identical design and execution as described in Figure 4.8, but a different liposome batch was used (batch 3). WST-1 measurements were performed, but are not included here due to inconsistent results. The cells were cultured in FA-free medium for 36 days before the experiment and the experiment was conducted in FA-free medium. Panel A and B show results from fluorescence microscope cell counting on nucleus morphology using DNR as a fluorescent probe. The data are average of two parallels and the deviation.

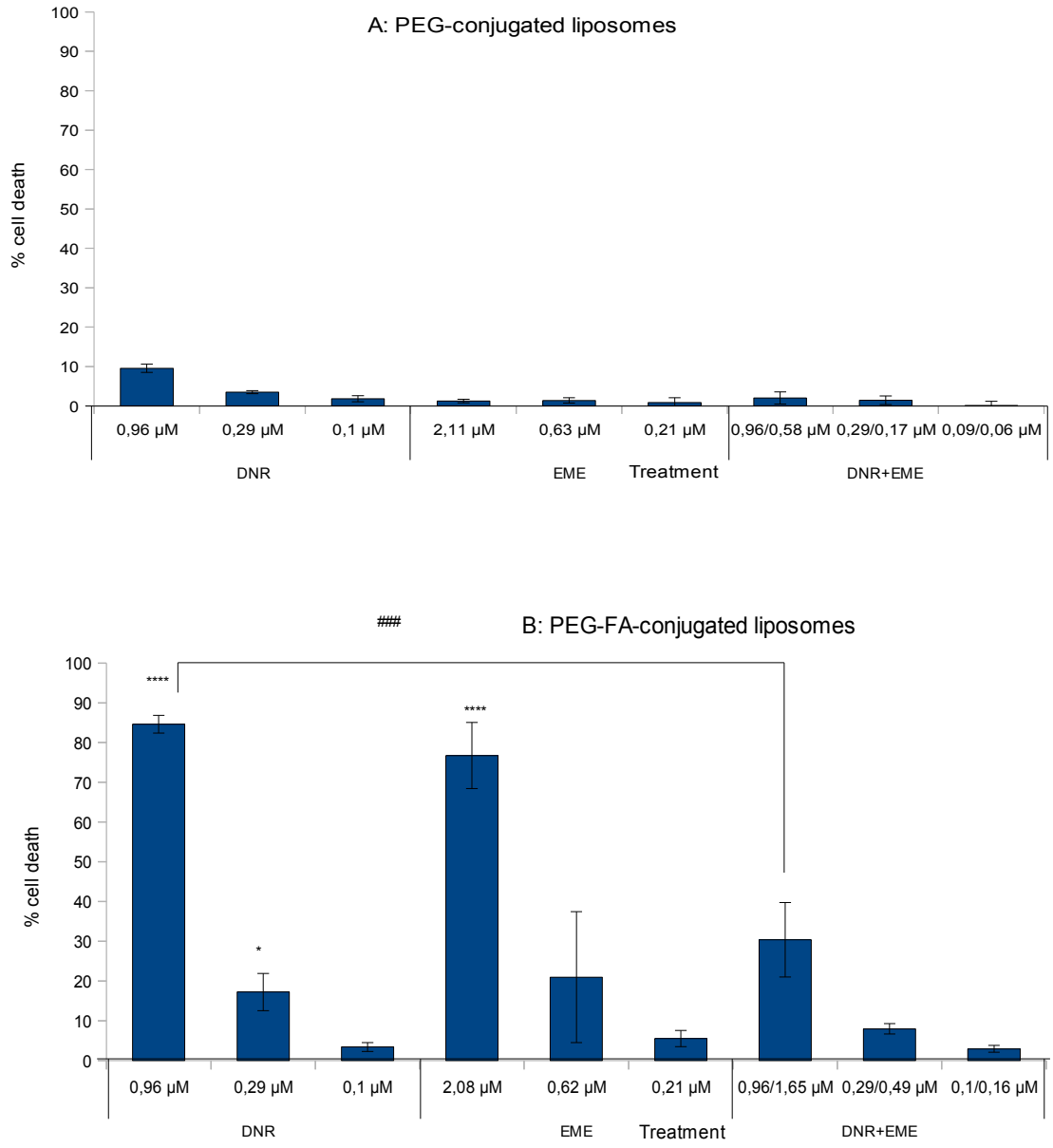

*Figure 4.10: Death induction in MOLM-13 SH p53 cells by different liposomes. Cells (40000 cells/well) were incubated with liposomes (batch 2) for 30 min in 48-well tissue culture dishes, washed 3 times, and incubated for 48 h before fixing. WST-1 measurements were performed, but are not included here due to inconsistent results. The cells were cultured in FA-free medium for 4 and 5 days before the experiment and the experiment was conducted in FA-free medium. Panel A and B show results from fluorescence microscope cell counting on nucleus morphology using DNR as a fluorescent probe. * refers to T-tests between PEG and PEG-FA treatments, while # refers to T-tests performed within the same liposome treatment. The data are average of four parallels (combined results from identical experiment performed on two different days) and the standard error.*

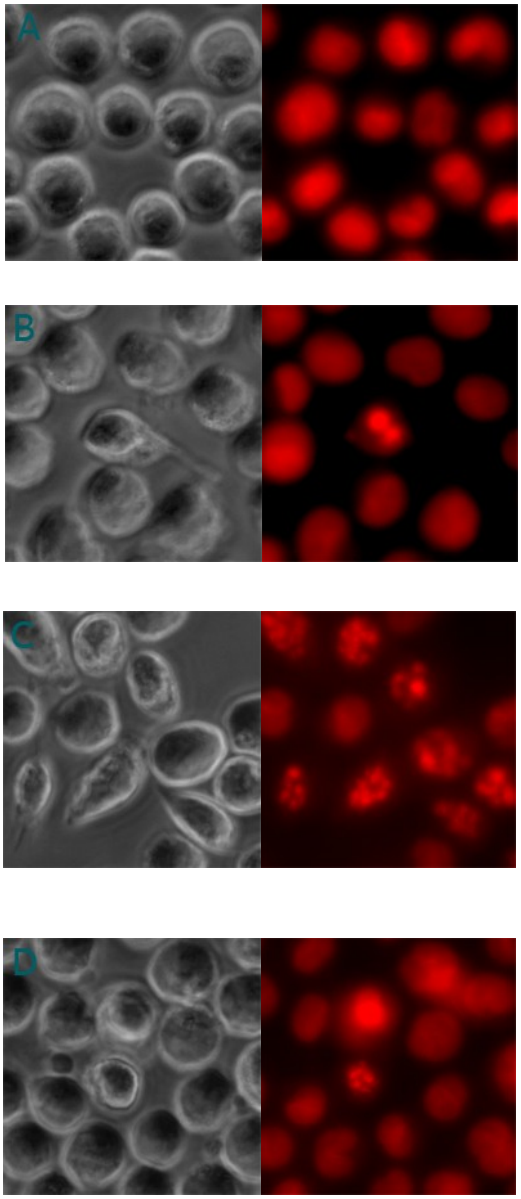

Figure 4.11: Cell and nucleus morphology of the MOLM-13 wt cell line treated with PEG-liposomes. A: control cells, B: DNR (0.96 μM) treated cells, C: EME (2.11 μM) treated cells, D: DNR+EME (0.96+1.09 μM) treated cells. Images to the left show surface morphology by phase contrast illumination, images to the right show nucleus morphology of nuclei stained with DNR, at laser cy3.5. Apoptosis morphology is characterised by condensed chromatin structures in a fragmented nuclei. In the light microscope, apoptotic cells are typically characterised by cell shrinkage, membrane blebs and an irregular surface.

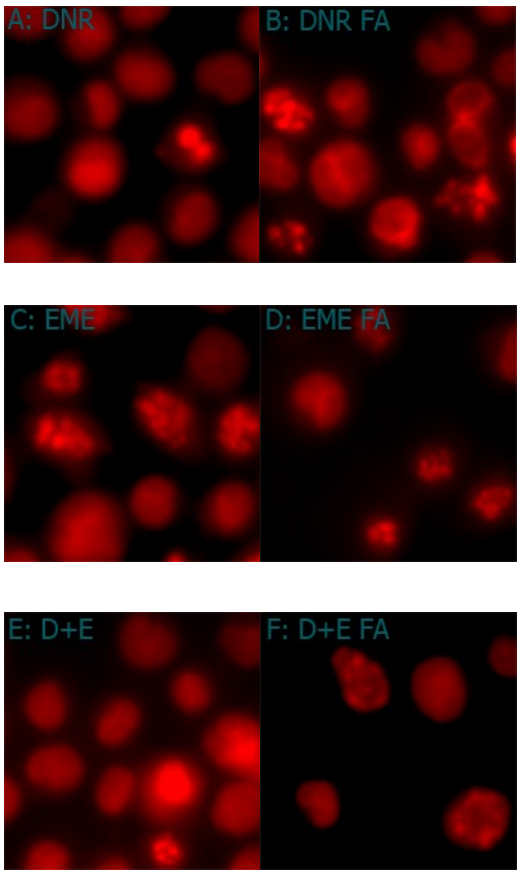

Figure 4.12: Nucleus morphology of the MOLM-13 wt cell line treated with PEG and PEG-FA conjugated liposomes: PEG-FA conjugated liposomes were more effective in inducing cell death than PEG conjugated liposomes. DNR was used to stain the nuclei for fluorescence microscopy. Images to the left show treatment with PEG-liposomes, images to the right PEG-FA-liposomes. A: DNR (0.96 μM) treated cells, B: DNR (0.96 μM) treated cells, C: EME (2.11 μM) treated cells, D: EME (2.08 μM) treated cells, E: DNR+EME (0.96 + 1.09 μM) treated cells, F: DNR+EME (0.96 + 1.31 μM) treated cells. Apoptosis morphology as described in Figure 4.11.

4.2.4 Optimisation of treatment regime with PEG-FA-conjugated liposomes

PEG-FA liposomes were established as more effective than PEG liposomes. We next wanted to investigate further for optimisation of PEG-FA-liposome treatment of AML cells by sequential incubation of liposomes. This was done on the basis of the work by Gausdal et al., who found that the protein synthesis inhibitor CHX was most effective when given after DNR addition (60).

PEG-FA liposomes loaded with DNR and PEG-FA liposomes loaded with EME were used in a pilot experiment performed in MOLM-13 cell lines (Figure 4.13). Adding PEG-FA-EME

liposomes subsequent to PEG-FA-DNR incubation was indeed more effective than incubation with both liposomes at the same time. The sequential incubation was also more effective than PEG-FA-DNR liposomes alone, but this difference was not statistically significant.

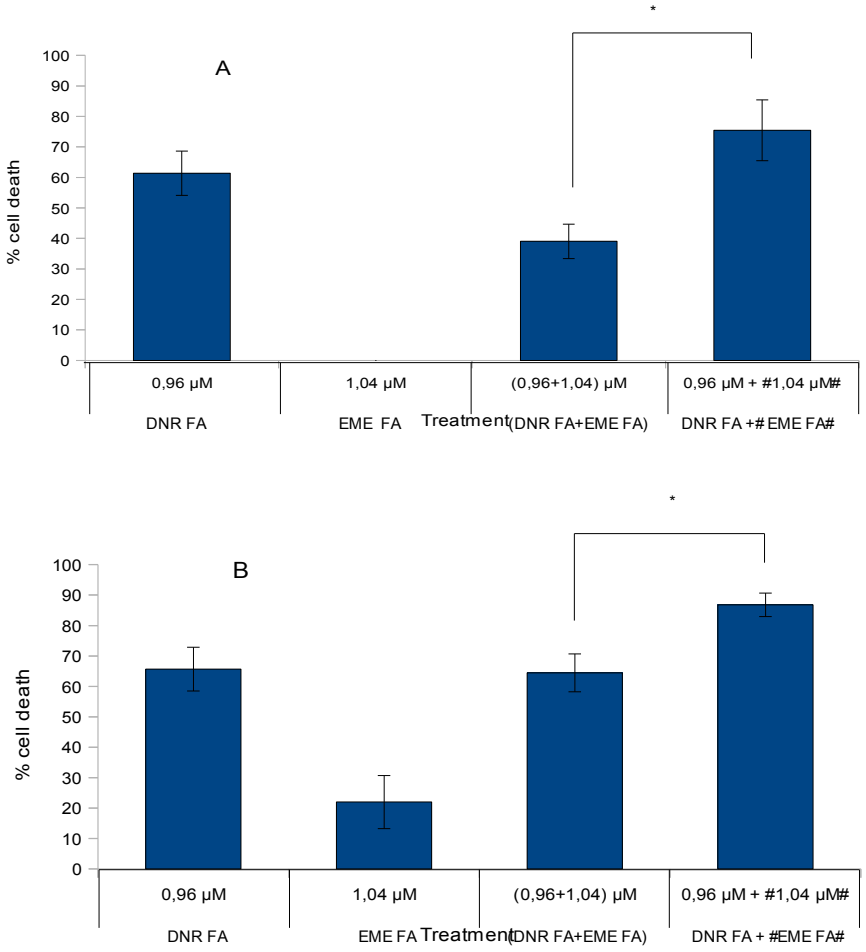

Figure 4.13: Death induction in MOLM-13 cells by PEG-FA-conjugated liposomes, sequential incubation. A: MOLM-13 wt, B: MOLM-13 SH p53. Cells (40000 cells/well) were incubated in 48-well tissue culture dishes with liposomes (batch 2) for 20 min, series 5 (DNR FA + #EME FA#): PEG-FA DNR only, all series were washed 3 times, series 5 was incubated with PEG-FA EME for 20 min, series 5 was washed 3 times, and finally all series incubated for 48 h before fixing of cells. The MOLM-13 wt and MOLM-13 SH p53 cells were cultured in FA-free medium for 9 and 15 days before the experiment was performed, respectively, and the experiment was conducted in FA-free medium. Panel A and B show results from fluorescence microscope cell counting on nucleus morphology using DNR as a fluorescent probe. The data are average of three parallels and the standard error.

We next decided to perform an extended experiment with additional doses of EME to investigate optimisation of doses. MOLM-13 SH p53 cells were chosen for the experiment because they seemed to be most vulnerable to liposome treatment (Figure 4.13).

This experiment did not show any statistically significant difference in effect for sequential incubation compared to simultaneous adding of liposomes (Figure 4.14). For the two lowest EME concentrations, simultaneous adding of liposomes seemed to be more effective, while sequential incubation was clearly most effective for the highest EME concentration. Sequential incubation was more effective than PEG-FA EME alone and PEG-FA DNR alone, except from in the lowest EME concentration where PEG-FA DNR alone appeared to be slightly more effective.

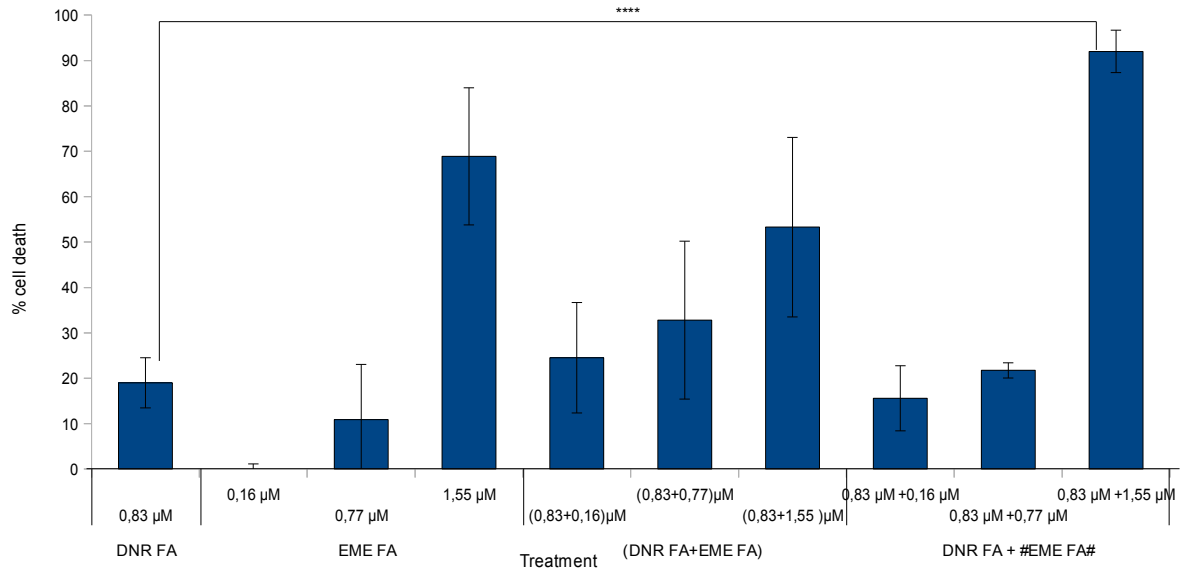

Figure 4.14: Death induction in MOLM-13 SH p53 cells, sequential incubation with PEG-FA-conjugated liposomes. Cells (40000 cells/well) were incubated in 48-well tissue culture dishes with liposomes (batch 3) for 20 min, series 5 (DNR FA + #EME FA#): PEG-FA DNR only, all series were washed 3 times, series 5 was incubated with PEG-FA EME for 20 min, series 5 was washed 3 times, and finally all series were incubated for 48 h before fixing of cells. The cells were cultured in FA-free medium for 8 days before the experiment was performed, and the experiment was conducted in FA-free medium. Results from fluorescence microscope cell counting on nucleus morphology using DNR as a fluorescent probe. The data are average of three parallels and the standard error.

4.2.5 Comparing the effect of free cytostatics against liposome-encapsulated cytostatics in MOLM-13 SH p53 cells

The effect of DNR and EME-incorporated liposomes in the MOLM-13 cell lines was clearly demonstrated, and it was also shown that PEG-FA liposomes were more effective than PEG-liposomes. However, it was desirable to compare the effect of liposomal drugs with the drugs in free form. An experiment was done based on DNR and EME doses given in a previous experiment (see Figure 4.10), and the design was ensured to be identical. Direct comparison between the effect of liposomal and free drug was now possible.

The free drug was clearly most effective for DNR and DNR+EME-treatments (Figure 4.15). For EME-treatments, however, PEG-FA-conjugated liposomes were in fact more effective than free drug, and the difference was statistically significant for the 2.08 µM dose.

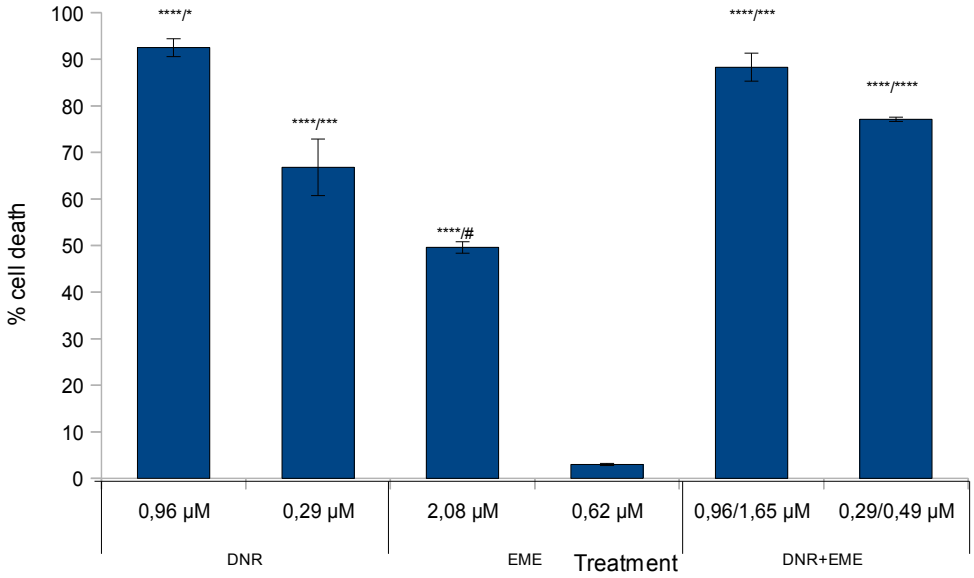

*Figure 4.15: Cell death induction by free DNR and EME in MOLM-13 SH p53 cells. The experimental design and execution was identical to that described in Figure 4.10, therefore the results are comparable. The cells were cultured in FA-free medium for 31 days before the experiment and the experiment was conducted in FA-free medium. Results from fluorescence microscope cell counting on nucleus morphology using DNR as a fluorescent probe. The data are average of three parallels and the standard error. * refer to when free cytostatics are most effective, # to when liposomal cytostatics are most effective; PEG-conjugated liposomes/PEG-FA-conjugated liposomes.*

4.2.6 Flow cytometry of PEG and PEG-FA containing fluorescent liposomes

The flow cytometry experiment was performed to investigate the uptake of liposomes into MOLM-13 SH p53 cells. We wanted to investigate the extent of uptake of liposomes, and also see if there was a difference in uptake of PEG-FA liposomes compared to PEG-liposomes, which the results from previous experiments suggested.

The results from this experiment are not shown graphically. In summary, we were not able to identify Texas Red fluorescence in any of the prepared samples compared to the control cells, suggesting that the liposomes were not taken up.

4.3 Evaluation of the efficacy of liposomes in PC-3 and LNCaP prostate cancer cell lines

Another cancer that is associated with over-expression of folic acid binding surface proteins is prostate cancer (41). We therefore wanted to test efficacy of the liposomes on the prostate cancer cell lines PC-3 and LNCaP. The LNCaP cell line is known to endogenously express PSMA (41, 42), a possible target for FA-conjugated liposomes (see section 1.2.2), whereas the PC-3 cell line does not (42). On the other hand, PC-3 cells have deficient p53 (66), which could make them more sensitive to the combination of DNR and protein synthesis inhibitor.

4.3.1. Efficacy of PEG-FA-conjugated liposomes vs PEG-conjugated liposomes in LNCaP and PC-3 prostate cancer cell lines

A pilot experiment was performed to investigate the efficacy of liposomes in prostate cancer cell lines. Nearly equivalent doses of cytostatics were given so that results were comparable between PEG-FA and PEG-conjugated liposomes. The experimental design and execution was identical for the PC-3 and LNCaP cell line.

Results for the PC-3 cells are shown in Figure 4.16. Empty liposomes were shown to have no effect on cell viability or cell death. Drug-incorporated liposomes induced cell death and reduced cell viability at concentrations below 8.22 μM EME, 0.53 μM DNR and 0.54+0.98 μM DNR+EME. Cell viability and cell counting results correlated well. PEG-FA liposomes were more effective than PEG liposomes. The DNR+EME combination was more effective than the drugs given separately for PEG-FA-conjugated liposomes, and the combination was somewhat less effective compared to

DNR alone for PEG-conjugated liposomes. Figure 20 shows cell and nucleus morphology of the PC-3 cell line, with DNR used as a fluorescent probe.

Results for the LNCaP cells are shown in Figure 4.17. The findings were essentially the same as for the PC-3 cells. Empty liposomes had no effect on cell viability and death, and the drug-incorporated liposomes induced cell death and reduced cell viability at concentrations lower than 2.17 µM EME, 0.53 µM DNR, and 0.54+1.52 µM DNR+EME. Cell viability and cell counting results correlated well. PEG-FA-conjugated liposomes were clearly more effective than PEG-liposomes. The cells seemed to be more vulnerable to DNR treatment than EME treatment. Figure 4.18 shows cell and nucleus morphology of LNCaP cells using Hoechst 33342 as a fluorescent probe.

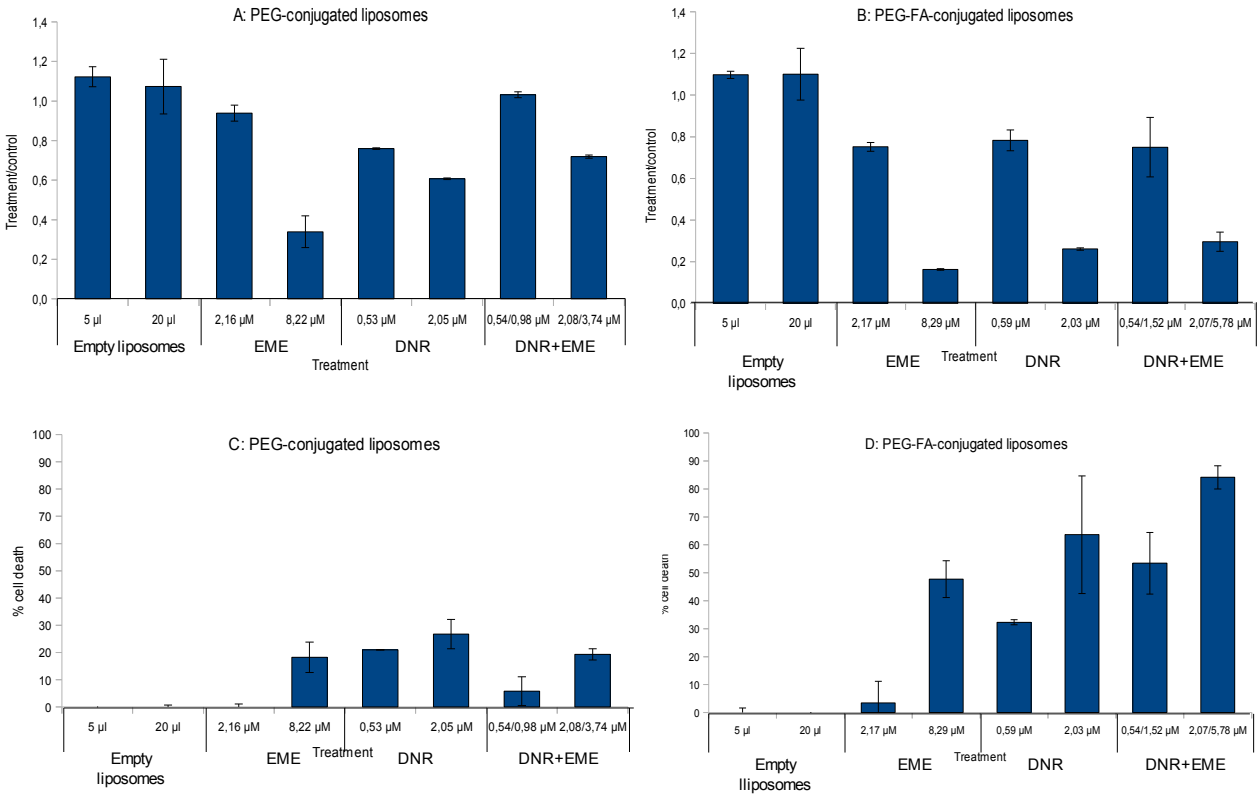

Figure 4.16: Death induction in PC-3 cells by different liposomes. Cells (3000 cells/well) were seeded in a 48-well tissue culture dish 2 days before the experiment. The cells were incubated with liposomes (batch 1) for 30 min, washed 2 times, and incubated for 72 h before WST-1 measurement and fixing of cells. Panel A and B show results from cell viability assay WST-1, panel C and D show results from cell counting on cell and nucleus morphology using Hoechst 33342 as a fluorescent probe. The data are average of two parallels and the deviation.

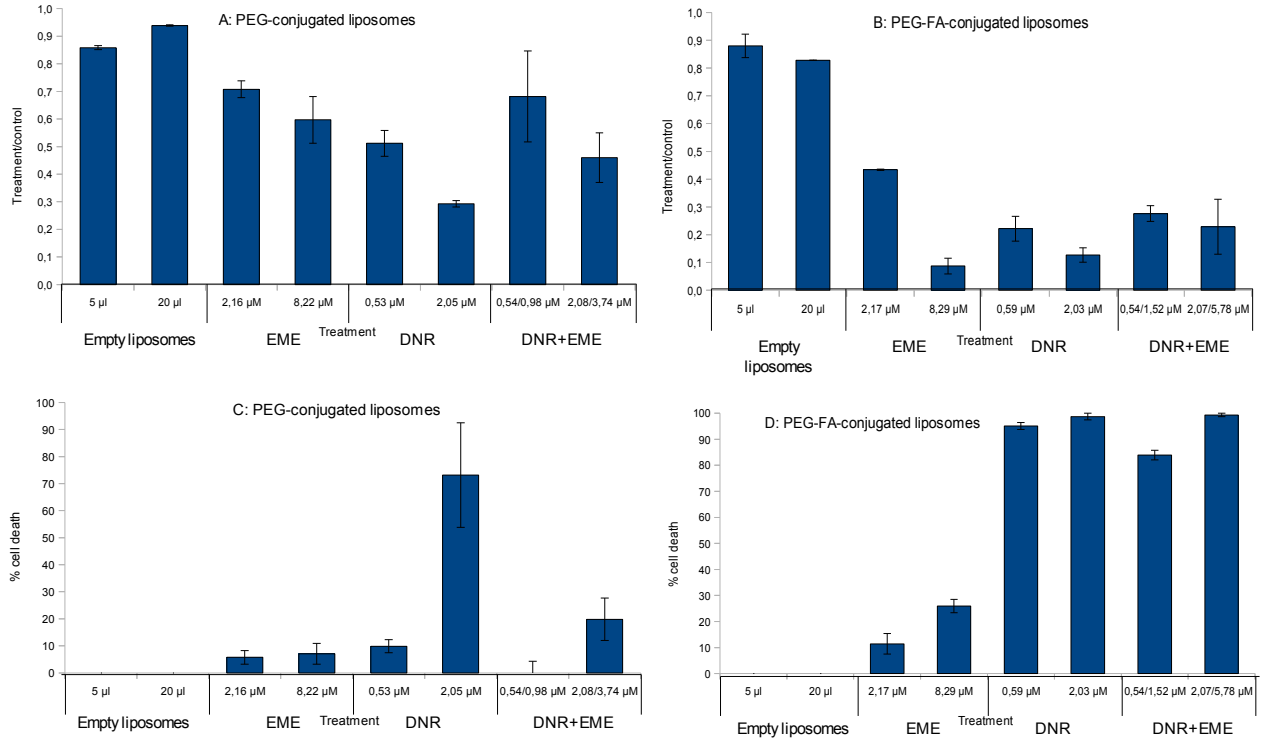

Figure 4.17: Death induction in LNCaP cells by different liposomes. Cells (3000 cells/well) were seeded in a 48-well tissue culture dish 2 days before the experiment. The cells were incubated with liposomes (batch 1) for 30 min, washed 2 times, and incubated for 72 h before WST-1 measurement and fixing of cells. Panel A and B show results from cell viability assay WST-1, panel C and D show results from cell counting on cell and nucleus morphology using Hoechst 33342 as a fluorescent probe. The data are average of two parallels and the deviation.

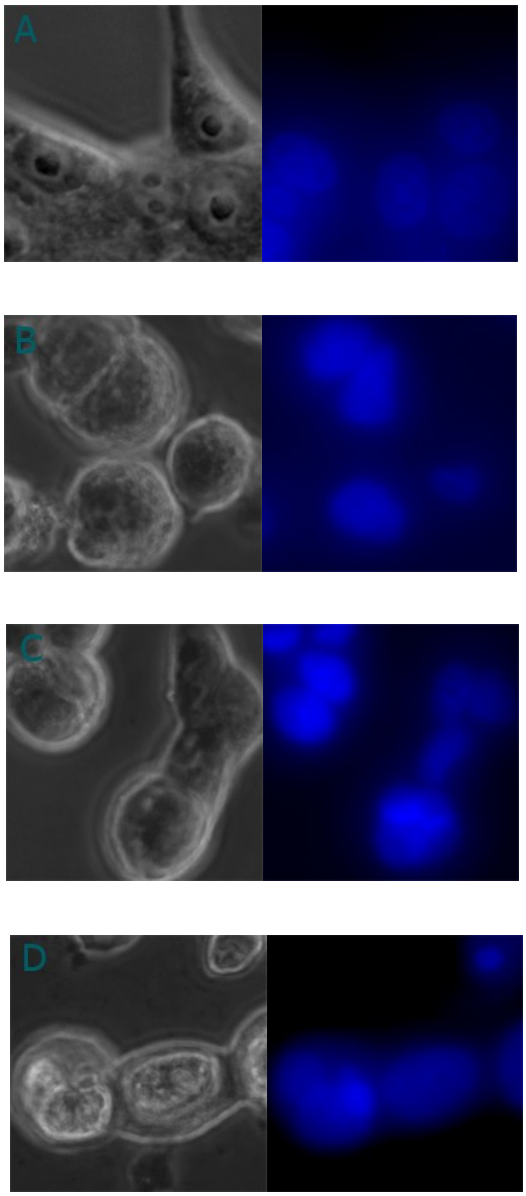

Figure 4.18: Cell and nucleus morphology of LNCaP cells treated with PEG-conjugated liposomes. Images to the left show surface morphology by phase contrast illumination. Images to the right show nucleus morphology using Hoechst 33342 as a fluorescent probe. Panel A: control cells, panel B: DNR (2.05 μM) treated cells, panel C: EME (8.22 μM) treated cells, panel D: DNR+EME (2.08+3.74 μM) treated cells.

4.3.2. Enforced expression of PSMA in the PC-3 cell line and evaluation of liposome efficacy

We next wanted to investigate if enforced expression of PSMA made PC-3 cells more vulnerable to liposome treatment.

First, a transient transfection of the PC-3 cell line with PSMA using calcium phosphate was attempted without success. Very few cells were transfected; only 20 cells per well in a 6-well tissue culture dish 48 h after the transfection. Experiments were not performed with these cells.

Next, a transient transfection of the PC-3 cells with PSMA was performed using lipofectamine. Half of the cells were transfected with empty vector to serve as a control in cell experiments. GFP was co-expressed as a marker for transfection efficiency. The transfection was quite successful, with 25% of the cells expressing GFP. GFP expression was estimated by cell counting in the fluorescence microscope (see pictures Figure 4.20).

Cell lysates for Western blotting were made with the aim of confirming PSMA expression. SDS-PAGE and Western blot was executed with help from Nina Lied Larsen. The blot showed very weak bands (Figure 4.19). However, two bands could be seen for LNCaP cells, the positive control, in an area consistent with the size of PSMA (Figure 4.19, lane 2). Bands were detected for NRK cells and all PC-3 cell samples (Figure 4.19, lane 1, 3, 4 and 5) at a different size, but disappointingly no band could be detected verifying PSMA-expression for the transfected PC-3 cells (lane 5). A possible explanation is that there were not enough transfected cells present in the PC-3 sample for a band to be detected. The blot could also indicate that the cells were not transfected with PSMA, as GFP is co-transfected in a separate plasmid, and can be expressed independently of PSMA.

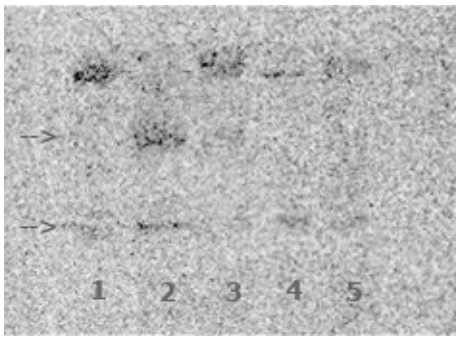

Figure 4.19: Western blot of PSMA. Lane 1: NRK cells used as a negative control, lane 2: LNCaP cells used as a positive control, lane 3: PC-3 cells, lane 4: Empty vector-transfected PC-3 cells, lane 5: PSMA-transfected PC-3 cells. Arrows indicate bands for PSMA in lane 2. 45 µg protein was loaded on the gel for each sample. Actin measurement was not performed.

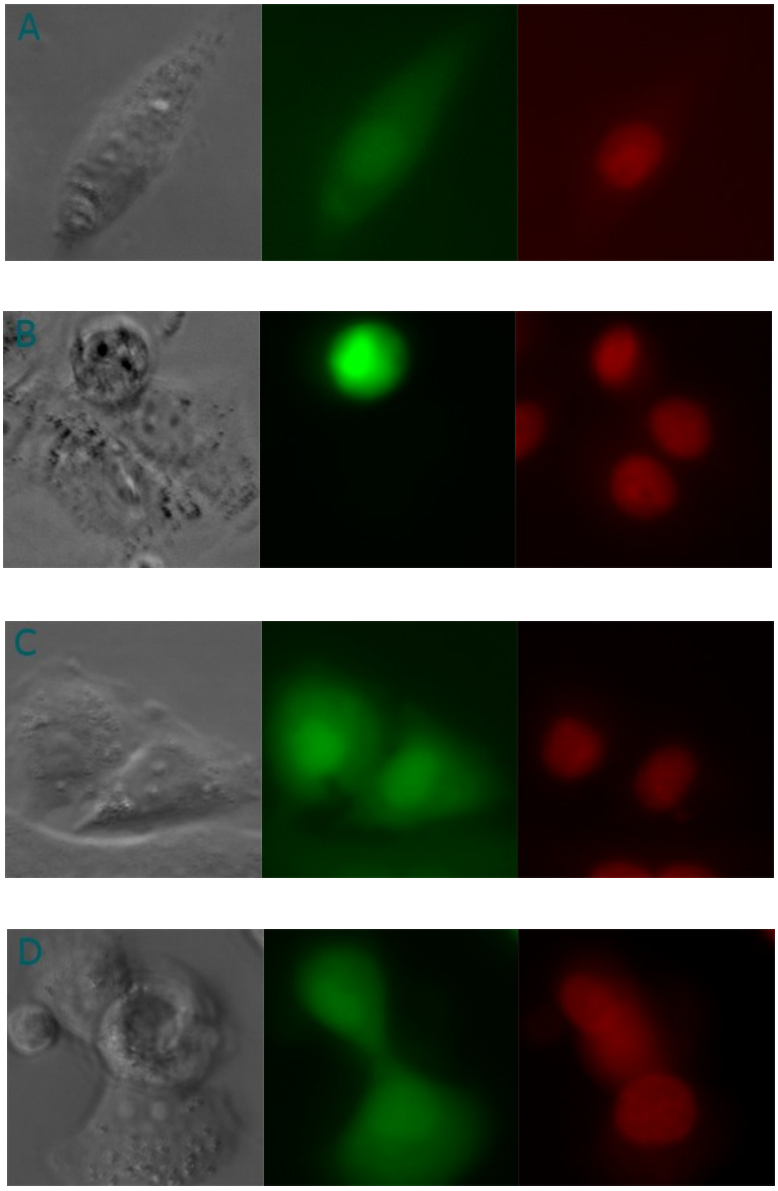

Figure 4.20: PC-3 cells transfected with GFP and PSMA, treated with drug-loaded PEG-conjugated liposomes. Images to the left show surface morphology by phase contrast illumination. Images in the middle show GFP-expressing cells, detected by the FITC laser. Images to the right show nucleus morphology using DNR as a fluorescent probe. A: Control cells, B: DNR (2.13 μM) treated cells , C: EME (2.41 μM) treated cells, D: DNR+EME (2.13+2.41 μM) treated cells.

Next, a cell experiment was performed on the transfected cells. The PEG-FA-conjugated liposomes were more effective for both PSMA-transfected and empty vector-transfected control cells and the difference in efficacy between the two cell types was not as large as expected (Figure 4.21). However, the transfection efficiency was only 25% judged by GFP-positive cells, only 50 cells were counted per well and PSMA was not successfully detected by Western blot (Figure 4.19).

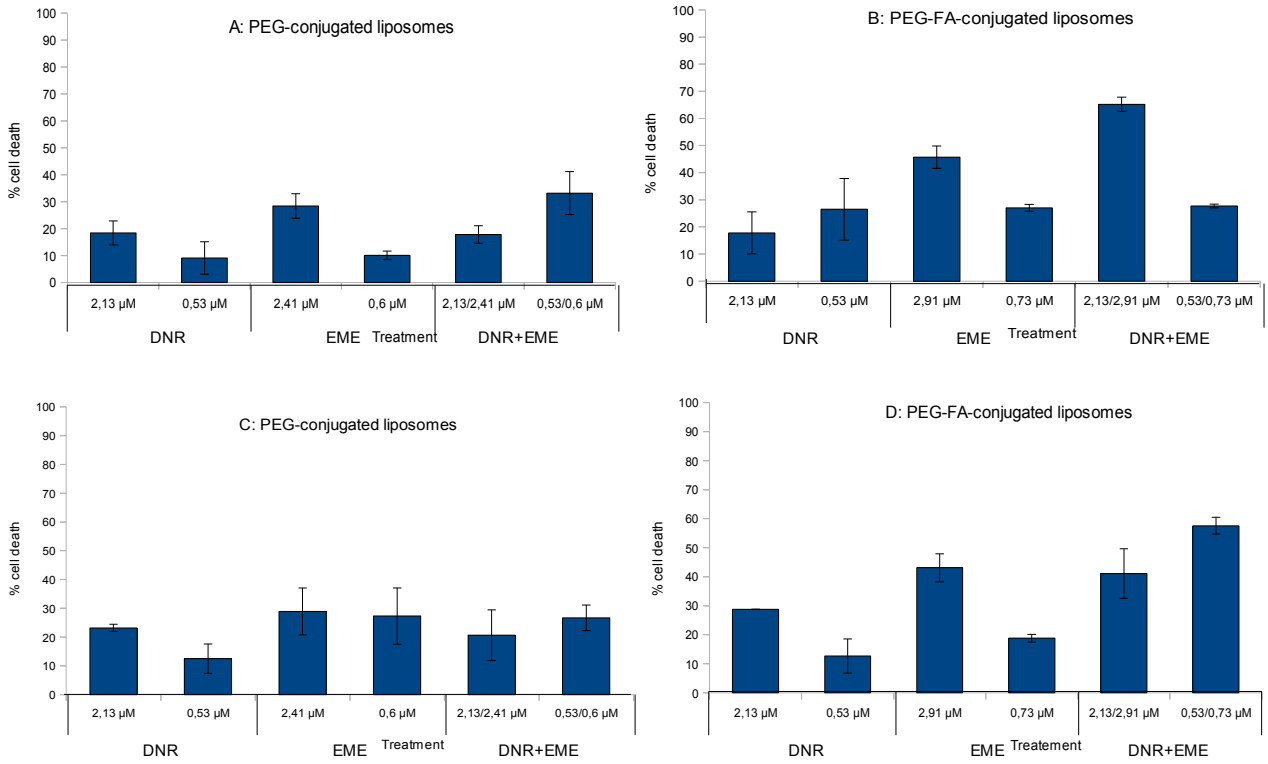

Figure 4.21: Comparison of the efficacy of liposomes between PSMA-transfected PC-3 cells and PC-3 control cells transfected with empty vector. Cells (5000 cells/well) were seeded in a 48-well tissue culture dish one day before the experiment. The cells were incubated with liposomes (batch 3) for 30 min, washed 2 times, and incubated for 48 h before fixing of cells. WST-1 measurements were performed but are not included here. Panel A and B show results for PSMA-transfected cells. Panel C and D show results for empty vector-transfected cells. DNR was used as a fluorescent probe for cell counting based on nucleus morphology (see figure 4.21). Only GFP-positive cells were counted, at least 50 cells per well. The data are average of two parallels and the deviation.

4.4 Effect of PEG-FA-conjugated liposomes on non-malignant cells

We next wanted to investigate if PEG-FA-conjugated liposomes could enhance drug effects in non-malignant cells. The NRK cell line was used for this purpose. The experimental design was identical to the experiment with prostate cancer cells described in Figure 4.21.

Results are shown in Figure 4.22. WST-1 results showed decreased metabolic activity for cells treated with liposomes containing EME and DNR+EME, and PEG-FA-liposomes seemed to give a larger decrease in metabolic activity than PEG liposomes. The decrease in metabolic activity

seen for EME and DNR+EME was not reflected entirely by cell counting. Results from fluorescence cell counting on nuclear morphology showed that PEG liposomes did not cause any cell death in the given concentrations. PEG-FA liposomes caused some cell death (10%) for the highest concentrations of DNR and EME. In comparison, MOLM-13 cell lines experienced 60 – 80% cell death at a DNR concentration of 0.96 µM (batch 2, PEG-FA liposomes) and 60 – 75% cell death at an EME concentration of 2.08 µM (batch 2, PEG-FA liposomes). The LNCaP and PC-3 cell lines experienced 100% and 60% cell death at a DNR concentration of 2.03 µM (batch 1, PEG-FA liposomes) and 25% and 50% cell death at an EME concentration of 8.29 µM (batch 1, PEG-FA liposomes), respectively.

In summary, liposome-incorporated cytostatics was seen to be far more cytotoxic for leukaemia and prostate cancer cell lines than for the non-malignant NRK cell line. Presence of FA on the liposomal surface enhanced drug efficiency also in NRK cell lines.

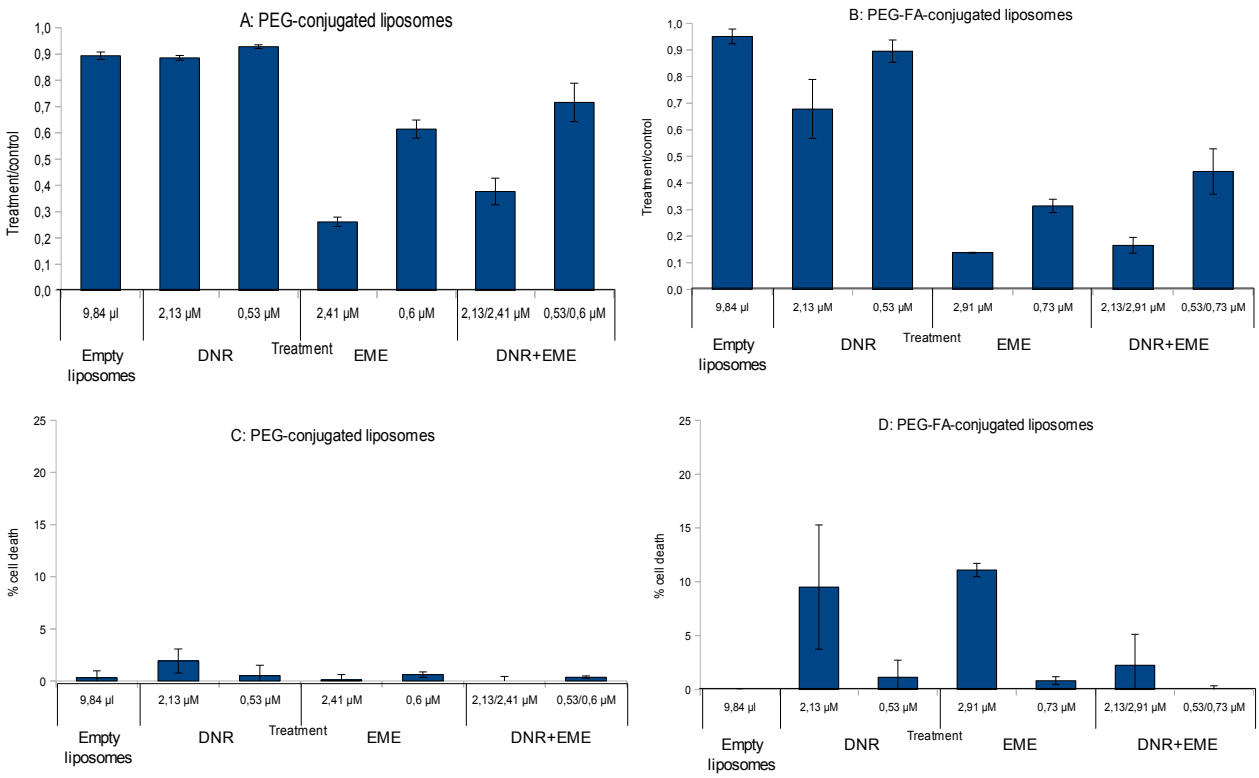

Figure 4.22: Death induction by liposomes in a non-malignant cell line: NRK cells. Cells (5000 cells/well) were seeded in a 48-well tissue culture dish 24 h before the experiment was performed. Cells were incubated with liposomes (batch 3) for 30 min, washed 2 times, and incubated for 48 h before WST-1 measurements and fixing of cells. Panel A and B show results from WST-1 measurements, panel C and D show results from fluorescence cell counting on nucleus morphology using DNR as a fluorescence probe. The data are average of three measurements and the standard error.

5. Discussion

5.1 Production of multifunctional liposomes

We were able to produce liposomes that combined several desirable properties for cancer treatment. The liposomes were PEGylated for minimal MPS recognition, prolonging circulation times in vivo. We were able to successfully incorporate DSPE-PEG-FA into the liposomes, creating FA-coated liposomes that enabled targeted drug delivery via FR-β and PSMA. Also, we were able to incorporate two cytostatics into a single liposome, obtaining a drug carrier for two different drugs. A synergistic effect of the drugs could thus be investigated by this system.

All the desired properties were incorporated into a single liposome, enabling targeted drug delivery and favourable alteration of pharmacokinetic properties of the drugs. The liposomes were designed to be stable and retain the cytostatics inside; thereby protecting cytostatics from degradation and elimination, and also protecting healthy tissues from the cytostatics, reducing toxic side-effects. This is especially promising for AML treatment with DNR, which suffers from serious cardiotoxic adverse effects (56).

For the empty liposomes, the measured ZP was substantially lower than for the drug-incorporated liposomes (see Table 4.8). This could be due to association of positively charged drug molecules (see Figure 1.6) to the negatively charged DSPE-PEG (73, 74) on the outside of the liposomes. Suspensions with a Zeta potential higher than +30 mV or lower than -30 mV are normally considered to exhibit colloidal stability (71). Our measurement results indicate that the liposome suspensions will aggregate over time, and it is more likely that drug-incorporated liposomes will aggregate since this zeta potential is closer to zero compared to the zeta potential of empty liposomes. However, flocculation or sedimentation was never visually observed for empty or drug-loaded liposome suspensions, the particle size was constant and PdI increased only slightly during 39 days of storage (Table 4.6). We therefore consider the colloidal stability to be satisfactory over the period of time that the liposomes were used. The suspensions were shaken before use to re-suspend liposome aggregates if any should be present.

The size of the liposomes increased modestly after suspending in sucrose. We consider the most likely explanation to be due to the low ionic strength of sucrose compared to PBS, which the liposomes normally have been suspended in. Low conductivity media extends the electrical double layer and hence the measured hydrodynamic diameter of the liposomes, which is measured by DLS (70). Supporting this view is the fact that the liposome size remained constant over three measurements. The size increase could also be due to sucrose molecules absorbing to the PEG

chains or, less likely, caused by leakage of water molecules over the lipid bilayer into the liposome core. Another factor that could affect our results both for ZP and size measurements is the viscosity of the medium (70, 71). Water was set to solvent during the measurements since sucrose was not an option in the software, and the viscosity of sucrose solution is higher than that of water (75-77).

The drug content of the liposomes was seen to vary among the batches, and the measured EME concentration was higher than the DNR concentration (Table 4.4). This phenomenon could be explained by the gel filtration. Since collection of liposomes were by visual inspection of the elute, the fractions containing DNR, which had a red colour, were larger than the un-coloured EME liposome fractions. For batch 3, the yielded fractions were 2.1 ml EME-liposomes and 3.5 ml DNR-liposomes. Hence, the DNR-containing fractions were more diluted and the concentration was lower. Also, EME could be located in the lipid bilayer due to its structural resemblance to cholesterol (see chemical structure of EME in Figure 1.5), which could contribute towards a higher apparent encapsulation efficiency for this drug. The incorporation of two drugs simultaneously turned out to be especially difficult to reproduce in terms of concentrations. Batch-to-batch variation was also seen to some extent in terms of size (Table 4.1).

No apparent drug-release was noted from the DNR-containing liposomes after 39 days of storage at 4°C in the dark. Drug-release was estimated by visual observation during gel filtration, and theoretically DNR could be retained in the column in low concentrations that were not visible. Therefore, a future improvement would be measuring drug leakage of the liposomes quantitatively. Stability testing performed by Herfindal on liposomes in serum at 37°C for 24 h showed that the DNR content did not decrease substantially (unpublished data). The drug-leakage of EME-containing liposomes was not measured since EME is un-coloured, making the gel filtration method impossible to use. Therefore the stability of these liposomes was not investigated as thoroughly as for DNR-containing liposomes. Drug-release of EME-containing liposomes needs to be investigated in the future.

PC content measurements of the liposomes were attempted without success (Table 4.3). There are several possible explanations to why we were not able to obtain reliable measurement results. Liposomes are composed of phospholipid bilayer membranes, and lysis of the liposomes is necessary for PC detection. The results suggest that the liposomes were not lysed. We suspect that the PEGylation of the liposomes could contribute to this. The PEG chains could induce sterical hindrance for the enzymatic reaction with PC, and this need to be subjected for the assay to work in our system. Cholesterol is also a part of our liposome formulation, which makes the packing of the phospholipids denser (48). This could make lysis of the liposomes more difficult.

The liposomes were used for up to 8 weeks after they were made, and it must be taken into

consideration that the stability in a time period over 39 days was strictly not tested. It would strengthen the experimental design if this had been performed routinely. More extensive stability testing of the liposomes is a future area of investigation. However, the results from the measurements at 39 days strongly suggested that the liposomes were stable for a longer period of time since no aggregates were detected and the size did not increase substantially (Table 4.5). In conclusion, for the use in this thesis we consider that the liposomes showed sufficient stability.

A flow cytometry experiment was performed to investigate the cellular uptake of liposomes. We were not able to detect a difference in emitted fluorescence between control cells and cells treated with liposomes. A possible explanation could be the very short incubation time of 10 min. A study showed that FA-conjugated liposomes were associated to FA-expressing cells within 30 min, and after 50 min incubation time receptor-mediated liposomal internalisation was observed (29). It is also possible that the washing procedures following the short incubation time were too vigorous. On the other hand, experiments performed on LNCaP cells showed liposomal uptake on confocal microscopy with an incubation time of 10 min (Herfindal 2012, pers.comm.). We also suspect that the laser and filter settings of the flow cytometer might have been wrong. Finally, there is a possibility that there was something wrong with the liposome batch or the Texas Red fluorochrome.

In summary, we were able to produce multifunctional liposomes that showed sufficient stability for the use in this thesis.

5.2 Efficacy of multifunctional liposomes in FR-expressing AML cell lines

PEG-FA-conjugated liposomes were clearly more effective than the PEG-conjugated liposomes in AML cell lines (Figure 4.5 and 4.8 – 4.10). A literature search did not reveal any studies that reviewed the expression of FR-β in MOLM-13 cells. However, we confirmed by Western blotting (Figure 4.7) that the MOLM-13 cell lines expressed FR-β, which indicated that targeted drug delivery was achieved via this receptor. The bands for the blot were weak, other bands were present and the FR antibody was suspected to be of poor quality due to wrong storage conditions. Western blot was performed on MV4-11 cells, a cell line known to express FR-β (22), with similar results (data not shown). Still, by Western blotting we detected a band that corresponds to the size of FR-β (Figure 4.7), and the results from our experiments strongly suggest the presence of functional FR due to the improved efficacy of PEG-FA-conjugated liposomes compared to PEG-conjugated liposomes. There was no visible difference in expression level between cells cultured in FA-free and FA-containing medium, although culturing in FA-free medium can induce up-regulation of FR (16).

Targeted drug delivery to AML cells via FR-β has been performed in several studies (22, 23), and our results confirm the success of this strategy. This in vitro success is promising for further animal experiments, and possibly in the future leading to a new treatment for AML. Liposomal drug delivery also has the potential of reducing the serious side-effects associated with the standard AML treatment, especially regarding to anthracycline cardiotoxitciy (56, 58). This could warrant the opportunity of treating more patients older than 60 years, a group of patients with very low disease survival (5).

Data suggest that AML originates from leukaemic stem cells (LSCs), a rare population of cells capable of self-renewal, proliferation and differentiation (11, 24). Cytarabin is notably ineffective against LSCs, and there is a need for targeted strategies to kill these cells (11). Since FR-β is frequently co-expressed with CD34 in AML cells, it is likely that LSCs express functional FR-β (15, 23). Therefore, FR-targeted liposomes could offer a means of targeting LSCs. It was demonstrated by Li and co-workers that FA-conjugated liposomes filled with doxorubicin decreased colony forming units in AML cells, suggesting that these liposomes could be used to target LSCs (22).

Cell cytotoxicity was the end point of measurement in the AML cell lines. Empty liposomes had no effect on cell cytotoxity, so the liposomes themselves were not considered a confounding factor in the interpretation of the results. WST-1 measurement results on the MOLM-13 cell lines gave inconsistent readings, and we concluded that fluorescence microscopy was the most reliable method, with cell death morphology as the end point. The WST-1 cell viability assay is dependent on the activity of mitochondrial enzymes of the cells. If a cell line has a generally low mitochondrial activity, the conversion of the tetrazolium salt will be low, and small differences in activity will have a large impact on the results. This could be a possible explanation to our results. Also, rupture of lysosomes could increase WST-1 turnover and produce false positive results.

The incubation time with liposomes was set to 20 or 30 min for all experiments. A study of targeted drug delivery in AML cells using FA-conjugated liposomal DOX reported an incubation time of 2 h (22). The relatively short incubation times used in this thesis provides a strict test for drug delivery via multifunctional liposomes, valuable for future in vivo experiments. Since we found a distinct increase in activity when using PEG-FA-conjugated liposomes with these relatively short incubation times, we conclude that this drug delivery device has potential also in in vivo experiments.

Two identical experiments were performed on the MOLM-13 wt cell line using two different liposome batches (Figure 4.8 and 4.9). The trend was clearly the same in both experiments: PEG-FA-conjugated liposomes were more effective than PEG-conjugated liposomes. This shows that we

were able to obtain similar results between different liposome batches. However, the first experiment (Figure 4.8) had a more pronounced difference in effect compared to the second experiment (Figure 4.9), which is likely to be due to the above-mentioned batch-to-batch variations.

When comparing the effect of the free cytostatics and liposomal cytostatics, it was seen that DNR was clearly more effective when given in free form. Another study reported that free DOX was found to be more toxic compared to PEG-FA-conjugated liposomal DOX in AML cells (22). DNR has been shown to inhibit parts of the endocytosis-machinery (unpublished data, Gausdal). This could explain our results, since FA-PEG-conjugated liposomes are internalised by FR receptor-mediated endocytosis (27). Free DNR enter cells via passive diffusion over the cell membrane (23), while liposomes are dependent on internalisation by endocytosis, which is inhibited by the drug it is carrying. Supporting this view is that EME was more effective in PEG-FA-conjugated liposomal form than in free form. In summary, by using liposomal DNR instead of free DNR, the toxicity is decreased. This can be transferred to healthy tissues, where potentially serious side-effects such as cardiotoxicity can be reduced.

In summary, our results in the AML cell lines were encouraging for further investigation of multifunctional liposomes targeting the FR.

5.3 Efficacy of multifunctional liposomes in prostate cancer cell lines

The multifunctional liposomes were effective also in prostate cancer cell lines (Figure 4.16, 4.17 and 4.21). The effective cytostatics concentrations were higher than for the AML cell lines. The FA-PEG-conjugated liposomes were demonstrated to be more effective than the PEG-conjugated liposomes.

The LNCaP cell line showed a better response towards PEG-FA-conjugated liposomes than the PC-3 cell line (Figure 4.16 and 4.17), and LNCaP cells seemed to be most sensitive for DNR treatment. LNCaP cells are known to express PSMA (41), which was our target for drug delivery by the PEG-FA-conjugated liposomes in this cell line. PSMA expression was confirmed by Western blotting, as shown in Figure 4.19. The results from our LNCaP experiments overall suggest that PSMA can be used as a target for drug delivery, and that this was successfully achieved. We do not know the mechanism for PEG-FA-conjugated liposomal uptake via the PSMA, but receptor-mediated endocytosis is a plausible mechanism (41). This could be investigated in future experiments. The sensitivity of LNCaP cells towards DNR offers a potentially new chemotherapy treatment for advanced prostate cancer. Targeted delivery of chemotherapeutics could be a future

preferred approach compared to hormone therapy, which is associated with numerous side-effects and development of resistant cells (36).

PC-3 cells were transfected with PSMA, but it is not sure whether the transfection was successful. The transfection procedure still needs optimisation. The Western blot did not show any band for PSMA in the transfected cells (Figure 4.19), possibly due to low concentrations of successfully transfected cells or problems with solubilisation of membrane proteins. The experiment performed with the PSMA-transfected cells showed only a modest, if any, increase in sensitivity towards PEG-FA-conjugated liposomes compared to the response seen for control cells (Figure 4.16 and 4.21), suggesting that the transfection efficiency for PSMA was low.

Despite the limited amounts of experiments showed in this thesis, the results from the LNCaP cells indicates PSMA as a target for drug delivery via FA-conjugated liposomes, and that DNR could be an effective drug in prostate cancer therapy.

5.4 Comparing the effect of DNR and DNR+EME in multifunctional liposomes

The effect of the DNR+EME combination was investigated on the basis of the work performed by Gausdal et al. (60). The DNR+EME combination was found to be less effective than DNR alone in MOLM-13 cells (Figure 4.8 – 4.10). This was true both for wt cells and cells with silenced p53, and there was no apparent difference in response towards the combination of drugs between the cell lines. However, we can not exclude the possibility that cell death occurred with a morphology we were unable to detect. The phenomenon of a “frozen” death type is described in AML cell lines by Gausdal et al. in a similar situation (60). In this study, the protein synthesis inhibitor CHX was seen to block visible signs of apoptosis induced by DNR, because the cells underwent massive conventional apoptosis after removal of the drug combination (60). This death morphology is not easily detected in the microscope. Unfortunately no other reliable method than cell counting on nucleus morphology was used for the AML cell lines, so if this phenomenon occurred it could have been overlooked. In future investigations cell death should be detected using other reliable methods, such as flow cytometry, ATP measurements, annexin/propidium iodide staining or LDH release measurements.

In PC-3 cells, the DNR+EME combination was more effective for PEG-FA-conjugated liposomes (Figure 4.16). In LNCaP cells, the effect for the combination was equal to DNR alone (Figure 4.17). PC-3 has defective p53, while LNCaP has intact p53 (66). Hence, these results were consistent with previous experience that cells with defective p53 seem to be more vulnerable to the

combination of DNR and a protein synthesis inhibitor (60) (Gausdal, 2012, unpublished data). This response demonstrates why transfection with PSMA of the PC-3 cell line was performed; theoretically allowing for an even better response towards PEG-FA-conjugated liposomes and the combination of drugs compared to the LNCaP cell line.

In the AML cell lines, sequential incubation of PEG-FA-conjugated liposomes containing DNR and EME was performed (Figure 4.13 and 4.14). Interestingly, the combination of drugs was seen to be more effective than DNR alone when sequentially incubated. This was consistent with findings by Gausdal et.al. (60). In this thesis, we found that the effect seemed to be concentration-dependent, because the relationship was not found to be true for lower EME concentrations (Figure 4.14). Administrating drugs sequentially is an approach that can be easily transferred to the clinic. The potential of improved therapeutic outcome that is suggested by sequential incubation can ultimately lead to a higher proportion of cured AML patients.

EME has been demonstrated to be a P-gp substrate, which could in part explain synergistic and additive effects between the drugs (65). Also, this means that combining other drugs with EME exhibits the potential of overcoming MDR, which is a common problem in cancer therapy (59). However, another aspect to take into consideration regarding combining DNR and EME for cancer therapy is the cardiotoxicity of both drugs. This was issue problematised by Larsson et al., who stated that the two drugs should not be used in combination (65). This, however, was discussed for drugs in free form, which is not comparable to drugs encapsulated in nanocarriers. Nanocarriers are useful in this setting to reduce toxicity, and can potentially allow for combining any drugs that are useful for cancer therapy.

An anthracycline was chosen for liposomal encapsulation with the aim of optimising an existing treatment form for AML. It is an advantage that DNR is a part of AML treatment, making the road to clinical use shorter. As described in section 1.4, EME is approved for use in humans and has a shorter way towards approval compared to other protein synthesis inhibitors. The role of combining DNR and EME for AML treatment and optimisation of treatment regimes is an issue for further investigation.

5.5 Conclusion and future investigations

An in vitro validation of multifunctional liposomes has been performed. Liposomes were successfully produced, and confirmed to have the desirable properties in terms of targeting leukaemia cancer cells in vitro. The liposomes were also demonstrated to be effective in prostate cancer cell lines. FR-expressing AML cell lines and a PSMA-expressing prostate cancer cell line were targeted by PEG-FA-conjugated liposomes.

The PEG-FA-conjugated liposomes also showed some increased toxicity compared to PEG-conjugated liposomes towards the prostate cancer PC-3 cell line not expressing PSMA (42) and the non-malignant NRK cell line (Figure 4.16 and 4.22). This could indicate that the liposomes are bound to other folate-binding proteins, or even non-specifically to membrane proteins. This effect needs to be investigated further. The NRK cells could be expressing the FR, since the FR-α is expressed in the kidney proximal tubules (15).

Future experiments should be performed with the aim of optimising liposome doses and treatment regimes, especially sequential incubation with liposomes, and also by exploring different incubation times with liposomes. Flow cytometry or confocal microscopy could be performed to investigate the uptake of liposomes in cancer cells. In AML cell lines, other reliable methods of measuring cell death such as flow cytometry, ATP measurements, annexin/propidium iodide staining and LDH release measurements should be applied, especially to investigate the possibility of "frozen" cell death for cells treated with a DNR+EME combination.

An alternative way of increasing FR expression in AML cell lines, is by ATRA treatment (22). This could be applied to investigate if an increase in effect of PEG-FA-conjugated liposomes was achieved.

The multifunctional liposomes produced in this thesis have several areas of future investigations. Stability testing should be performed on a regular basis and over a longer period of time to evaluate the shelf life. This would include finding a means of measuring EME leakage to discover if EME-containing liposomes suffer from this. The zeta potential measurements showed interesting results indicating drug association to PEG chains. Evaluating the liposome structure at a molecular level would be an interesting future area of investigation. Also, the PC content was never measured in these batches. However, the final quality check of the liposomes will be their ability to selectively kill malignant cells expressing FA-binding membrane proteins. In our system, this was successfully achieved.

In conclusion, targeted drug delivery via multifunctional liposomes has been demonstrated to be effective in vitro. Further studies are necessary to explore the efficacy of these liposomes in

animal models for cancer. Based on the results presented in this thesis, animal experiments have been initiated to investigate if it is possible to prolong life-time of MOLM-13-transplanted mice using PEG-FA-conjugated liposomes loaded with DNR or DNR and EME. Many of the advantages of targeted drug delivery to cancer cells can not be demonstrated by in vitro studies, such as passive targeting via the EPR effect and favourable altering of pharmacokinetic properties of the drug: reduction of side-effects, prolonged circulation times, improved therapeutic index and protection of the drug from degradation. The above-mentioned animal experiments will investigate these advantageous properties of multifunctional liposomes in cancer therapy.

References

1. Atul Metha VH, editor. Haematology at a Glance. 3rd ed. Chichester: Wiley-Blackwell; 2009.

2. Dohner H, Estey EH, Amadori S, Appelbaum FR, Buchner T, Burnett AK, et al. Diagnosis and management of acute myeloid leukemia in adults: recommendations from an international expert panel, on behalf of the European LeukemiaNet. Blood. [Practice Guideline
Research Support, Non-U.S. Gov't
Review]. 2010 Jan 21;115(3):453-74.

3. Schmaier AH, Lazarus, H.M., editor. Concise Guide to Hematology. 1st ed. Chichester: Wiley-Blackwell; 2012.

4. Reya T, Morrison SJ, Clarke MF, Weissman IL. Stem cells, cancer, and cancer stem cells. Nature. [Review]. 2001 Nov 1;414(6859):105-11.

5. Burnett A, Wetzler M, Lowenberg B. Therapeutic advances in acute myeloid leukemia. J Clin Oncol. [Review]. 2011 Feb 10;29(5):487-94.

6. Canzoniero JV, Bhatnagar B, Baer MR, Gojo I. Upfront therapy of acute myeloid leukemia. Curr Oncol Rep. [Review]. 2011 Oct;13(5):361-70.

7. Haematology NAf. Acute myeloid leukaemia (AML) Programme of Action. Brinch, L; Kahrs, J; Strømsheim, J P; Tangen, J M; Waage, A; 2003. p. 14.

8. Villela L, Bolanos-Meade J. Acute myeloid leukaemia: optimal management and recent developments. Drugs. [Research Support, N.I.H., Extramural
Review]. 2011 Aug 20;71(12):1537-50.

9. Matsuo Y, MacLeod RA, Uphoff CC, Drexler HG, Nishizaki C, Katayama Y, et al. Two acute monocytic leukemia (AML-M5a) cell lines (MOLM-13 and MOLM-14) with interclonal phenotypic heterogeneity showing MLL-AF9 fusion resulting from an occult chromosome insertion, ins(11;9)(q23;p22p23). Leukemia. [Case Reports]. 1997 Sep;11(9):1469-77.

10. Appelbaum FR, Rowe JM, Radich J, Dick JE. Acute myeloid leukemia. Hematology Am Soc Hematol Educ Program. [Review]. 2001:62-86.

11. Roboz GJ. Novel approaches to the treatment of acute myeloid leukemia. Hematology Am Soc Hematol Educ Program. [Review]. 2011;2011:43-50.

12. Patrick GL. An Introduction to Medicinal Chemistry. 3rd ed. Oxford: Oxford University Press; 2005.

13. Kantarjian H, O'Brien S, Cortes J, Wierda W, Faderl S, Garcia-Manero G, et al. Therapeutic advances in leukemia and myelodysplastic syndrome over the past 40 years. Cancer. [Review].

2008 Oct 1;113(7 Suppl):1933-52.
14. Jemal A, Clegg LX, Ward E, Ries LA, Wu X, Jamison PM, et al. Annual report to the nation on the status of cancer, 1975-2001, with a special feature regarding survival. Cancer. 2004 Jul 1;101(1):3-27.
15. Salazar MD, Ratnam M. The folate receptor: what does it promise in tissue-targeted therapeutics? Cancer Metastasis Rev. 2007;26(1):141-52.
16. Elnakat H, Ratnam M. Distribution, functionality and gene regulation of folate receptor isoforms: implications in targeted therapy. Adv Drug Deliv Rev. [Research Support, U.S. Gov't, P.H.S.
Review]. 2004 Apr 29;56(8):1067-84.
17. Deng Y, Zhou X, Kugel Desmoulin S, Wu J, Cherian C, Hou Z, et al. Synthesis and biological activity of a novel series of 6-substituted thieno[2,3-d]pyrimidine antifolate inhibitors of purine biosynthesis with selectivity for high affinity folate receptors over the reduced folate carrier and proton-coupled folate transporter for cellular entry. J Med Chem. [Research Support, N.I.H., Extramural]. 2009 May 14;52(9):2940-51.
18. Stover PJ. Physiology of folate and vitamin B12 in health and disease. Nutr Rev. [Review]. 2004 Jun;62(6 Pt 2):S3-12; discussion S3.
19. Zhao X, Li H, Lee RJ. Targeted drug delivery via folate receptors. Expert Opin Drug Deliv. [Research Support, N.I.H., Extramural
Research Support, U.S. Gov't, Non-P.H.S.
Review]. 2008 Mar;5(3):309-19.
20. Qiu A, Jansen M, Sakaris A, Min SH, Chattopadhyay S, Tsai E, et al. Identification of an intestinal folate transporter and the molecular basis for hereditary folate malabsorption. Cell. [Research Support, N.I.H., Extramural]. 2006 Dec 1;127(5):917-28.
21. Low PS, Henne WA, Doorneweerd DD. Discovery and development of folic-acid-based receptor targeting for imaging and therapy of cancer and inflammatory diseases. Acc Chem Res. [Review]. 2008 Jan;41(1):120-9.
22. Li H, Lu Y, Piao L, Wu J, Liu S, Marcucci G, et al. Targeting human clonogenic acute myelogenous leukemia cells via folate conjugated liposomes combined with receptor modulation by all-trans retinoic acid. Int J Pharm. [Research Support, N.I.H., Extramural]. 2010 Dec 15;402(1-2):57-63.
23. Pan XQ, Zheng X, Shi G, Wang H, Ratnam M, Lee RJ. Strategy for the treatment of acute myelogenous leukemia based on folate receptor beta-targeted liposomal doxorubicin combined with receptor induction using all-trans retinoic acid. Blood. [Research Support, Non-U.S. Gov't

Research Support, U.S. Gov't, P.H.S.]. 2002 Jul 15;100(2):594-602.
24. Roboz GJ, Guzman M. Acute myeloid leukemia stem cells: seek and destroy. Expert Rev Hematol. [Review]. 2009 Dec;2(6):663-72.
25. Xiong S, Yu B, Wu J, Li H, Lee RJ. Preparation, therapeutic efficacy and intratumoral localization of targeted daunorubicin liposomes conjugating folate-PEG-CHEMS. Biomed Pharmacother. [Research Support, Non-U.S. Gov't]. 2011 Feb;65(1):2-8.
26. Lee RJ, Low PS. Folate-mediated tumor cell targeting of liposome-entrapped doxorubicin in vitro. Biochim Biophys Acta. [In Vitro]. 1995 Feb 15;1233(2):134-44.
27. Lee RJ, Low PS. Delivery of liposomes into cultured KB cells via folate receptor-mediated endocytosis. J Biol Chem. 1994 Feb 4;269(5):3198-204.
28. Gabizon A, Horowitz AT, Goren D, Tzemach D, Mandelbaum-Shavit F, Qazen MM, et al. Targeting folate receptor with folate linked to extremities of poly(ethylene glycol)-grafted liposomes: in vitro studies. Bioconjug Chem. [Research Support, Non-U.S. Gov't]. 1999 Mar-Apr;10(2):289-98.
29. Goren D, Horowitz AT, Tzemach D, Tarshish M, Zalipsky S, Gabizon A. Nuclear delivery of doxorubicin via folate-targeted liposomes with bypass of multidrug-resistance efflux pump. Clin Cancer Res. [Research Support, Non-U.S. Gov't]. 2000 May;6(5):1949-57.
30. Dasgupta PK, Roger S., editor. ABC of prostate cancer. 1st ed: Wiley-Blackwell; 2012.
31. Martin JM, Supiot S, Berthold DR. Pharmacotherapeutic management of locally advanced prostate cancer: current status. Drugs. [Research Support, Non-U.S. Gov't
Review]. 2011 May 28;71(8):1019-41.
32. Yao V, Berkman CE, Choi JK, O'Keefe DS, Bacich DJ. Expression of prostate-specific membrane antigen (PSMA), increases cell folate uptake and proliferation and suggests a novel role for PSMA in the uptake of the non-polyglutamated folate, folic acid. Prostate. [Research Support, N.I.H., Extramural
Research Support, Non-U.S. Gov't
Research Support, U.S. Gov't, Non-P.H.S.]. 2010 Feb 15;70(3):305-16.
33. Yao V, Parwani A, Maier C, Heston WD, Bacich DJ. Moderate expression of prostate-specific membrane antigen, a tissue differentiation antigen and folate hydrolase, facilitates prostate carcinogenesis. Cancer Res. [Research Support, Non-U.S. Gov't
Research Support, U.S. Gov't, Non-P.H.S.]. 2008 Nov 1;68(21):9070-7.
34. Kreftregisteret. www.kreftregisteret.no. 2012.
35. Cooperberg MR, Moul JW, Carroll PR. The changing face of prostate cancer. J Clin Oncol. [Research Support, N.I.H., Extramural

Research Support, Non-U.S. Gov't
Review]. 2005 Nov 10;23(32):8146-51.
36. Walczak JR, Carducci MA. Prostate cancer: a practical approach to current management of recurrent disease. Mayo Clin Proc. [Review]. 2007 Feb;82(2):243-9.
37. Weissbach L, Altwein J. Active surveillance or active treatment in localized prostate cancer? Dtsch Arztebl Int. [Meta-Analysis
Review]. 2009 May;106(22):371-6.
38. Cannata DH, Kirschenbaum A, Levine AC. Androgen deprivation therapy as primary treatment for prostate cancer. J Clin Endocrinol Metab. [Case Reports
Evaluation Studies
Historical Article
Review]. 2012 Feb;97(2):360-5.
39. Nishiyama T. Androgen deprivation therapy in combination with radiotherapy for high-risk clinically localized prostate cancer. J Steroid Biochem Mol Biol. [Research Support, Non-U.S. Gov't
Review]. 2012 Apr;129(3-5):179-90.
40. Crawford ED, Flaig TW. Optimizing outcomes of advanced prostate cancer: drug sequencing and novel therapeutic approaches. Oncology (Williston Park). [Review]. 2012 Jan;26(1):70-7.
41. Ghosh A, Heston WD. Tumor target prostate specific membrane antigen (PSMA) and its regulation in prostate cancer. J Cell Biochem. [Research Support, U.S. Gov't, P.H.S.
Review]. 2004 Feb 15;91(3):528-39.
42. Pinto JT, Suffoletto BP, Berzin TM, Qiao CH, Lin S, Tong WP, et al. Prostate-specific membrane antigen: a novel folate hydrolase in human prostatic carcinoma cells. Clin Cancer Res. [Comparative Study
Research Support, Non-U.S. Gov't
Research Support, U.S. Gov't, P.H.S.]. 1996 Sep;2(9):1445-51.
43. Buhler P, Wolf P, Elsasser-Beile U. Targeting the prostate-specific membrane antigen for prostate cancer therapy. Immunotherapy. [Review]. 2009 May;1(3):471-81.
44. Musacchio T, Torchilin VP. Recent developments in lipid-based pharmaceutical nanocarriers. Front Biosci. [Review]. 2011;16:1388-412.
45. Ferrari M. Cancer nanotechnology: opportunities and challenges. Nat Rev Cancer. [Research Support, Non-U.S. Gov't
Research Support, U.S. Gov't, P.H.S.

Review]. 2005 Mar;5(3):161-71.
46. Haley B, Frenkel E. Nanoparticles for drug delivery in cancer treatment. Urol Oncol. [Review]. 2008 Jan-Feb;26(1):57-64.
47. Yu B, Tai HC, Xue W, Lee LJ, Lee RJ. Receptor-targeted nanocarriers for therapeutic delivery to cancer. Mol Membr Biol. [Research Support, N.I.H., Extramural
Research Support, U.S. Gov't, Non-P.H.S.
Review]. 2010 Oct;27(7):286-98.
48. Bitounis D, Fanciullino R, Iliadis A, Ciccolini J. Optimizing Druggability through Liposomal Formulations: New Approaches to an Old Concept. ISRN Pharm. 2012;738432:9.
49. Bae KH, Chung HJ, Park TG. Nanomaterials for cancer therapy and imaging. Mol Cells. [Research Support, Non-U.S. Gov't
Review]. 2011 Apr;31(4):295-302.
50. Torchilin V. Multifunctional and stimuli-sensitive pharmaceutical nanocarriers. Eur J Pharm Biopharm. [Review]. 2009 Mar;71(3):431-44.
51. Sawant RR, Torchilin VP. Challenges in development of targeted liposomal therapeutics. Aaps J. 2012 Jun;14(2):303-15.
52. Blanco E, Hsiao A, Mann AP, Landry MG, Meric-Bernstam F, Ferrari M. Nanomedicine in cancer therapy: innovative trends and prospects. Cancer Sci. [Research Support, U.S. Gov't, Non-P.H.S.
Review]. 2011 Jul;102(7):1247-52.
53. Herfindal L. NIM, Milankovic S.S. Bruk av nanokolloidar i behandling av sjukdomar. Naturen. 2012;In press.
54. Blume G, Cevc G. Molecular mechanism of the lipid vesicle longevity in vivo. Biochim Biophys Acta. [Comparative Study
Research Support, Non-U.S. Gov't]. 1993 Mar 14;1146(2):157-68.
55. Klibanov AL, Maruyama K, Torchilin VP, Huang L. Amphipathic polyethyleneglycols effectively prolong the circulation time of liposomes. FEBS Lett. [In Vitro
Research Support, U.S. Gov't, P.H.S.]. 1990 Jul 30;268(1):235-7.
56. Minotti G, Menna P, Salvatorelli E, Cairo G, Gianni L. Anthracyclines: molecular advances and pharmacologic developments in antitumor activity and cardiotoxicity. Pharmacol Rev. [Research Support, Non-U.S. Gov't
Review]. 2004 Jun;56(2):185-229.
57. Kim HP, Gerhard B, Harasym TO, Mayer LD, Hogge DE. Liposomal encapsulation of a synergistic molar ratio of cytarabine and daunorubicin enhances selective toxicity for acute myeloid

leukemia progenitors as compared to analogous normal hematopoietic cells. Exp Hematol. [Comparative Study
Research Support, Non-U.S. Gov't]. 2011 Jul;39(7):741-50.
58. O'Brien ME, Wigler N, Inbar M, Rosso R, Grischke E, Santoro A, et al. Reduced cardiotoxicity and comparable efficacy in a phase III trial of pegylated liposomal doxorubicin HCl (CAELYX/Doxil) versus conventional doxorubicin for first-line treatment of metastatic breast cancer. Ann Oncol. [Clinical Trial
Clinical Trial, Phase III
Comparative Study
Multicenter Study
Randomized Controlled Trial
Research Support, Non-U.S. Gov't]. 2004 Mar;15(3):440-9.
59. Akinboye ES, Bakare O. Biological activities of emetine2011.
60. Gausdal G, Gjertsen BT, McCormack E, Van Damme P, Hovland R, Krakstad C, et al. Abolition of stress-induced protein synthesis sensitizes leukemia cells to anthracycline-induced death. Blood. [Research Support, Non-U.S. Gov't]. 2008 Mar 1;111(5):2866-77.
61. UK D. http://www.medicines.org.uk/EMC/searchresults.aspx?term=Ipecacuanha&searchtype=QuickSearch. 2012.
62. Medicine UNLo. http://chem.sis.nlm.nih.gov/chemidplus/jsp/common/Toxicity.jsp (Emetine toxicity). 2012 [cited 2012 29.05].
63. Medicine UNLo. http://chem.sis.nlm.nih.gov/chemidplus/jsp/common/Toxicity.jsp (Cycloheximide toxicity). 2012 [cited 2012 29.05].
64. Moller M, Herzer K, Wenger T, Herr I, Wink M. The alkaloid emetine as a promising agent for the induction and enhancement of drug-induced apoptosis in leukemia cells. Oncol Rep. [Research Support, Non-U.S. Gov't]. 2007 Sep;18(3):737-44.
65. Larsson DE, Hassan S, Larsson R, Oberg K, Granberg D. Combination analyses of anti-cancer drugs on human neuroendocrine tumor cell lines. Cancer Chemother Pharmacol. [Research Support, Non-U.S. Gov't]. 2009 Dec;65(1):5-12.
66. Li W, Liu Y, Li XX, Yu Y, Wu JJ, Wang Q, et al. MAPKs are not involved in triptolide-induced cell growth inhibition and apoptosis in prostate cancer cell lines with different p53 status. Planta Med. [Research Support, Non-U.S. Gov't]. 2011 Jan;77(1):27-31.
67. Gates SB, Mendelsohn LG, Shackelford KA, Habeck LL, Kursar JD, Gossett LS, et al. Characterization of folate receptor from normal and neoplastic murine tissue: influence of dietary folate on folate receptor expression. Clin Cancer Res. 1996 Jul;2(7):1135-41.

68. Kane MA, Elwood PC, Portillo RM, Antony AC, Najfeld V, Finley A, et al. Influence on immunoreactive folate-binding proteins of extracellular folate concentration in cultured human cells. J Clin Invest. [Research Support, Non-U.S. Gov't
Research Support, U.S. Gov't, P.H.S.]. 1988 May;81(5):1398-406.
69. Gubernator J. Active methods of drug loading into liposomes: recent strategies for stable drug entrapment and increased in vivo activity. Expert Opin Drug Deliv. [Review]. 2011 May;8(5):565-80.
70. Ltd MI. DLS technical note MRK656-01: Dynamic Light Scattering: An Introduction in 30 Minutes. 2012.
71. Ltd MI. Zetasizer Nano series technical note MRK654-01: Zeta Potential - An introduction in 30 minutes. 2012.
72. abcam. http://www.abcam.com/FOLR2-antibody-ab56067.html. 2012.
73. Moribe K, Maruyama K, Iwatsuru M. Estimation of surface state of poly(ethylene glycol)-coated liposomes using an aqueous two-phase partitioning technique. Chem Pharm Bull (Tokyo). 1997 Oct;45(10):1683-7.
74. Immordino ML, Dosio F, Cattel L. Stealth liposomes: review of the basic science, rationale, and clinical applications, existing and potential. Int J Nanomedicine. [Review]. 2006;1(3):297-315.
75. Uribe S, Sampedro JG. Measuring Solution Viscosity and its Effect on Enzyme Activity. Biol Proced Online. 2003;5:108-15.
76. Aulton ME, editor. Aulton's Pharmaceutics: The design and manufacture of medicines. 3rd ed. Leicester: Churchill Livingstone Elsevier; 2007.
77. Rabe S, Krings U, Berger RG. Dynamic flavor release from sucrose solutions. J Agric Food Chem. [Research Support, Non-U.S. Gov't]. 2003 Aug 13;51(17):5058-66.